2019

O-linked beta N-acetylglucosamine (O-GlcNAc) post-translational modifications govern axon regeneration

BOSTON UNIVERSITY

SCHOOL OF MEDICINE

Dissertation

O-LINKED BETA N-ACETYLGLUCOSAMINE (O-GLCNAC) POST-TRANSLATIONAL MODIFICATIONS GOVERN AXON REGENERATION

by

DANIEL GARRISON TAUB

B.A., Hampshire College, 2012

Submitted in partial fulfillment of the

requirements for the degree of

Doctor of Philosophy

2019

Approved by

First Reader _____

Christopher V. Gabel, Ph.D.
Associate Professor of Physiology & Biophysics

Second Reader _____

Benjamin Wolozin, M.D, Ph.D.
Professor of Pharmacology and Neurology

DEDICATION

I dedicate this work to my loving and supportive family. My wife Stefanie Giera, Ph.D. My father Mark Taub, my mother Marcia Taub, and my step-mother Nita Taub. My brother and step-brother Griffin Taub and Zacc Powell. My grandparents Michael and Sylvia Taub and Corrine and Donald Roudi. Lastly, my two loving dogs, Savannah and Lulu Taub.

ACKNOWLEDGMENTS

First, I need to thank my advisor Christopher V. Gabel, Ph.D. His support and mentorship over the years has been a blessing. I knew the second I started working that I would want to join the lab for my thesis work and it is not easy to leave. My committee chair Olga Gurksy, Ph.D. for being ever-positive and pushing me to be better. Benjamin Wolozin, M.D., Ph.D. my second reader, provided me with invaluable research and career advice for which I'm very thankful. R. Andrew Zoeller, Ph.D. gave me crucial feedback early on in this work. Zhigang He, B.M., Ph.D., my external member, helped to elevate and translate these findings into a mammalian model and think about problems globally. I need to thank the Department of Physiology & Biophysics, specifically Esther Bullitt, Ph.D., Carter Cornwall, Ph.D., and David Atkinson, Ph.D. who advised me on all matters throughout my thesis. I also need to thank Shoumita Dasgupta, Ph.D. and Gregory Viglianti, Ph.D. for helping me develop my teaching skills. Lastly, my friends: the whole Gabel Lab, the He lab at Harvard, the Francis lab at UMass Worchester, the Driscoll lab at Rutger's, Jonathan Szeber, Jackson Schipke, Alicia Wooten, Grace Olinger, Tim Norman, Jie Yang, Nick Frame, and Tina Lisk.

O-LINKED N-BETA-ACETYLGLUCOSAMINE (O-GLCNAC) POST-TRANSLATIONAL MODIFICATIONS GOVERN AXON REGENERATION

DANIEL GARRISON TAUB

Boston University School of Medicine, 2019

Major Professor: Christopher V. Gabel, Ph.D. Professor of Physiology & Biophysics

ABSTRACT

Axonal regeneration within the mammalian central nervous system following traumatic damage is limited and interventions to enable regrowth is a crucial goal in regenerative medicine. The nematode *Caenorhabditis elegans* is an excellent model to identify the intrinsic genetic programs that govern axonal regrowth. Here we demonstrate that alterations in O-linked N- beta-acetylglucosamine (O-GlcNAc) post-translational modifications of proteins can increase the regenerative potential of individual neurons. O-GlcNAc are single monosaccharide protein modifications that occur on serines/threonines in nucleocytoplasmic compartments. Changes in O-GlcNAc levels serve as a sensor of cellular nutrients and acts in part through the insulin-signaling pathway. Loss of O-GlcNAc via mutation of the O-GlcNAc Transferase (OGT), the enzyme that adds O-GlcNAc onto target proteins, enhances regeneration by 70%. Remarkably,

hyper-O-GlcNAcyation via mutation of the O-GlcNAcase (OGA), the enzyme that removes O-GlcNAc from target proteins, also enhances regeneration by 40%. Our results shed light on this apparent contradiction by demonstrating that O-GlcNAc enzyme mutants differentially modulate the insulin-signaling pathway. OGT mutants act through AKT1 to modulate glycolysis. In contrast, OGA mutants act through the FOXO/DAF-16 transcription factor to improve the mitochondrial stress response. These findings reveal for the first time the importance of O-GlcNAc post-translational modifications in axon regeneration and provide evidence that regulation of metabolic programs can dictate the regenerative capacity of a neuron.

TABLE OF CONTENTS

LIST OF TABLES

LIST OF FIGURES

LIST OF ABBREVIATIONS

ACK ..... Activated CDC42 Kinase

AGE-1 ..... Ageing Alteration/homolog of PI3K

AKT ..... Protein Kinase B

ALM ..... Anterior Lateral Microtubule Neuron

ARK-1 ..... A Ras-regulating Kinase/homolog of ACK

CAMK ..... Calcium/Calmodulin-dependent Protein Kinase

CREB ..... cAMP response-element binding protein

DAF-16 ..... Abnormal Dauer Formation-16/homolog of FOXO

DAF-18 ..... Abnormal Dauer Formation-18/homolog of PTEN

DAF-2 ..... Abnormal Dauer Formation-2/homolog of insulin receptor

ER ..... Endoplasmic Reticulum

FOXO ..... Forkhead box protein O

GSK ..... Glycogen Synthase Kinase

HBP ..... Hexosamine Biosynthetic Pathway

JNK ..... Jun Nuclear Kinase

KIN-2 ..... Protein Kinase-2/homolog of PKA

MAPK ..... Mitogen Activated Protein Kinase

MAPKK ..... Mitogen Activated Protein Kinase Kinase

MAPKKK ..... Mitogen Activated Protein Kinase Kinase Kinase

MTOR ..... Mammalian Mechanistic Target of Rapamycin

NGM ..... Nematode Growth Media

O-GLCNAC ..... O-linked beta N-acetylglucosamine

OGA ..... O-GlcNAcase

OGT ..... O-GlcNAc Transferase

PI3K ..... Phosphoinositide 3-kinase

PKA ..... Protein Kinase A

PTEN ..... Protein Kinase B

SGK ..... Serum Glucocorticoid Kinase

TPR ..... Tetratricopeptide Repeat

CHAPTER 1:

1.1 Introduction

The nervous system is a complex organ composed of neurons and glia that govern nearly every aspect of an organism's physiology. Both conscious and unconscious cognitive aspects, such as thinking, controlling breathing, and movement, are intricately controlled by this system. Accordingly, dysfunction of this system is catastrophic and is exemplified by the large number of human diseases with nervous system etiologies, such as neuronal injury, Alzheimer's, Parkinson's, and Amyotrophic Lateral Sclerosis. At the center of all these diseases is the functional unit called the neuron, which is a highly specialized cell responsible for carrying and storing information and communicating in networks to allow functionality.

1.2 Architecture and Information Flow of the Axon

Neurons adapt many highly specific morphologies but contain several core elements vital to their function in information flow. From the polarized cell body, two microtubule-based structures are essential for neuronal function. The axon is a long microtubule projection with an actin/spectrin-based cytoskeleton for strength and flexibility. The microtubule direction projecting from the cell body is plus-end-out, meaning that the tubulin subunits are assembled in a fashion which the plus-end is exposed at the end of the tract. The end of the axon generally connects, more commonly

known as synapses, with its target cell, which can be various cell types such as other neurons or muscle cells. Dendrites are the other microtubule-based projection extending from the cell body and they are generally thinner in circumference than the axon. In contrast to the axon, the dendrites adopt a minus-end-out conformation and the cytoskeleton is arranged in patches of actin with occasional spectrin lattices but not as highly ordered as in the axon (Stiess and Bradke, 2011). In general, the dendrites represent a receptive field, detecting and integrating signals whereas the axon carries information to other cells. Information is carried electrochemically. By altering the membrane potential of the neuron in the dendritic field, a threshold is reached and an electric wave called an action potential spreads down the axon toward the axon terminals, thereby controlling neuronal communication either electrically via gap junctions or chemically via exocytosis to affect its target cell.

1.3 *Caenorhabditis elegans* in Neuroscience Research

The nematode *Caenorhabditis elegans* (*C. elegans*) has emerged as a powerful model to study neuroscience from a single cell to a systems biology level. Established as a model organism in the early 1970's by Sydney Brenner, *C. elegans* provides many advantages such as a transparent body, a fully sequenced genome, and rapid generation times (Brenner, 1974; Consortium, 1998). They exist predominantly in a hermaphroditic form and produce clonal progeny. However, a small percentage of males does exist and the ratio of males to hermaphrodites can be increased by altering environmental conditions. *C. elegans* lives in soil all over the world, in which they eat bacteria and are

preyed upon by other nematode species, fungi, and pathogens (Corsi et al., 2015). The common laboratory strain, designated N2, was isolated from a mushroom compost pile in Bristol, England and is the prototype for most experiments. The typical lifespan of *C. elegans* starts as an egg and progresses through four larval stages until adulthood is reached roughly 46 hours after hatching at 20°C (Figure 1.1). The lifespan of *C. elegans* is dramatically affected by temperature, genetic background, and dietary influences. For example, the time to adulthood is only around 35 hours when grown at 25°C. In adulthood, *C. elegans* can live two to four weeks in which they are most fertile in the beginning week. In the absence of food, larval *C. elegans* in the L1/L2 stages can undergo an alternate lifecycle, termed dauer, in which they become thin, move less, and do not develop. When food is reintroduced, they revert back to their normal lifecycle. In contrast to their natural environment, *C. elegans* are cultured on an agar-based media which is supplemented with a lawn of Escherichia coli (*E. coli*). OP50 is the traditional *E. coli* strain of choice whereas RNAi experiments utilize HT115 (DE3) bacteria, due to its IPTG-inducible polymerase activity that is used for induction of RNAi.

An extensive genetic toolbox is available for *C. elegans* research. Large-scale mutagenesis projects, individual laboratory genome modification, and natural population diversity have resulted in mutations in almost every open reading frame and most strains are readily available through the Caenorhabditis Genetics Center at the University of Minnesota (Consortium, 2012). Genes that cannot be targeted by mutagenesis can be knocked down with RNAi in which bacteria that produce RNAi are fed directly to the nematodes (Beifuss and Gumienny, 2012; Kamath and Ahringer, 2003). Further, the

adoption of CRISPR/Cas9 technologies for *C. elegans* has allowed specific point mutations or other designer genome modifications to be rapidly produced (Dickinson and Goldstein, 2016). The fast generation times coupled with highly accessible genetics allows for unprecedented in vivo forward genetic screening. These tools have elucidated important axon growth and regeneration pathways, as discussed later.

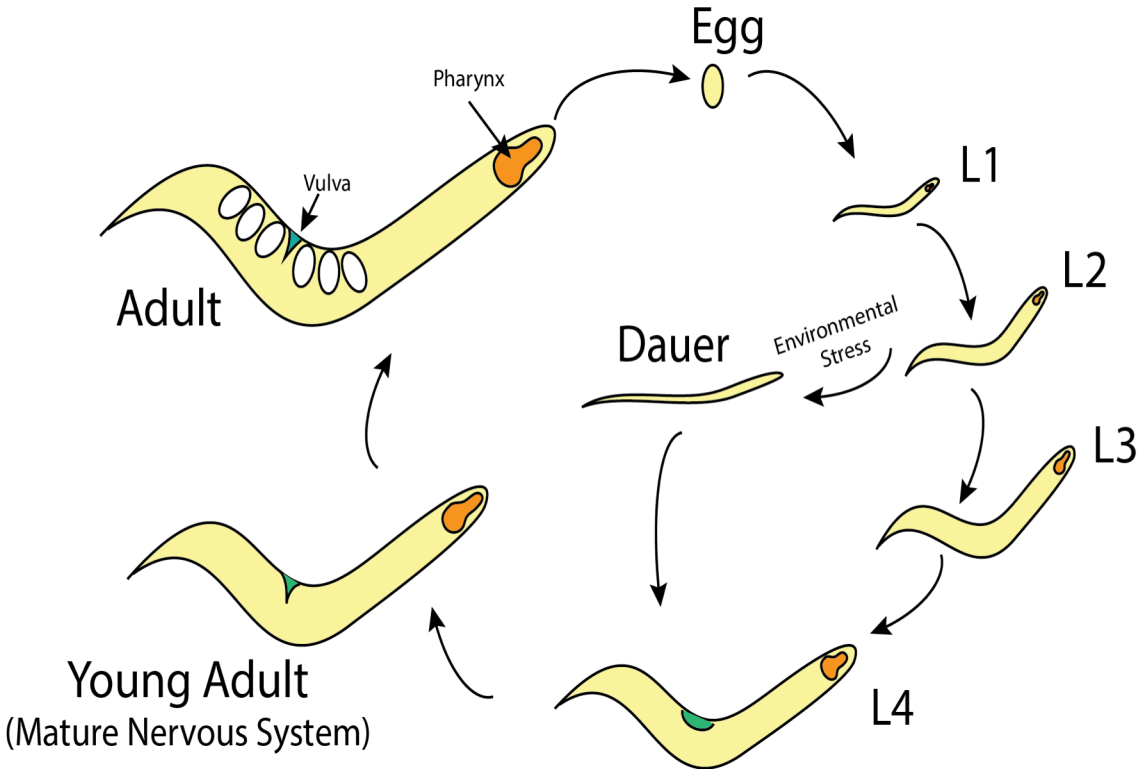

Figure 1.1 The Lifecycle of *Caenorhabditis elegans*

The progression from egg, through the larval stages, to the adult stages is detailed. This can be tracked by examining vulval development (highlighted in green). The pharynx at the head of the animal is labeled in orange.

The *C. elegans* nervous system is well-defined and highly stereotyped across individuals. It consists of 302 neurons and 50 glial-like cells (White et al., 1986). However, unlike the mammalian nervous system, these glial cells are not needed for myelination or trophic support. Neurons adopt a wide range of morphologies dependent on function ranging from the highly branched and elaborated PVD mechano/thermosensitive neurons that cover the majority of the body to the more simplistic ALM mechanosensory neurons with only a single axon extending to the head. In contrast to mammalian neurons, *C. elegans* neurons do not have spiking action potentials but more likely have graded regenerative potentials like plateau potentials (Liu et al., 2009). Whereas action potentials are stereotypical in amplitude, duration, and waveform, graded potentials do not display this behavior. Aside from these features, *C. elegans* neurons behave largely as neurons from other species displaying specialized morphologies, information conveyed by changes in membrane potential, and synapses. The specific set of neurons examined in this work are the touch receptor neurons, a class of mechanosensory neurons responsible for detecting light touch (Figure 1.2) (Chalfie and Sulston, 1981). There are six of these neurons classified by location in the body. The Anterior Lateral Microtubule (ALM) and Anterior Ventral Microtubule (AVM) neurons innervate the anterior side whereas the Posterior Lateral Microtubule (PLM) and the Posterior Ventral Microtubule (PVM) neurons innervate the posterior of the animal (Chalfie and Sulston, 1981; White et al., 1986). These neurons are tightly linked to the cuticle and upon cuticle deflection, mechanosensitve ion channels open to depolarize the neuron leading to changes in movement depending on the origin of the deflection

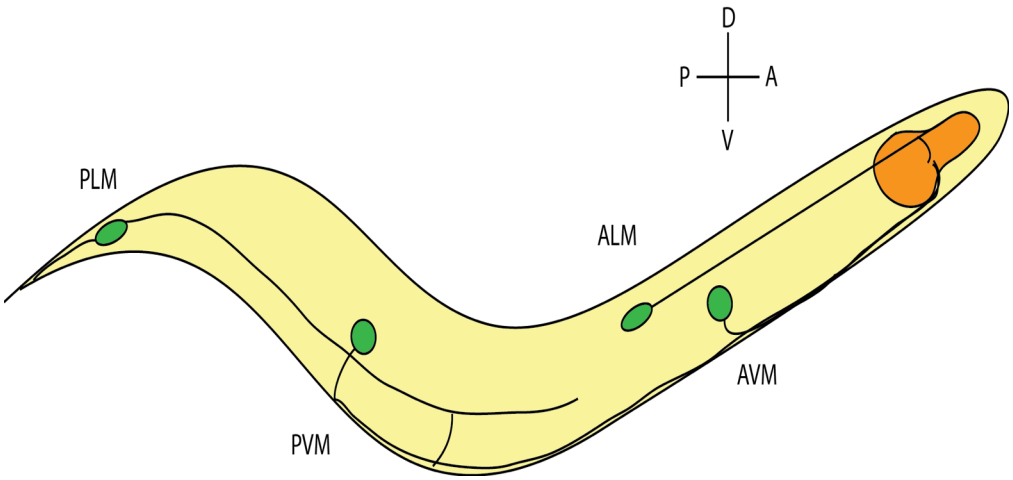

Figure 1.2 The Mechanosensory Neurons of *Caenorhabditis elegans*

Mechanosensory cell bodies in green have both anterior and posterior positions to detect light touch in the environment. The main target of the regeneration in this work is the ALM, which extends a single axon anteriorly and synapses within the nerve ring.

(O'Hagan et al., 2005). For example, animals touched in the anterior region will reverse to avoid the source of the touch. In contrast to mammalian central nervous system neurons, *C. elegans* neurons can generate new growth upon injury and the regenerative response of the mechanosensory neurons in particular has been well-studied (Gabel et al., 2008; Pinan-Lucarre et al., 2012).

1.4 Cell Intrinsic Factors Governing Axon Regeneration

Injury to axons or dendrites of the central nervous system is a huge public health burden and often devastating to the patients affected. The National Institutes of Health currently estimates that 1.4 million people per year are afflicted. Unfortunately, therapeutic prospects are limited as the central nervous system does not functionally regenerate. There are many hypotheses as to why regeneration does not occur ranging from lack of cellular competence to loss of axonal guidance cues in adulthood. Indeed, both cell intrinsic and extrinsic factors contribute to a regenerative response. Over a century ago, Santiago Ramon y Cajal, the founding father of neuroscience, agreed with his contemporaries like Max Bielschowsky and Walther Spielmeyer that the adult nervous system is fixed in nature and lacks the capacity to regenerate. Yet a detailed look into his drawings illustrates that some regeneration is indeed possible, albeit limited. Functionally, it is without question that lesions of the mammalian nervous system rarely regenerate fully. However, pioneering work from Albert Aguayo and colleagues in the 1980s demonstrated that regenerative capacity relied heavily on the environment. Upon grafting of a piece of the sciatic nerve (part of the peripheral nervous system) into the

injured spinal cord, axon regeneration was readily observed. However, transplanting a piece of the optic nerve (part of the central nervous system) into the injured sciatic nerve resulted in little regeneration. Further work investigating the prohibitive growth environment of the central nervous system identified many factors that can perturb regeneration including myelin-associated proteins and scar tissue formation. However, work in the 2000s clearly demonstrated that activation of intrinsic programs can override environmental cues. Cultured spinal cord neurons are repulsed and avoid by myelin-associated glycoprotein. By applying trains of action potentials, thereby increasing intracellular calcium and activating the calcium-dependent adenylyl cyclase, increased production of cAMP allowed these axons to bypass areas with inhibitive myelin signals. Further, administration of dibutyryl cAMP after injury can also overcome the myelin-dependent blocks in regeneration. These studies and others highlight the importance of the intrinsic response to a beneficial regenerative response after injury.

Neurons injured in a post-mitotic state have to enter a growth state in order to regenerate. During development, the axonal growth program is up-regulated and includes a glycolytic metabolic profile, expression of cell-surface receptors to interpret external guidance cues, and various factors to promote microtubule growth. The guidance of axonal growth is governed by a growth cone, an actin-based structure that extends fillopodia to assess the external environment and decide the direction of growth (Song and Poo, 1999). A prominent example of this is the Slit/Robo signaling pathway in the developing mammalian nervous system. Developing axons express Robo-receptors at the growth cone to detect Slit-ligands, generally mediating a repulsive response away from

the ligand source (Dickson and Gilestro, 2006). This is important in the development of commissural neurons to control when and where axons cross the midline, thereby properly connecting the two symmetrical halves of the nervous system. However, these guidance cues, guidance receptors, metabolic capacity, and axonal growth programs are lost or turned off after development thereby limiting the regenerative response during adulthood (He and Jin, 2016). A good example of this is the guidance and regeneration of the Anterior Ventral Microtubule neuron in *C. elegans*. During development, guidance of the axon to its target in the ventral nerve cord requires a dorsally-derived repulsive cue mediated by the Slit/Robo and TGF-beta pathways and a ventrally-derived attractive cue mediated by the DCC/netrin pathway. However, during adulthood, although the Slit signal is still expressed in the dorsal body, it is non-essential for correct guidance. Further, TGF-beta expression is also still present dorsally but the neurons appear to be unresponsive to the signal, as genetic mutants display no alterations in adulthood axon guidance. Regeneration of axons after injury requires the following steps: 1) membrane resealing 2) breakdown and cleanup of damaged cellular components 3) formation of a new growth cone 4) axon extension 5) re-connecting with post-synaptic targets (Figure 1.3). *C. elegans*, as well as a variety of other model organisms, have provided us with insight into steps one through four, although step 5 remains a challenge.

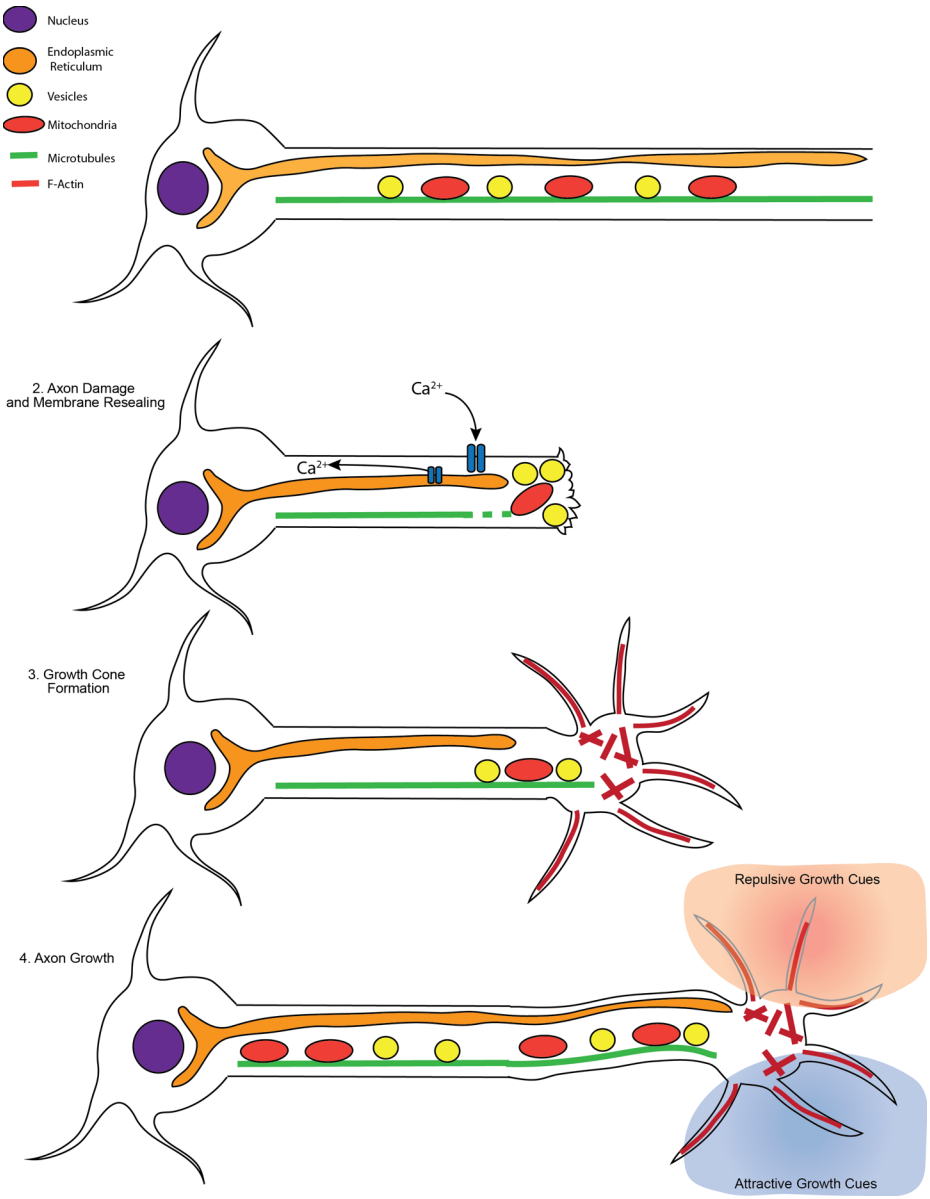

Figure 1.3. Steps of Axon Regeneration

1. Intact polarized neuron.
2. Axonal injury followed by a back-propagating calcium wave and membrane resealing.
3. Clearance of the damaged cellular contents and initiation of the growth cone
4. Cytoskeleton polymerization, axon extension, and signaling pathways dictate the regenerative growth

Through the efforts of forward genetic screening, several important pathways have emerged as being essential for a pro-regenerative response including calcium and cyclic AMP signaling, mTOR signaling, the p38 Mitogen Activated Kinase (MAPK) pathway, and insulin-signaling.

1.4.1 Calcium/cyclic AMP Signaling:

Most studies suggest calcium acts at the initial steps of regeneration and is particularly important in membrane resealing and growth cone formation. After injury, a drastic increase in intracellular calcium is observed and a wave of calcium propagates back toward the cell body (Cho et al., 2015; Sun et al., 2014). The spatiotemporal dynamics of this increase are important for the regenerative response by acting on a number of distinct cellular targets. Axon damage causes an initial influx of calcium followed by mobilization of calcium stores in the endoplasmic reticulum (ER) and presumably other intracellular sinks like the mitochondria, although this hasn't been thoroughly investigated (Sun et al., 2014). The temporal dynamics of this initial wave occurs over the span of minutes but sustained elevation of calcium levels at the site of injury has been observed and hypothesized to be important in the regenerative response. The contribution of calcium from the ER is significant (~40-50%) and is mediated primarily by the ryanodine receptor (*unc-68*). Indeed, loss-of-function mutations in the *unc-68* gene significantly decrease the amount of calcium released and the corresponding amount of regeneration (Sun et al., 2014). Likewise, enhancing intracellular calcium

levels through a gain-of-function mutation in the *unc-19* voltage-gated calcium channel increases regenerative outgrowth (Ghosh-Roy et al., 2010). However, drastic sustained increases in calcium is harmful and leads to cell death as illustrated by a gain-of-function mutation in the *mec-4* sodium/calcium channel which leads to calcium-mediated necrosis (Bianchi et al., 2004). It is then clear that the calcium response governs the life or death decision of the neuron after injury and its properly governed dynamics are crucial to effective regeneration. Calcium exerts its effects on regeneration through many different effectors either with or without the calcium-binding protein calmodulin. A well-studied example is the calcium/calmodulin-dependent kinases (CAMKs). Gain-of-function of the CAMKII (*unc-43*) produces a drastic decrease in regenerative outgrowth, whereas loss-of-function mutations have no phenotype, suggesting that it is a negative regulator of regeneration (Chung et al., 2016). Further elucidation of the myriad of targets of calcium signaling is bound to uncover additional regeneration-associated genes.

A prominent effect of calcium elevation in neurons is the activation of the enzyme adenylyl cyclase which generates the second messenger cyclic AMP from ATP. Indeed, experiments applying dibutyryl-cAMP or the adenylyl cyclase activator forskolin to injured axons saw an enhancement in regeneration. Further characterization in *C. elegans* revealed that cAMP elevation could significantly enhance axon regeneration in mechanosensory neurons (Ghosh-Roy et al., 2010). Epistasis experiments revealed that the effects of cAMP were downstream of calcium signaling as elevation of cAMP was sufficient to induce robust regeneration in the presence of an IP3-inhibitor which suppresses ER calcium release. In addition, enhancing intracellular calcium signaling in

addition to cAMP did not have an additive effect on regeneration suggesting they act in a common pathway (Ghosh-Roy et al., 2010). As with calcium, the effects of cAMP on regeneration appear to act at many levels. In mammalian models, cAMP rises leads to the activation of protein kinase A (PKA) which in turn activates the cAMP-Response Element Binding (CREB) transcription factor. Activation of this pathway leads to the up-regulation of regeneration-associated genes such as arginase I, which promotes polyamine synthesis and relieves the inhibition on regeneration by myelin-associated proteins (Cai et al., 2002; Cai et al., 1999).

In contrast to mammals, the effect of cAMP on axon regeneration in *C. elegans* is largely independent of the CREB homolog crh-1. Instead, cAMP signaling acts on certain basic leucine zipper (bZip) family proteins such as cebp-1 and jun-1, although how cAMP transduces this signal is still unclear (Li et al., 2015). One model has been proposed in which the PKA homolog kin-2 phosphorylates the ETS-4 protein. Once phosphorylated, it can form a complex with CEBP-1 to activate target genes important in the initiation of the MAPK-signaling pathway (Li et al., 2015). Thus, although an enhanced regenerative phenotype is observed in both mammals and *C. elegans* upon increasing cAMP signaling, the molecular mechanisms appear largely different. To what extent there exists a degree of overlap remains to be studied.

1.4.2 PTEN/mTOR Signaling

As developmental growth programs are often shut off in post-mitotic neurons, a targeted genetic screen was conducted in retinal ganglion cells in mice using an inducible

AAV-transmitted Cre recombinase to identify neuronal growth factors involved in regeneration (Park et al., 2008). Of the genes tested, including p53, Smad4, Dicer, LKB1, and retinoblastoma (Rb), PTEN (phosphatase and tensin homolog) had the greatest effect on both neuronal survival and regenerative outgrowth. PTEN is an important phosphatase in the phosphoinositide 3-kinase (PI3K)/mammalian target of rapamycin (mTOR) signaling pathway and directly reduces PI3K activity through its phosphatase activity. However, in the absence of PTEN, PI3K is activated leading to the activation of the mTOR signaling complex and further activation of cap-dependent protein translation via the ribosomal S6 kinase 1 and the eukaryotic initiation factor 4E binding protein (Park et al., 2008). Hence the activation of this pathway leads to new protein synthesis, among other actions. Similar mechanisms exist in *C. elegans* in which mutants in the PTEN-homolog, daf-18, can enhance axon regeneration and this effect can be blocked by administration of the mTOR inhibitor rapamycin (Byrne et al., 2014). Whether the downstream actions of mTOR are conserved in *C. elegans* remains unknown.

1.4.3 The p38 and c-Jun N-Terminal Kinase (JNK) Mitogen-Activated Protein Kinase Pathways

Mitogen-activated protein kinase (MAPK) signaling cascades are crucial for axon regeneration but dispensable for initial axon development (Hammarlund et al., 2009). MAPKs have been recognized to play an important role in mediating extracellular signals and stresses into injury-response programs and two specific pathways are essential for regeneration in *C. elegans*. A RNAi screen for factors that influence axon regeneration in

a mutant with spontaneous axon breaks first discovered the Dual-Leucine Zipper (DLK) Kinase 1, which encodes a mitogen-activated protein kinase kinase kinase (MAPKKK) (Hammarlund et al., 2009). Loss-of-function mutations in *dlk-1* prevented regeneration from occurring while over-expression promoted a regenerative response. Further genetic epistasis experiments determined that DLK-1 activated the mitogen-activated protein kinase kinase (MAPKK), MAPKK4, which then acted upon the mitogen-activated protein kinase (MAPK), *pmk-3*/p38 (Nix et al., 2011). The activation of *pmk-3* then leads to the subsequent activation of transcription factors that govern the response to injury. Upon injury, a combination of calcium mediated signals coupled with microtubule destabilization triggers DLK-1 activation, although the exact mechanisms remain unclear. Previous work suggests that upon an increase in cytosolic calcium, DLK-1 can change from an inactive heteromeric protein consisting of DLK-1 short and long isoforms to an active homomeric protein consisting of DLK-1 long. This then can proceed to activate the rest of the signaling cascade (Yan and Jin, 2012).

In parallel to the p38 MAPK pathway, exists the c-Jun N-terminal Kinase (JNK; KGB-1 in *C. elegans*) MAPK pathway which cross-regulate one another (Nix et al., 2011). Similar to the p38 pathway, the JNK pathway consists of a MAPKKK (MLK-1) signaling to a MAPKK (MEK-1) and then activating the JNK MAPK (KGB-1). At each step in this pathway, there exists the opportunity for cross-regulation. Exactly why this complex MAPK signaling is necessary for regeneration is unclear. As MAPKs respond to a variety of stressors, the combination of these two pathways onto convergent targets may represent a rheostat to control signaling intensity or duration. The end step of both of

these pathways is the activation of the PMK-3 and KGB-1 MAPKs. Their subsequent molecular actions have begun to be defined and appear to act at the transcriptional level. PMK-3, for example, activates the CCAATT/enhancer-binding protein CEBP-1. The targets of CEBP-1 are just being revealed but initial studies suggest that calcium/cAMP signaling triggers the formation of a CEBP-1 transcriptional complex. The transcription of the SVH-2 receptor tyrosine kinase is up-regulated and, upon activation by the SVH-1 ligand, activates the JNK pathway to regulate axon regeneration (Li et al., 2015). How this complex pathway functions in a spatiotemporal fashion is not yet understood.

1.4.4 The Insulin-Signaling Pathway

The insulin-signaling pathway was recently identified as an important pathway in the age-related decline in regenerative ability (Figure 1.4). This pathway is highly conserved from mammals to *C. elegans*, although mammals have one insulin growth factor which binds to the insulin receptor, whereas, *C. elegans* have forty insulin-like ligands for one insulin receptor (DAF-2) (Murphy and Hu, 2013). The complexity of signaling of these ligands remains an active area of research but initial studies suggest tissue-specific expression of insulin-like ligands with both agonistic and antagonistic effects on DAF-2. Why *C. elegans* has such a large evolutionary expansion of insulin-like ligand genes remains unknown. Once a ligand binds to the DAF-2 receptor tyrosine kinase, a signaling cascade is initiated ultimately resulting in the regulation of the FOXO transcription factor, DAF-16. Upon DAF-2 activation, the Phosphoinositide 3-kinase (AGE-1) is activated, which converts phosphatidylinositol 4,5-bisphosphate to

phosphatidylinositol (3,4,5)-triphosphate in the membrane. This promotes the recruitment of the kinase AKT-1 to the membrane for phosphorylation and activation by a variety of kinases including PDK and mTORC2. Activation of AKT-1 influences a number of downstream targets, but notable for the insulin-signaling pathway, AKT-1 phosphorylates DAF-16 to inhibit its transcriptional activity by promoting its nuclear exclusion (Murphy and Hu, 2013). Other kinases may act in parallel to AKT-1 in order to inhibit or promote DAF-16 activity including AKT-2 and SGK-1 (Hertweck et al., 2004; Xiao et al., 2013).

The DAF-16 transcription factor regulates hundreds of genes involved in numerous processes including metabolism and cellular stress response. Interestingly, DAF-16 appears to activate tissue-specific genes, as neuronal DAF-16 targets differ greatly from intestinal target genes (Kaletsky et al., 2016). Further diversifying the actions of DAF-16, there are eight different DAF-16 isoforms produced by differential promoter usage, which contain different tissue expression profiles, the presence or absence of the DNA-binding domain, and several different N-terminal domains (Kwon et al., 2010). DAF-16 acts on target genes by binding to a canonical DAF-16 binding motif, determined in vitro to be TTGTTTAC (Furuyama et al., 2000).

The insulin-signaling pathway and set of regulated genes is the subject of intense research due to the ability of DAF-2 mutants to live twice as long as wildtype *C. elegans* (Dorman et al., 1995; Kimura et al., 1997). This drastic extension of lifespan is dependent on the DAF-16 transcription factor and several downstream genes. In addition to aging, DAF-2 mutants also have extended regenerative capacity in older animals (Byrne et al.,

2014). Using the GABAergic motor neurons, it was found that the percentage of axons that regenerate in five-day old DAF-2 mutants is greater than in the wildtype, and this effect was dependent on DAF-16. Co-immunoprecpitation and identification of DAF-16 targets revealed that the DLK-1 gene is regulated by DAF-16 and mutation of DLK-1 abolishes the enhanced regeneration seen in aged DAF-2 mutants (Byrne et al., 2014). However, DAF-16 has hundreds of potential targets and other groups have found other DAF-16 target genes to influence axon regeneration, such as the forkhead-9 transcription factor (Kaletsky et al., 2016). Likely DAF-16 has a number of cell-intrinsic and -extrinsic actions that influence the regenerative capacity of a neuron.

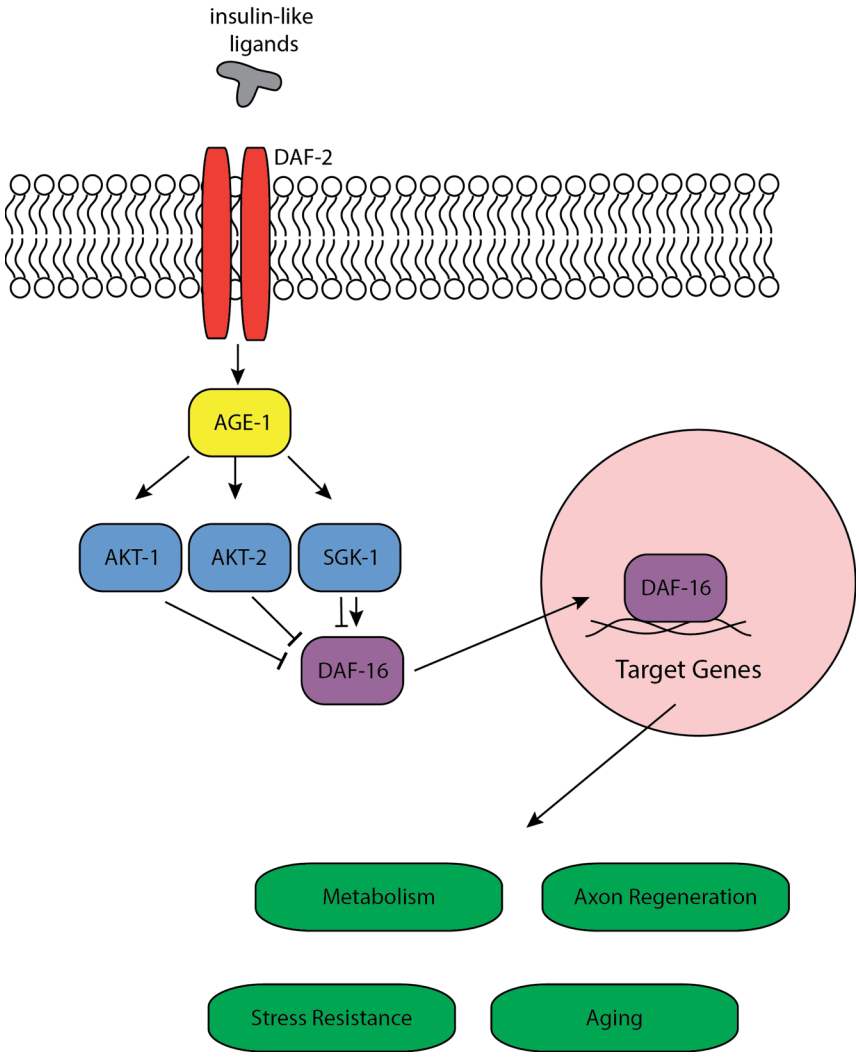

Figure 1.4 The Insulin Signaling Pathway and its Targets

Insulin ligands activate the DAF-2/INSR leading to the activation of downstream kinases. This converges on the DAF-16/FOXO transcription factor to regulate genes involved in many aspects of neuronal physiology.

1.5 O-GlcNAc: An evolutionarily conserved nutrient sensor

In order to survive, an organism must be able to detect and respond to changes within its environment. Likewise, cellular assessment of fitness also occurs to govern important cellular decisions such as survival and growth. The mechanisms underlying the detection of cellular fitness are being uncovered and a number of these are nutrient sensors to enable the cell to optimize its metabolic response given its available resources. Examples of these nutrient sensors include the AMP-activated protein kinase, which detects levels of ATP and AMP, and the sterol regulatory-element binding protein pathway, which responds to changes in sterols. Glucose is an important energy source and its use, storage, and mobilization must be carefully monitored. O-linked beta-N-acetylglucosamine (O-GlcNAc) post-translational modifications of serines/threonines are a glucose-responsive effector of proteins (Figure 1.5). The substrate, UDP-GlcNAc, is generated by the hexosamine biosynthetic pathway (HBP) which utilizes 2-5% of total cellular glucose (Marshall et al., 1991; McClain and Crook, 1996). Accordingly, O-GlcNAc levels increase in response to increasing glucose levels and act to modify a plethora of proteins. In fact, O-GlcNAc is likely the most abundant protein post-translational modification. The addition and removal of O-GlcNAc to target serines/threonines is catalyzed by one set of enzymes, the O-GlcNAc Transferase (OGT) and the O-GlcNAcase (OGA) (Hart et al., 2007). This glycosylation occurs in nucleocytoplasmic compartments and is different from the O-linked and N-linked glycosylations that occur in the endoplasmic reticulum in that they are not branched or

extended. O-GlcNAc addition or removal from target proteins has complex consequences for protein behavior. In the simplest case, O-GlcNAc competes with phosphorylation to prevent protein activation. However, more complex cases suggest a dynamic interplay between phosphorylation and O-GlcNAcylation that has a variety of effects on protein conformation and behavior.

Although O-GlcNAc modifies hundreds of proteins, alterations in O-GlcNAc dynamics produce distinct phenotypes which suggests there is a logical flow of information being transferred to alter cellular dynamics. Key pathways affected include the insulin-signaling pathway, calcium signaling, and the stress response, although many more are likely to be identified (Forsythe et al., 2006; Hanover et al., 2005; Ngoh et al., 2011; Zachara et al., 2004). Studies of O-GlcNAc were initially deterred by the lack of mass spectrometry tools for detection, the lack of specific chemical inhibitors, and the embryonic/perinatal lethality of mutants in the mouse O-GlcNAc enzymes (Hart et al., 2007). However, recent technological advances in all areas have allowed in depth study of this modification to begin. The following sections demonstrate the results of altered O-GlcNAc signaling in humans, mice, and *C. elegans*. Table 1 summarizes the information.

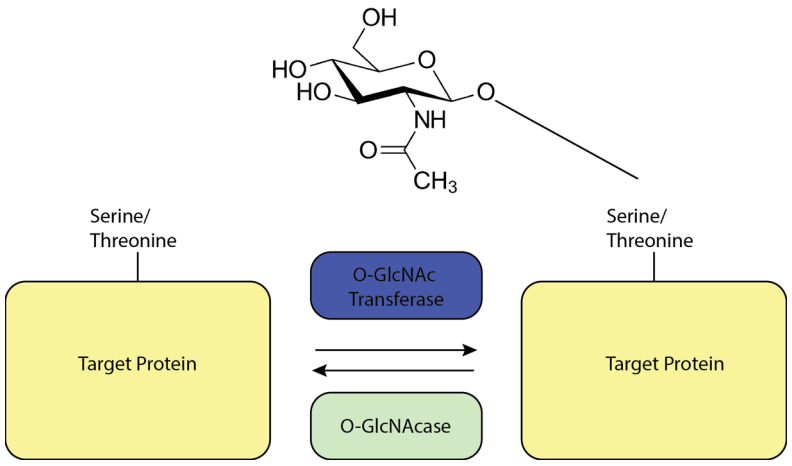

Figure 1.5 Schematic detailing O-GlcNAc Addition and Removal on Proteins

The O-GlcNAc Transferase recognizes proteins using its tetratricopeptide repeat domain and adds the O-GlcNAc moiety to target serines/threonines. The O-GlcNAcase is a specific hydrolase that removes this modification. This occurs in nucleocytoplasmic compartments.

1.5.1 Human SNPs in the O-GlcNAc Transferase and O-GlcNAcase Genes:

Single nucleotide polymorphisms in the OGT and OGA genes have been associated with human disease. The OGT enzyme has N-terminal tetratricopeptide repeats (TPR) used to interact with target substrates and a C-terminal catalytic domain. Hemizygous polymorphisms in the TPR region have been associated with X-linked Intellectual Disability (Vaidyanathan et al., 2017; Willems et al., 2017). The first mutation leads to aberrant splicing of the target mRNA and no protein is translated. The second is a missense mutation which changes arginine 284 to a proline results in an enzyme with decreased protein stability and reduced substrate glycosylation in HEK293T cell lysates, although global O-GlcNAc levels in patient-derived fibroblasts remain unaffected (Willems et al., 2017). As the mutation is located in the substrate recognition domain, it is possible that only certain OGT substrate interactions are affected and this might not be detected when looking at global O-GlcNAc levels. Alternatively, OGT in mammals has a second catalytic function which cleaves the transcriptional co-regulator Host Cell Factor 1 (HCF1) producing N-and-C-terminal subunits that regulate different cellular activities. HCF1 is another gene also associated with X-linked Intellectual Disability and the catalysis was affected in patient-derived fibroblasts (Willems et al., 2017). Whether OGT is important as a glycosyltransferase, a protease, or both in X-linked Intellectual Disability remains unknown.

SNPs in the OGA gene have also been identified. A survey to identify SNPs associated with type II diabetes in Mexican Americans, identified a SNP localized to intron 10 that lead to a 2.27 times increased risk in developing diabetes and a significant decrease in the age of onset (Lehman et al., 2005). Interestingly, the risk was conferred in the heterozygous state and no homozygous subjects were found. While detailed molecular studies of this SNP have not been performed, intron 10 contains an alternative stop codon, which may suggest its involvement in differential expression of various isoforms of OGA/MGEA5.

1.5.2 Disruption of O-GlcNAc Signaling in Mouse Models:

As mentioned above, deletion of OGT is perinatal lethal in mice but a combination of different promoters driving tissue-specific expression have begun to elucidate the role of OGT in cellular functions (Shafi et al., 2000). O-GlcNAc appears to be particularly important in the neurons of the central nervous system as mutation of OGT in all neurons using the synapsin-I-Cre and a floxed OGT allele results in lethality by postnatal day 10 (O'Donnell et al., 2004). However, by using more targeted Cre promoters, such as alpha-CaMKII, disrupting OGT results in adult obesity (Lagerlof et al., 2016). This is caused by a reduction in excitatory synaptic activity in neurons of the paraventricular nucleus of the hypothalamus. Without this activity, the signal to cease feeding is not transmitted and hyperphagia occurs (Lagerlof et al., 2016). In addition, O-GlcNAc appears to be important for memory. cAMP response element binding protein

(CREB) is heavily modified by O-GlcNAc in an activity-dependent manner. The addition of O-GlcNAc to CREB suppresses its transcriptional activity by reducing its ability to bind with an important coactivator. Without binding to the CRTC-coactivator, CREB cannot sufficiently induce gene transcription and initiate memory formation(Rexach et al., 2012).

Deletion of OGA in mice also results in perinatal lethality (Keembiyehetty et al., 2015). This phenotype was associated with severe hypoglycemia. Analysis of the liver revealed that there was a reduction in glycogen stores suggesting that glucose homeostasis is disrupted. The respiratory exchange ratio is the ratio of the amount of CO_2 produced to the amount of O_2 consumed. Ratios of 0.70 are indicative of oxidative lipid metabolism and ratios closer to 1.00 suggest carbohydrate metabolism, as oxidative lipid metabolism consumes more O_2. Heterozygous OGA mutants display a clear preference toward carbohydrate metabolism. This suggests that OGA mutants prefer to utilize carbohydrates as a substrate for metabolic processes and that this shunt toward carbohydrate use is not sustainable and eventually leads to lethality (Keembiyehetty et al., 2015). Using a nestin-Cre targeted to all neurons revealed important functions for OGA in the brain (Olivier-Van Stichelen et al., 2017). While OGA brain-conditional knockouts were viable, fertile, and had similar longevity to wildtype controls, they had a reduction of size in certain brain regions such as the olfactory bulb and the anterior pituitary. In addition, these mice exhibited fatty liver syndrome and 50% higher body fat likely due to the hypopituitary development and resulting endocrine disruption, although

this remains to be tested (Olivier-Van Stichelen et al., 2017). Accordingly, circulating levels of adiponectin and insulin were increased while IGF levels were decreased. Interestingly, OGA brain-conditional knockouts displayed a massive increase in cellular proliferation in the brain but altered neurogenesis. The resulting neuronal/cellular phenotype is quite complex and requires further study using neuronal-population specific knockouts.

1.5.3 Disruption of O-GlcNAc Signaling in Caenorhabditis elegans Models:

In contrast to mice, mutation of OGT or OGA is well-tolerated in *C. elegans* although OGT and OGA mutants live slightly shorter and longer lives, respectively (Love et al., 2010). As in mice, similar effects on body fat and sugar content are observed, but curiously, disruption of OGT or OGA produces similar results with less triglyceride storage but more glycogen storage (Forsythe et al., 2006). This is hypothesized to be due to the increase in inhibitory GSK-3β phosphorylation leading to a release on glycogen synthase and increase in glycogen formation and storage (Forsythe et al., 2006). It is somewhat paradoxical that both OGT and OGA mutants display similar organismal metabolic phenotypes and exhibit similar effects on GSK-3β phosphorylation, especially if a mutually exclusive model for O-GlcNAc and phosphorylation is occurring on GSK-3β.

O-GlcNAc mutant *C. elegans* also display an altered stress response. OGT mutants are more susceptible to heat and toxic exposures while OGA mutants are resistant (Love et al., 2010; Rahman et al., 2010). At the neuronal level, O-GlcNAc also appears to serve a neuroprotective role, although in the opposite direction. The introduction of various human neurodegenerative alleles produces neurodegeneration in *C. elegans* resulting from tauopathy, polyglutamine expansion, or amyloid aggregation (Wang et al., 2012). Loss of OGT appears neuroprotective whereas loss of OGA appears to exacerbate the neurodegeneration. For example, introducing the Htn-Q150 allele, which has the human huntingtin protein and a tract of 150 glutamine residues, in a subset of amphid neurons results in neurodegeneration of ASH neurons. At day eight of adulthood, 59.4% of neurons were degenerating and 8.9% were dead in wildtype animals whereas OGT mutants had 10.4% degenerating and 0% dead and OGA mutants had 35.9% degenerating and 51.3% dead (Wang et al., 2012). The examples provided above illustrate that while O-GlcNAc modifies many diverse proteins, the resulting phenotypes after modification are quite specific and therefore it is likely that specific pathways are affected. It is likely that the lack of cell-specific manipulations of O-GlcNAc levels have led to differing conclusions in *C. elegans* studies. Organismal effects on metabolism or growth rates could be leading to non-intrinsic effects.

1.6 Goal of this Dissertation:

The multitude of effects O-GlcNAc exerts on neuronal physiology, metabolism, and the stress response place it at a prime position to respond to neuronal injury and

influence axon regeneration. When the research for this dissertation began, the knowledge of the role of O-GlcNAc in neurons was limited. Axonal growth in cultured embryonic neurons was significantly affected by O-GlcNAc modulation but the underlying mechanism remained elusive. In embryonic chicken forebrain neurons, over-expression of the O-GlcNAcase and, therefore, a reduction of O-GlcNAc levels increased axon length primarily by affecting branching and corresponding branch length. Likewise, knocking out the O-GlcNAc Transferase in developing mouse neurons in culture resulted in enhanced axon length, whereas over-expressing OGT reduced axon growth. A CREB siRNA abolished the effects suggesting O-GlcNAc was modifying CREB to influence axon length. Further, one study suggested that the O-GlcNAc levels are enhanced in the growth cone of developing axons suggesting its importance in this specialized structure. These studies and others compelled us to examine the effects of O-GlcNAc on axon regeneration.

The goal of this dissertation is to 1.) determine whether O-GlcNAc signaling influences axon regeneration, 2.) determine mechanistically how this is achieved, and 3.) establish whether the results can be translated to a mouse model of axonal injury.

Gene	Organism	Type of Lesion	Phenotypes	References
OGT				
	Homo sapiens	SNP	X-linked intellectual disability and developmental delay; craniofacial alterations	Willems et al., 2017; Vaidyanathan et al., 2017
	Mus musculus	Cre-mediated Whole Organism Knockout	perinatal lethal	Shafi et al., 2000
		Cre-mediated Neuron Knockout	lethality at postnatal day 10	O'Donnell et al., 2004
		Cre-mediated Paraventricular Nucleus of the Hypothalamus Knockout	obesity and hyperphagia; reduced excitatory potentials in alpha-CAMKII neurons	Langerlof et al., 2017
	Caenorhabditis elegans	Large-scale deletion	decreased lifespan, increased glycogen, decreased triacylglycerols, inhibits dauer formation, sensitive to heat-stress, neuroprotective	Forsynthe et al., 2006; Love et al., 2010; Rahman et al., 2010; Wang et al., 2012
OGA				
	Homo sapiens	SNP	Increased risk of developing diabetes in Mexican-Americans	Lehman et al., 2005
	Mus musculus	Cre-mediated Whole Organism Knockout	neonatal lethality associated with reduced glycogen levels and hypoglycemia	Keembiyehetty et al., 2015
		Cre-mediated Neuron Knockout	developmental delay, increased cellular proliferation, altered neurogenesis and differentiation, obesity with fatty liver syndrome, decreased circulating free fatty acids, increased circulating triacylglycerides, increased circulating insulin, decreased circulating IGF	Oliver-Van Stichelen et al., 2017
	Caenorhabditis elegans	Large-scale deletion	increased longevity, increased glycogen, decreased triacylglycerols, promotes dauer formation, resistant to heat-stress, exacerbates neurodegeneration	Forsynthe et al., 2006; Love et al., 2010; Rahman et al., 2010; Wang et al., 2012

Table 1: Summary of the Influence of O-GlcNAc on Physiology Across Organisms

CHAPTER TWO

Methods

2.1 *C. elegans* strains and culture

All strains were cultured and maintained at 20°C on Nematode Growth Media agar plates [3g NaCl, 22g bactoagar, 2.5g bactopeptone, 1mL of 5mg/mL cholesterol in 100% ethanol, 1mL of 1M $CaCl_2$, 1mL of 1M Mg_2SO_4, 25mL of 1M KPO_4, 975 mL of H_2O] seeded with OP50 *E. coli*, except in RNAi experiments as noted. Strains were obtained from the Caenorhabditis Genetics Consortium (CGC at the University of Missouri) and the National Bioresource Project (NBRP; Japan). Select strains in this work were gifts from Monica Driscoll (PTN73), Rik Korswagen (KN131), and Michael Nonet (NM2637). To visualize the mechanosensory neurons (ALM & PLM neurons), strains were crossed into either SK4005 (zdis5 [p*mec4*::GFP]) or KWN177 [p*mec-4*::mCherry; *unc-119*+] background. A full list of all strains and sample sizes is provided in Appendix 1.

The generation of males for crossing between strains was conducted by taking 30 L4 hermaphrodite nematodes and heatshocking them at 25°C for 5-6 hours, then returning them to 20°C. Males in the next generation were searched for, picked out, and mated accordingly.

2.2 Axon Regeneration Assay with an Infrared Femtosecond Laser

To induce a highly local, specific, and reproducible axonal injury in *Caenorhabditis elegans*, a Coherant Mantis infrared laser was used. In this system, a sapphire crystal doped with titanium is excited by a green pump laser to emit a mode-locked pulsed, infrared wave beam. An optoacoustic pulse picker generates a 10 kHz train of 100 femtosecond pulses, which is then guided into the back of an inverted microscope. Using a high NA objective (such as the 60X NA 1.4 used in this work), allows for high spatial resolution of the beam. The use of an infrared beam with a wavelength spread around 800nm is used for tissue penetration, as tissue at these wavelengths is almost transparent. Using a pulsed beam, as compared to continuous, leads to higher peak energies for a given laser power. Further, the pulses are spaced in time so that energy between each pulse dissipates and does not lead to excess tissue damage (Gabel, 2008).

Single nematodes were placed on a stiff agarose pad composed of 8% agarose in Nematode Growth Buffer (NGM), which is fixed on a glass slide. A 2:1 ratio of 0.05 micron polystyrene microspheres (PolySciences Inc.):NGM buffer was spread across the pad and individual nematodes were picked onto the pad. A glass coverslip was gently placed over the nematodes in solution and the coverslip was fixed in place with a 1:1 ratio of paraffin and petroleum jelly. Done correctly, animals were completely immobilized without chemical treatment (Kim et al., 2013). In total, the laser surgery to rescue took < 15 minutes. After being mounted on the slide, the nematodes were mounted on a Nikon TI-2000 inverted fluorescent microscope and surgeries were

performed with a Nikon 60X NA 1.4 oil objective. Axons of the Anterior Lateral Microtubule (ALM) and Posterior Lateral Microtubule (PLM) neurons were severed at 20μM and 40μM from the neuronal cell body, producing a 20μM gap. A 10-kHz train of 100 femtosecond pulses in the near infrared (800 nm) with pulse energies of 15-30 nJ/pulse, was generated and axotomy consisted of 3-5 short laser exposures (0.25s each) resulting in vaporization at the focal point and severing of the targeted axon. After surgery, nematodes were rescued by removing the coverslip, placing them in fresh NGM buffer, and moving them to a new NGM agar plate to recover. Regeneration was analyzed by placing nematodes on a 2% agarose pad containing 5mM sodium azide for immobilization. Z-stacks of the regrowth were imaged with a Nikon 40X NA 1.3 oil objective at the designated time point. Time points analyzed in this work were 1, 3, 5, 12, and 24 hours after injury. For the 1-hour, 3-hour, and 5-hour time points, animals were maintained on the slide and desiccation was prevented by sealing the slide in paraffin wax. For the 12-hour, 24-hour, and 48-hour time points, animals were rescued with NGM buffer after axotomy and placed on NGM agar plates seeded with OP50 until reimaging. A maximum intensity projection of the Z-Stack was produced with ImageJ/FIJI Imaging Software and regeneration was measured by tracing the new outgrowth. It is worth noting that this approach loses information in the Z-direction but we have not found it to affect our analysis.

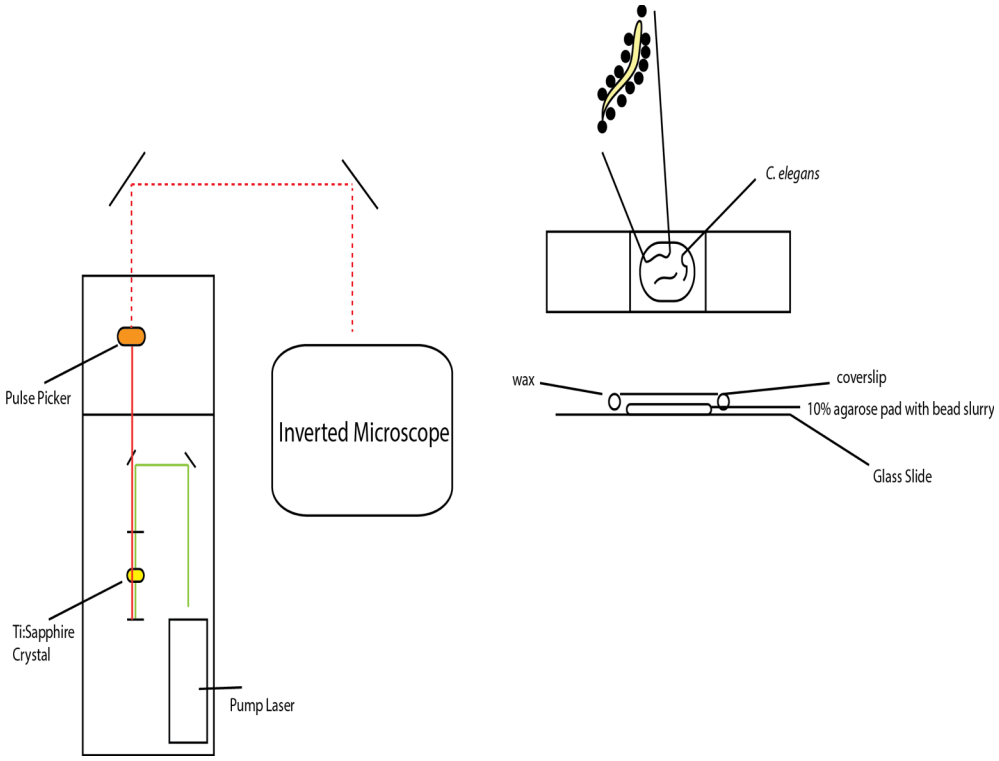

Figure 2.1 Schematic of the Laser Axotomy Protocol

Left: Generation of infrared pulsed laser is by pumping a Ti:Sapphire crystal with a green laser. Once the infrared beam is generated, it is shunted to a pulse picker. This is then diverted into the microscope.

Right (Top): C. elegans are immobilized with polystyrene beads and affixed to a glass slide.

Right (Bottom): A sandwich slide is made in which a 10% agarose pad with a slurry of polystyrene beads is placed on a glass slide. C. elegans are placed in the bead slurry and a coverslip is placed on top. The coverslip is held in place by a mixture of paraffin wax and petroleum jelly.

2.3 Filopodial Dynamics:

Filopodia were quantified at 1-hour, 3-hour, and 5-hour time points and imaged on a Nikon inverted microscope at 60X, as detailed above. Filopodia were defined as novel finger-like growths appearing from either the cell body or the cut site. The first appearance of novel filopodia was recorded at 1 or 3 hours post-injury and quantified. Filopodia were counted at 1, 3, and 5 hours post-injury and dynamics were analyzed over time.

2.4 Drug Treatments in *C. elegans*

For all drug treatments, the drug was dissolved in NGM agar plates and animals were cultured on them for 24 hours before and 24 hours after injury. Thiamet G (Cayman Chemical), to inhibit the O-GlcNAcase was dissolved in 100% EtOH and used at a concentration of 2μM. ST045849 (TimTec), to inhibit the O-GlcNAc Transferase, was dissolved in DMSO and used at a concentration of 50μM. Rapamycin (LC Laboratories), to inhibit mTOR, was dissolved in DMSO and used at a concentration of 100μM, as in Byrne et al., 2014. Glucose (Sigma) at 1, 10, and 100mM and phloretin at 1mM (Cayman Chemical), to inhibit glucose transporters, were dissolved in NGM Buffer. 2-deoxy-D-glucose (DOG) was dissolved in NGM buffer and used at a concentration of 5 and 10mM. The calcium chelator EGTA was used at a concentration of 7.5mM.

2.5 *In vivo* Calcium Imaging:

Calcium imaging was conducted by using *C. elegans* with the calcium-responsive genetically-encoded indicator GCaMP3 expressed specifically in the mechanosensory neurons under the *mec-4* promoter (Sun et al., 2014). GCaMP is a modified GFP with calmodulin, enabling GFP fluorescence as a function of calcium binding to calmodulin. In addition, this construct is then linked to an mCherry tag by an SL2 linker to enable ratiometric calcium imaging. This strain was crossed into *ogt-1* mutants for analysis of calcium dynamics.

For calcium imaging experiments, *C. elegans* were placed on 4% agarose pads with 0.2% tetramisole, an acetylcholine receptor agonist which paralyzes the muscles to prevent movement (Sun et al., 2014). The femtosecond laser was calibrated to produce 25nJ pulses and each injury consisted of three 0.5 second exposures. The ALM neuron was identified and an axonal cut site was determined 20 micrometers from the cell body. A timelapse movie consisting of 30 seconds before cutting and 5 minutes after cutting was recorded in both green and red channels simultaneously by taking the fluorescent signal, dividing it into red and green counterparts, and diverting this signal to independent regions of a CCD camera. Analysis was achieved by taking the ratio of green to red as follows:

(1) Relative Calcium Signal = [Green – Green Background]/[Red – Red Background]

Signals were then normalized to the starting timepoint and graphs generated with Matlab as changes compared to starting baseline over time.

2.6 Western Blotting in whole *C. elegans* lysates

To assess protein O-GlcNAc levels, 200 young adult worms of each genotype were isolated by rinsing the agar plates with M9 buffer and washing and pelleting the animals three times by spinning down at 1,000 xg for 5 minutes. Animals were resuspended in 40 uL of Lysis Buffer (20 mM Tris-Cl, 137 mM NaCl, 10% glycerol, 1% Triton X-100 and 1X protease and phosphatase inhibitor cocktail (AbCam)) and sonicated using maximum power output (10 second sonication, 30 second off – repeated 3 times). The lysate was then cleared by centrifugation at 15,000 xg for 20 minutes.

Samples were mixed with 2X or 6X Laemmli Buffer and 1X DTT and heated at 95°C for 10 minutes. Western blotting was conducted by running 16 microliters of sample and 5 microliters of ladder (Chameleon 800 Li-COR) on a 2-10% gel (NuPage) with 1X MOPS running buffer (BioRad) at 200V for 1 hour. Proteins were transferred to a low-fluorescence PVDF membrane using 1X Transfer buffer with Methanol at 35V for 1 hour. The membrane was blocked in blocking buffer in TBS (Odyssey) and then incubated with anti-O-GlcNAc (RL2 – EMD Millipore) and anti-beta-tubulin overnight at 4°C. A combination of anti-mouse (Green – 700nm) and anti-rabbit (Red – 800nm) infrared secondary antibodies were used for detection with the Licor Odyssey detector.

An infrared ladder was used to assess and verify protein size (LiCOR). Densitometry was conducted with Licor ImageStudio Lite (Li-COR).

2.7 Mechanosensory Neuron-Specific RNAi Feeding

To assess the function of certain genes, an RNAi feeding protocol was developed based in part off of a previous protocol(Calixto et al., 2010). Bacteria from both the Ahringer and Vidal libraries were used. Colonies were streaked out on bacterial agar plates containing carbenicillin (100μg/mL) and grown at 37°C overnight. The next day, colonies were selected and grown in 6 mL of LB with carbenicillin (100μg/mL) overnight at 37°C. From this subculture, 200μL was spread onto NGM agar plates containing carbenicillin (100μg/mL) and 2 mM IPTG. Plates were dried and incubated at room temperature for two days in the dark under aluminum foil to protect the IPTG from degradation.

For mechanosensory neuron specific RNAi gene knockdown, TU3568 (*sid-1*(pk3321) *him-5*(e1490) V; *lin-15B*(n744) X; uIs71 [(pCFJ90) p*myo-2*::mCherry + p*mec-18*::sid-1]) was employed (Calixto et al., 2010). This strain has RNAi sensitivity specifically in the mechanosensory neurons and is RNAi resistant in all other tissues. This is enabled by expressing the double-stranded RNA channel, *sid-1*, in the mechanosensory neurons but mutating this channel in all other tissues (Calixto et al., 2010). We validated this approach in several ways. First, RNAi against GFP in the mechanosensory neurons significantly reduced the signal. Secondly, we treated these

worms with RNAi against targets that are known embryonic lethal or have developmental defects that prevent reaching to adulthood (*daf-15, hmgr-1*, and *itr-1* among others). In any case, we did not see any embryonic lethality or developmental defect (data not shown). TU3568 was crossed into both the *ogt-1* and *oga-1* mutant backgrounds. Six to ten gravid adults were bleached and embryos were allowed to hatch and crawl onto RNAi-bacteria plates. Once the F1 generation reached adulthood, 30 gravid adults were picked onto fresh plates and allowed to lay eggs for 3-4 hours. The day 1 adults of the F2 generation were then analyzed in our regeneration assay as detailed above.

2.8 GSK-3 Overexpression Studies

GSK-3 is a known regulator of axon regeneration and is also influenced by O-GlcNAcylation. To assess the impact of GSK-3 on axon regeneration in the *ogt-1* mutant, KN131 (huIs24 [p*hsp-16.2*::*gsk-3*; *gpa-15*::gfp; *dpy-20*(+)]; *mec-7*::GFP) was crossed into *ogt-1* (ok1474) mutants. This strain has the *gsk-3* gene under the control of the heat-shock *hsp-16.2* promoter (Korswagen et al., 2002). Axotomies were performed as detailed in the axon regeneration protocol. After axotomy, nematodes were either placed at 30°C for 2 hours to induce *gsk-3* expression and then returned to 20°C or kept at 20°C. Regeneration was examined 24 hours after injury.

2.9 DAF-16 Subcellular Localization

To determine if DAF-16 subcellular localization was influenced by O-GlcNAc status, nuclear/cytoplasmic localization of DAF-16 was determined by crossing CF1139

daf-16(mu86); muIs61 [(pKL78) *daf-16*::GFP + *rol-6*(su1006)] with *oga-1* mutants (Lin et al., 2001). GFP localization was observed at the young adult stage by placing animals on 2% agar pads with 0.1% tetramisole for immobilization. Images were taken with a Nikon 20X objective. Animals were analyzed by examining the localization of the GFP signal in intestinal cells as either primarily nuclear or cytoplasmic. As a positive control to ensure DAF-16 can translocate into the nucleus, animals were heat-shocked at 37°C for 15 minutes to induce nuclear localization of DAF-16::GFP.

2.10 Oxidative Stress Imaging

Imaging of oxidative stress using the mitoROGFP sensor was performed with a Zeiss LSM 700 Laser Scanning Confocal Microscope (Melentijevic et al., 2017). mitoROGFP is a redox-sensitive GFP with cysteines placed at amino acids 147 and 204. These cysteines undergo reversible reduction/oxidation which in turn alters the ability of the molecule to be excited at either around 400nm or around 480nm. Oxidation of these cysteines increases excitation at 400nm, while reduction enhances 480nm excitation. A ratio of the emission at around 510nm between the two excitation wavelengths provides a relative oxidative status of the cellular environment. Uncut controls or 3 hours post cut *C. elegans* were mounted on 8% agarose pads and immobilized with a bead slurry as described above. Sequential line scanning was performed with 1.5% laser intensity and 450 gain. Ratiometric imaging was performed by dividing mean emission intensity at 518 nm resulting from 405 nm excitation to that resulting from 488 nm excitation after background subtraction using Image J. Representative images were created using the

ImageJ RatioPlus plugin and assigning pixel values to a LUT chart in order to visualize oxidative status of the mitochondria in the cell body.

2.11 Mitochondrial Tracking

Imaging dynamics of mitochondria was performed by crossing NM3627 jsIs1073 [p*mec-7*::TagRFP-mito::CB*unc-119*]; jsIs821 [p*mec-7*::GFP::*rab-3*; *unc-119*] with *ogt-1* and *oga-1* mutants (Kumar et al., 2010). Axons were cut as above but 60 micrometers from the cell body. Reimaging occurred as above with a five-minute time-lapse in one Z-plane at one frame per second. Kymographs and data analysis were conducted with Kymolyzer (Pekkurnaz et al., 2014). In this program, a line in the X/Y plane is chosen corresponding to the axon. In our studies, we chose the 60 micrometers before the axonal injury immediately adjacent to the neuronal cell body. This was to normalize axon length and width as much as possible, as regenerating processes can be thinner and exhibit branched complexity that make it difficult to trace a line. Once chosen, a kymograph is made by taking the line selected in X/Y, redrawing it to a straight line in X, and taking the time component and placing it in the Y direction. Thus, a straight line with constant Y is interpreted as no movement whereas changes in Y are interpreted as movement. Each particle was individually traced by hand and total length travelled, speed (micrometers/sec), and percent of time in motion were examined.

2.12 Axon Regeneration in Mouse Cortical Neurons *in vitro*

All mouse experiments and culture preparation were conducted in the laboratory of Zhigang He at Harvard University. Animals were cared for according to the standards set by the Harvard University Institutional Animal Care and Use Committee (IACUC) (IACUC #18-04-3670R). Mouse cortical neurons were isolated by obtaining timed pregnant C57BL/6 mice from Charles River Labs. Embryonic day 18 neuronal cultures were isolated by euthanization of the pregnant female via CO2 and rapid cervical dislocation. The embryos were then removed and isolated into a dish. The head of each embryo was rapidly decapitated, the skull removed, and the cortex isolated. Neuronal cells were then isolated by both mechanical and chemical means. Neurons were plated at a density of 150,000 per well in 6 cm dishes on glass coverslips coated in laminin. Neurons were cultured with neurobasal media supplemented with B27 and glutamine, changed every other day, and allowed to mature at 37°C for seven days in culture. Cultures were transported to Boston University in temperature controlled chambers in under 20 minutes the day before axotomy experiments.

Following maturation, neuronal cultures were treated with either DMSO or 2 μM of ST045849 (OGT inhibitor) for 12 hours. Neuronal medium was then changed to Hibernate Low Fluorescence Media supplemented with B27, glutamine, and the corresponding drug. Neurons were placed in a temperature-controlled chamber on a Nikon Ti-2000 inverted fluorescent microscope and imaged using a Nikon 60X objective. Axons were cut with the same laser system mentioned above but with a higher pulse rate

of 1Mhz. Axons were cut 60um away from the cell soma and followed for 6 hours post-injury. The percent of neurons displaying a growth cone by 6 hours were measured, as well as axonal outgrowth.

2.13 Optic Nerve Crush and Axon Regeneration in Mice *in vivo*

All procedures and anesthetics were approved by Harvard University Institutional Animal Care and Use Committee (IACUC) (IACUC #18-04-3670R). One month old male 10X backcrossed OGT floxed mice, B6.129-Ogt tm1Gwh/J, were used for the optic nerve injury and regeneration analysis. Optic nerves were injected with either Cre recombinase (n=6) or vehicle control (n=6). Expression was induced for 2 weeks. Optic nerves were crushed with forceps. After 2 weeks, the axonal tracer CTB-555 was injected and 2 days later retinas and optic nerves were dissected and isolated. Whole mount staining of the retina and optic nerve was performed for analysis of the axonal regeneration and the retinal ganglion cell survival.

CHAPTER THREE

Results

3.1 The Influence of O-GlcNAc on Axon Regeneration in *Caenorhabditis elegans*

To assess the role of O-GlcNAc on axon regeneration in *C. elegans*, we utilized mutants with large deletions in the coding regions of the O-GlcNAc Transferase (OGT) and O-GlcNAcase (OGA) genes. As with other organisms, *C. elegans* only encodes one gene for each enzyme. These mutants were obtained by large-scale mutagenesis during the *C. elegans* Gene Knockout Project. The *ogt-1* (ok1474) mutant has a 1300bp deletion and is a functional null mutant. The *oga-1* (ok1207) mutant is a 1700bp deletion resulting in a removal of exons 3-7, deleting the entire catalytic domain and resulting in a functional null mutant. We confirmed these mutants functionally by western blotting against O-GlcNAc. Accordingly, *ogt-1* mutants display no detectable O-GlcNAcylation whereas *oga-1* mutants display hyper-O-GlcNAcylation (Figure 3.1).

The mechanosensory neurons of *C. elegans* are a classic model of regeneration due to their simple morphology and proximity to the surface, which greatly facilitates laser axotomy. To visualize these neurons, we crossed the *ogt-1* and *oga-1* mutants into the *zdis5* background, which encodes a GFP under the mechanosensory-specific *mec*-4 promoter. We then took day 1 adults and

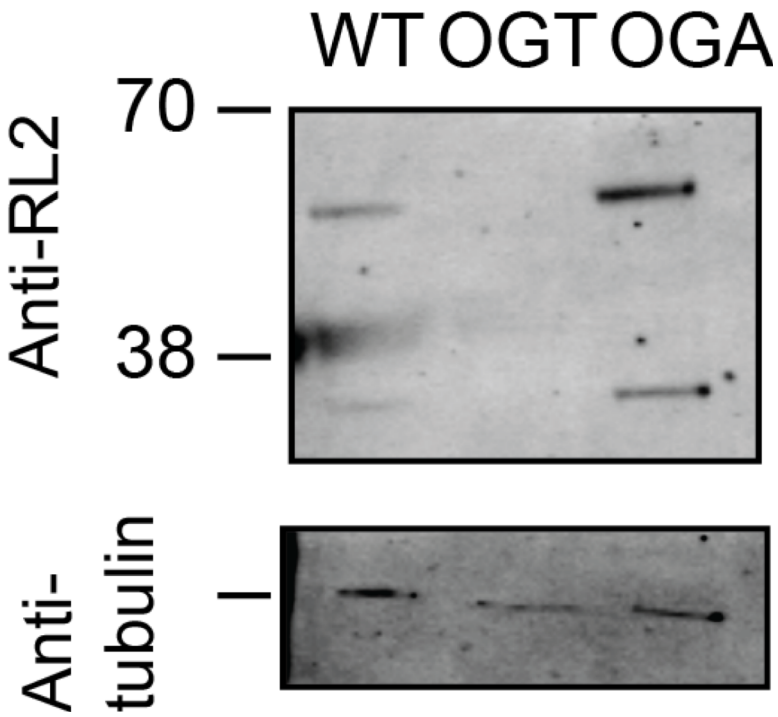

Figure 3.1 Protein O-GlcNAc Levels are Altered in O-GlcNAc Mutants

Representative western blot of O-GlcNAc levels in wildtype and O-GlcNAc mutant whole worm lysates. Anti-RL2 ant antibody primarily detects two O-GlcNAcylated nucleoporins. Tubulin was used as a loading control.

examined their regenerative growth 24 hours after injury of the Anterior Lateral Microtubule (ALM) neuron. Surprisingly, both *ogt-1*

and *oga-1* mutants displayed enhanced regeneration with ~70% and ~40% regrowth above wildtypes, respectively (Figure 3.2). In addition, we examined a different neuron to confirm our findings. Examining the Posterior Lateral Microtubule (PLM) neuron also revealed that both *ogt-1* and *oga-1* mutants can enhance regeneration, although in this case the *oga-1* mutant had greater regenerative potential than the *ogt-1* mutant (Figure 3.2).

3.1.2. O-GlcNAc Acts Cell Intrinsically to Enhance Axon Regeneration

To assess whether the effect of O-GlcNAc on axon regeneration is cell-intrinsic or extrinsic, we utilized a mechanosensory neuron-specific RNAi strain (TU3568) which has the *sid-1* dsRNA channel knocked out in all cells and then reintroduced specifically in the mechanosensory neurons under the *mec-18* promoter. This allows for neuron-specific knockdown of target genes without influencing other tissues. We cultured *C. elegans* on *ogt-1* or *oga-1* RNAi producing bacteria for two generations and then examined 24-hour regenerative growth. Knockdown of both *ogt-1* and *oga-1* specifically in the mechanosensory neurons significantly enhanced axon regeneration in the ALM (Figure 3.3). This suggests that the effect of O-GlcNAc on regeneration is cell-intrinsic.

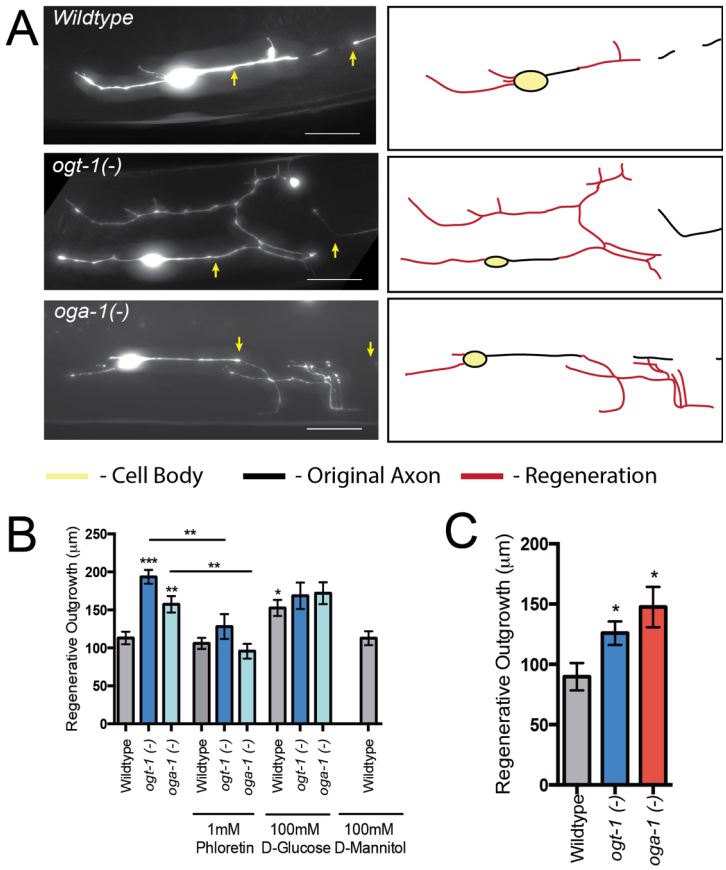

Figure 3.2 O-GlcNAc Mutants Have Enhanced Axon Regeneration

A - Representative images of axon regeneration in the ALM neuron 24 hours after laser axotomy in wildtype and O-GlcNAc mutants. Scale bar: 20 micrometers.

B - Average regenerative outgrowth of ALM neuron 24 hours after injury for wildtype and O-GlcNAc mutants with and without treatment of a glucose transport inhibitor (phloretin), D-glucose, or D-mannitol.

C - Average regenerative outgrowth of PLM neuron 24 hours after injury for wildtype and O-GlcNAc mutants.

Shown is mean ± s.e.m. One-way ANOVA ***p<0.001, **p<0.01, *p<0.05. Stars compare groups to wildtype control except for brackets that indicate specific comparisons.

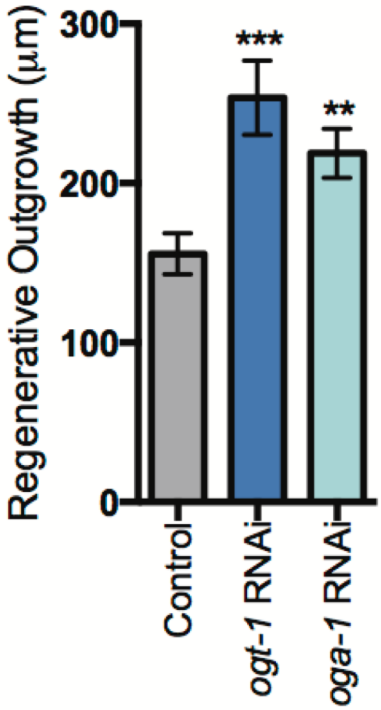

Figure 3.3 O-GlcNAc acts Cell Intrinsically to Enhance Regeneration

Average regenerative outgrowth 24 hours after injury with RNAi knockdown of *ogt-1* and *oga-1* in the mechanosensory neurons. Shown is mean ± s.e.m. One-way ANOVA ***p<0.001, **p<0.01

3.1.3. O-GlcNAc Modifying Small Molecule Inhibitors Can Enhance Axon Regeneration

We then determined whether pharmacological intervention targeting the O-GlcNAc enzymes could also enhance axon regeneration. To inhibit the OGT, we treated *C. elegans* with 50μM ST045849. This inhibitor was discovered through high-throughput chemical screening and is proposed to inhibit the OGT by binding to the active site. Treatment of *C. elegans* with 50μM ST045849 for 24 hours produced a significant decrease in O-GlcNAc levels, as detected by western blotting (Figure 3.4, western not shown). Treating *C. elegans* with ST045849 for 24 hours before injury and 24 hours after injury resulted in enhanced regeneration compared to DMSO treated controls (Figure 3.4). To inhibit the OGA, we utilized Thiamet G, a highly characterized inhibitor which resembles a glucosamine moiety to inhibit the active site of the OGA. Treatment of *C. elegans* for 24 hours with 2μM Thiamet G resulted in enhanced O-GlcNAc levels (Figure 3.4). In addition, treating *C. elegans* for 24 hours before and after injury resulted in significantly enhanced regeneration compared to EtOH treated controls (Figure 3.4). The results above suggest that modulation of O-GlcNAc levels toward one extreme or the other can significantly enhance axon regeneration in a neuron-intrinsic manner.

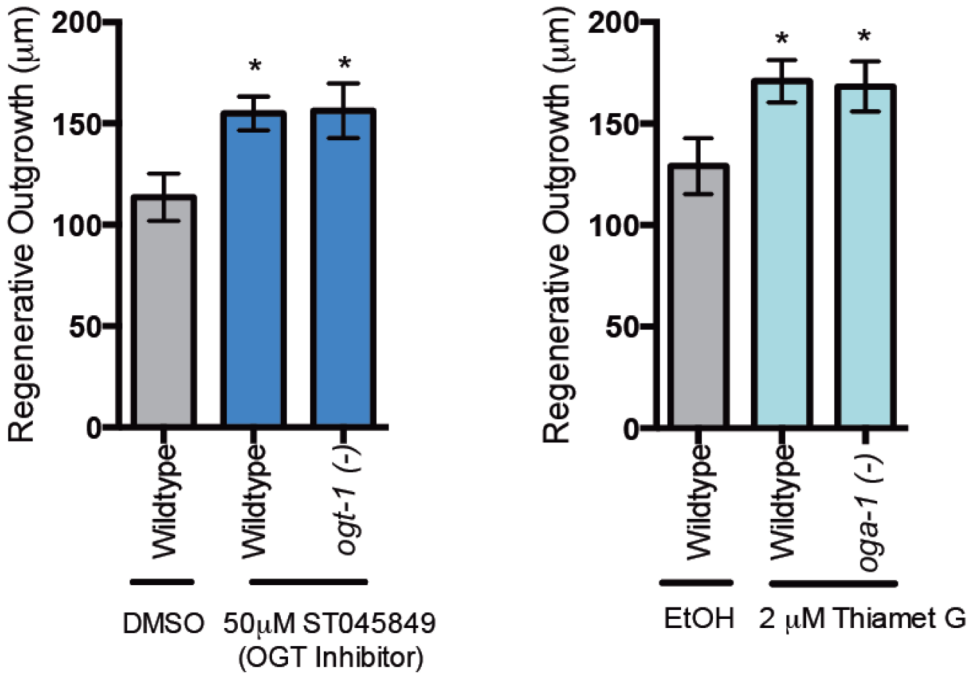

Figure 3.4 O-GlcNAc Small-Molecule Inhibitors Enhance Regeneration

(Left) Average regenerative outgrowth 24 hours after injury of wildtype or *ogt-1* mutants with and without the OGT inhibitor (ST045849).

(Right) Average regenerative outgrowth 24 hours after injury of wildtype or *oga-1* with and without the OGA inhibitor (Thiamet G).

3.2 O-GlcNAc Acts at a Late Stage of Axon Regeneration

Axon regeneration involves the resealing of the membrane, initiation of a growth cone, and axon extension. These events occur at distinct times in *C. elegans* with resealing and component degradation occurring within the first few hours, a growth cone forms between 3-5 hours, and axon extension occurs between 6-24 hours. We conducted time-lapse analysis of growth in *ogt-1* and *oga-1* mutants and examined regrowth at 1, 3, 5, 12, and 24 hours. Interestingly, axon regrowth in both mutants was indistinguishable from wildtypes from 0 to 12 hours post injury. However, between 12 and 24 hours post injury, regeneration of both *ogt-1* and *oga-1* was enhanced above wildtypes suggesting that both mutants act at a later stage of axon regeneration (Figure 3.5).

We also examined filopodial dynamics, which are actin-based early extensions. Previous work has identified these transient structures extending from both the site of damage and the cell body preceding axonal extension (Sun et al., 2014). We found that neither the *ogt-1* or *oga-1* mutants displayed differences compared to wildtype in the time to first filopodial extension when examining 1 and 3 hour timepoints. By 1 hour post injury, roughly 40% of neurons display filopodia. The remaining 60% display filopodia by 3 hours post injury. We then examined the dynamics of filopodia by measuring the number of them in the same neuron between 1, 3, and 5 hours.

As we have seen previously, filopodial number increases with time in wildtypes. We see that *ogt-1* and *oga-1* mutants follow a similar trend with the exception that *oga-1* mutants display significantly fewer filopodia at the 5-hour time point (Figure 3.5).

To confirm that O-GlcNAc mutants act at a late-stage of regeneration, we examined the relationship between DLK-1, an early effector of regeneration, and the O-GlcNAc mutants. DLK-1 is a Dual Leucine Zipper Kinase which acts in the conserved p38 MAPK pathway to enable regeneration through a multitude of mechanisms. As DLK-1 is a known early modulator of axon regeneration (Nix et al., 2014), we hypothesized that mutations in *dlk-1* should knockdown both *ogt-1* and *oga-1* regeneration. Mutations in *dlk-1* modestly reduce wildtype axon regeneration 24 hours after injury in accordance with what our lab and others have observed (Chung et al., 2016). Further, mutations in *dlk-1* significantly suppressed both *ogt-1* and *oga-1* mutant regeneration in accordance with *dlk-1* being upstream temporally (Figure 3.6).

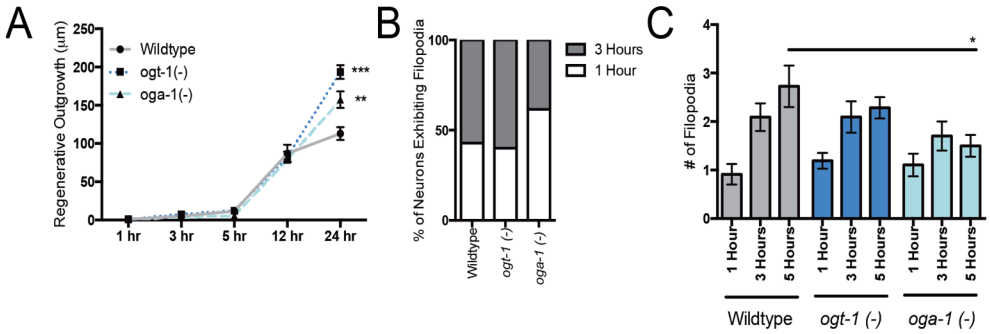

Figure 3.5 Dynamics of Axonal Outgrowth in O-GlcNAc mutants

A. Time-lapse of axon regeneration 1hr, 3hr, 5hr, 12hr, and 24hr after injury.

B. Percent of neurons displaying filopodia at 1 hr and 3 hr post-injury.

C. Number of filopodia over time between wildtype, *ogt-1*, and *oga-1* mutants.

Shown is mean ± s.e.m. One-way ANOVA ***p<0.001, **p<0.01, *p<0.05. Stars compare groups to wildtype control except for brackets that indicate specific comparisons.

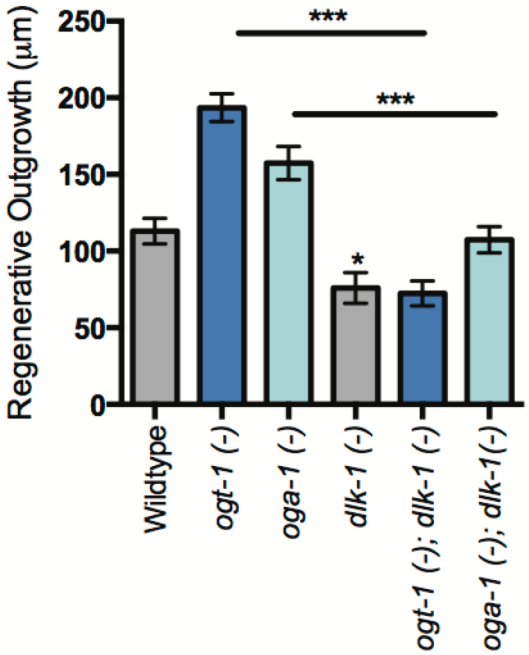

Figure 3.6 DLK-1 Loss-of-Function Inhibits O-GlcNAc Mutant Regeneration

Genetic epistasis analysis of 24 hour regeneration between *dlk-1* mutants and O-GlcNAc mutants. Shown is mean ± s.e.m. One-way ANOVA ***p<0.001, **p<0.01, *p<0.05. Stars compare groups to wildtype control except for brackets that indicate specific comparisons.

3.3 O-GlcNAc is a Nutrient Responsive Post-Translational Modification during Axon Regeneration

The O-GlcNAc modification responds dynamically to changes in glucose as O-GlcNAc synthesis is dependent on glucose metabolism through the hexosamine biosynthetic pathway. We examined whether altering glucose levels in our regeneration assays could influence regeneration. Western blots revealed that 100mM D-glucose supplementation elevated O-GlcNAc levels to an extent similar to what we observed in *oga-1* mutants (Figure 3.7). Treating wildtype animals with 100mM glucose for 24 hours before and after axon injury resulted in a significant increase in axon regeneration (Figure 3.2). Glucose treatment did not further enhance regeneration seen in *ogt-1* and *oga-1* mutants. In addition, treatment of *C. elegans* with 100mM D-mannitol as an osmolarity control had no effect on wildtype regeneration (Figure 3.2). We then inhibited glucose uptake with 1mM phloretin, a dose previously established in *C. elegans*. Treatment with phloretin did not affect wildtype but significantly suppressed both *ogt-1* and *oga-1* mutant regeneration (Figure 3.2). From these results, we conclude that O-GlcNAc is responsive to changes in glucose and that both *ogt-1* and *oga-1* regeneration are dependent on glucose. Mutants lacking O-GlcNAc post translational modifications could be enhancing glucose utilization in compensation for a perceived metabolic deficit and thus require glucose transport and utilization, whereas, *oga-1* mutants require glucose to generate the O-GlcNAc

moiety through the hexosamine biosynthetic pathway and therefore also require glucose transport.

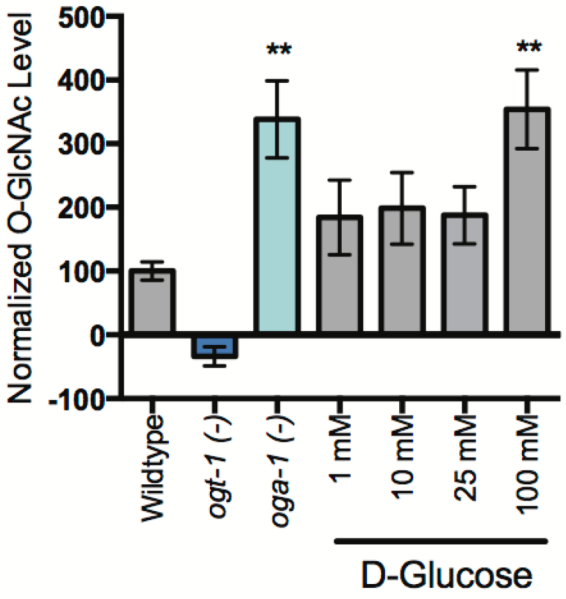

Figure 3.7 O-GlcNAc is a Glucose-Responsive Modification

O-GlcNAc levels as measured by western blotting as in Figure 3.1. O-GlcNAc (RL2 signal) levels normalized to tubulin. 100mM glucose treatment enhances O-GlcNAc levels to an extent comparable with *oga-1* mutants. n=3-5 lysates per condition.

3.4 O-GlcNAc does not act through calcium-dependent mechanisms

Several lines of evidence from mouse studies *in vitro* and *in vivo* have suggested that O-GlcNAc can modify and affect the function of proteins important in calcium signaling (Rengifo et al., 2007). During axon regeneration, calcium signaling is important in nearly all aspects, from membrane resealing to axonal extension (He and Jin, 2016). Proteomics have revealed that the inositol triphosphate receptor (IP3R), which governs the mobilization of calcium stores from the endoplasmic reticulum, and the calcium/calmodulin-dependent kinase (CAMK), an important effector kinase, are O-GlcNAcylated (Erickson et al., 2013; Rengifo et al., 2007). Both of these proteins play an essential role in axon regeneration. Endoplasmic reticulum release of calcium through both the IP3R and the ryanodine receptor, is the primary factors responsible for the enhanced calcium release upon axonal injury and this response is important for regeneration in *C. elegans* (Sun et al., 2014). O-GlcNAcylation of the IP3R in cultured mouse neurons inhibits the channel, whereas lack of O-GlcNAcylation promotes the open state (Rengifo et al., 2007). The sites of the IP3R that are O-GlcNAcylated are conserved in the *C. elegans* gene, *itr-1*. We hypothesized that lack of O-GlcNAcylation, via the *ogt-1* mutant, may enhance regeneration by increasing IP3R activity and calcium release. We generated double mutants between the O-GlcNAc mutants and a partial loss-of-function *itr-1* mutant allele, as the complete

knockout is not viable. Loss of *itr-1* function did not alter *ogt-1* mutant regeneration (Figure 3.8).

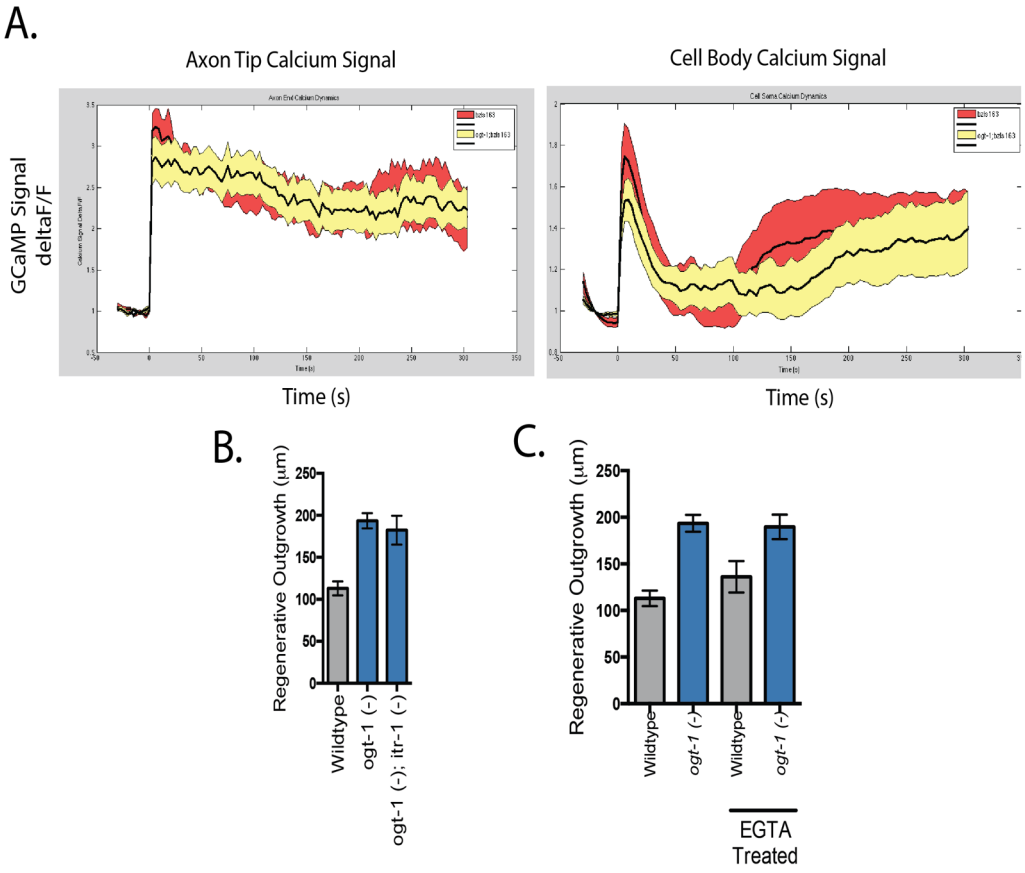

Figure 3.8 Calcium Dynamics are not Responsible for OGT Mutant Regeneration

A. GCaMP calcium signal before and after axonal injury in the axon tip (Left) and the cell body (Right). Red trace is wildtype and Yellow trace is *ogt-1* mutant. Time is 5 minutes.

B. Effect of *itr-1* loss-of-function mutant on 24-hr. regeneration of *ogt-1* mutant.

C. Effect of EGTA treatment on *ogt-1* and wildtype 24-hr. regeneration.

We then examined calcium dynamics during regeneration in the *ogt-1* mutant. Our previous work has revealed that calcium release from the ER makes up a large portion of the calcium signal upon axonal injury (Sun et al., 2014). This elevation in calcium can continue up to five hours post-injury and is important for the regenerative response, as mutants in the ryanodine receptor do not have these calcium dynamics and fail to regenerate to the extent of wildtypes. We utilized GCaMP3.0 to examine these calcium dynamics. Analysis of five minute videos after injury revealed no significant difference in the calcium dynamics between wildtype and *ogt-1* mutants (Figure 3.8). Examining levels up to five hours post-injury also revealed no significant difference (Figure 3.8). This data further suggested a lack of involvement of the ITR-1 and the ER calcium response.

Finally, we inhibited global calcium levels by applying the calcium chelator EGTA to our culture conditions. We found that altering calcium levels during experiments, with calcium in our buffers and NGM plates gave us wide variability. To eliminate this, we treated plates with 7.5mM EGTA for 24 hours before placing *C. elegans* on them. In addition, we used a calcium-free S-buffer to transfer worms during our cutting protocol and supplemented EGTA in the pads used to hold the worms on the microscope. Using this approach, we found that EGTA addition did not affect regenerative outgrowth in *ogt-1* or *oga-1* mutants (Figure 3.8). We concluded from this series of data that O-GlcNAc likely does not act through calcium-dependent mechanisms to enhance axon regeneration.

3.5 O-GlcNAc does not act through cyclic AMP-dependent mechanisms

O-GlcNAc has previously been shown to modulate axon growth in cultured neurons and memory formation in mice through directly modifying the cAMP Responsive Element Binding (CREB) protein (Rexach et al., 2012). CREB is a transcription factor within the cAMP signaling pathway, which is also important for a pro-regenerative response. Elevations in cAMP leads to the activation of Protein Kinase A (*kin-2*) and the activation of the CREB (*crh-1*) transcription factor and other bZip (*cebp-1* and *ets-4*) transcription factors to elevate the transcription of genes which enhance regeneration (Li et al., 2015). To examine whether the cAMP signaling pathway is important for the enhanced regeneration of the O-GlcNAc mutants, we generated double mutants between the O-GlcNAc mutants and the CREB transcription factor, *crh-1*. Loss of *crh-1* function did not affect either *ogt-1* or *oga-1* mutant regeneration (Figure 3.9). Likewise, using a phosphodiesterase (*pde-4*) mutant, which has been previously shown to enhance regeneration by decreasing cAMP degradation, did not have any effect on the regeneration of *ogt-1* or *oga-1* mutants (Figure 3.9). However, *pde-4* single mutants display enhanced regeneration akin to the *ogt-1/oga-1* alleles. This suggests two different scenarios. First, the two signaling pathways act independent from one another, as loss of *crh-1* function had no effect and enhancing the cAMP pathway was not additive, suggesting we have hit a ceiling for regenerative length at the 24-hour time point. Second, that O-GlcNAc and

cAMP pathways are redundant at some unknown level. Given the lack of involvement of the major downstream transcription factor *crh*-1/CREB and calcium dependent pathways which are important for cAMP mediated regeneration, we favor a model in which O-GlcNAc and cAMP signaling have independent effects on regeneration.

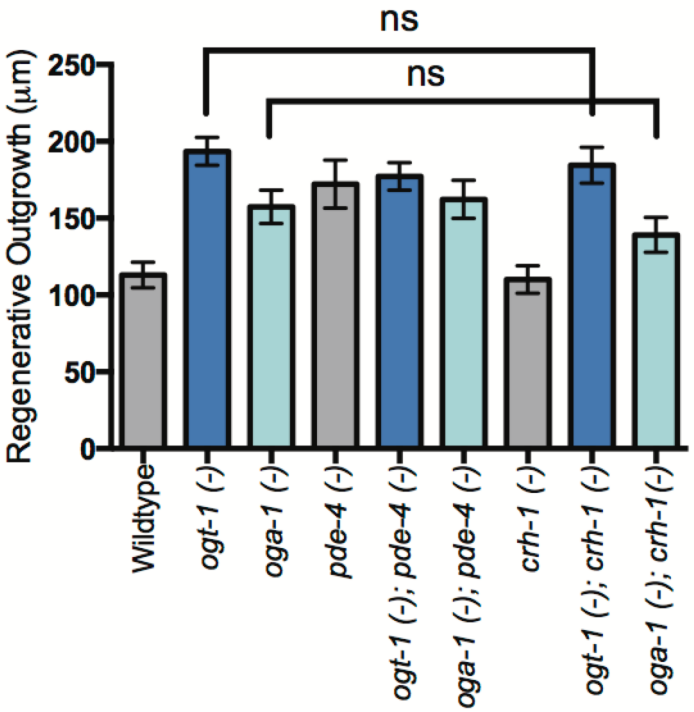

Figure 3.9 Cyclic AMP Pathway is not Essential for O-GlcNAc Mutant Regeneration

Loss of *pde-4* function (enhancing cAMP levels) enhances regeneration but has no effect on *ogt-1* or *oga-1* mutant regeneration. Loss of the downstream transcription factor controlled by cAMP, *crh-1*/CREB, has no impact on O-GlcNAc mutant regeneration. Shown is mean ± s.e.m. One-way ANOVA ns is not significant.

3.6 O-GlcNAc Acts through a Toggle Switch-like Mechanism in the Insulin-Signaling Pathway

Advances in mass spectrometry technology revealed that components of the insulin-signaling pathway in mammals are highly modified by O-GlcNAc (Whelan et al., 2010). Modifications occur at multiple strata of the pathway enabling rapid temporal response to changing intracellular nutrient status. For example, the insulin-receptor substrate (an adapter which interacts with the insulin receptor), the AKT kinase, and the FOXO transcription factor have all been identified as targets of O-GlcNAc (Whelan et al., 2010). In general, addition of O-GlcNAc results in the inhibition of insulin-signaling. Genetic epistasis analysis has also found that components of the insulin-signaling pathway interact with O-GlcNAc to govern lifespan, metabolism, and the stress response in *C. elegans* (Love et al., 2010; Rahman et al., 2010). We performed a large genetic epistasis screen by generating double mutants between components of the insulin-signaling pathway and O-GlcNAc enzymes. We examined the insulin receptor (*daf-2* e1370), the phosphotide inositide kinase (*age-1*), the AGC kinases (*akt-1* ok525, *akt-2* ok393, and *sgk-1*), the FOXO transcription factor (*daf-16* mu86). The results revealed the possibility of a toggle-like switch mechanism that governs regeneration in the O-GlcNAc mutants.

3.7 Lack of O-GlcNAc Enhances Axon Regeneration through AKT-1

Examining the insulin-signaling pathway revealed that the enhanced regeneration of *ogt-1* mutants displayed a complex interaction (Figure 3.10). Loss-of-function of *ogt-1;daf-2* resulted in regeneration comparable to either single mutant, suggesting they act within a similar pathway. Likewise double mutants between *ogt-1;age-1* also had regeneration similar to either *ogt-1* or *age-1* single mutants. Interestingly, loss of *akt-1* function specifically inhibited *ogt-1* regeneration to an extent comparable to wildtype. Mutations in *akt-2* had no effect on *ogt-1* regeneration. This suggests that *ogt-1* mutants act specifically through *akt-1* activation to enhance axon regeneration. In accordance with this, loss of *daf-16* function had no effect on *ogt-1* mutant regeneration (Figure 3.10).

3.8 ARK-1 is Genetically Upstream of AKT-1 during Regeneration of OGT mutants

Canonically, the PI3K (*age-1*) is an upstream activator of AKT-1 in the insulin-signaling pathway. However, we clearly see that *ogt-1* mutant regeneration is dependent on AKT-1 but independent of AGE-1 suggesting there is a different upstream activator (Figure 3.10). A known alternative upstream activator is the activated Cdc42 non-receptor tyrosine kinase (ACK).

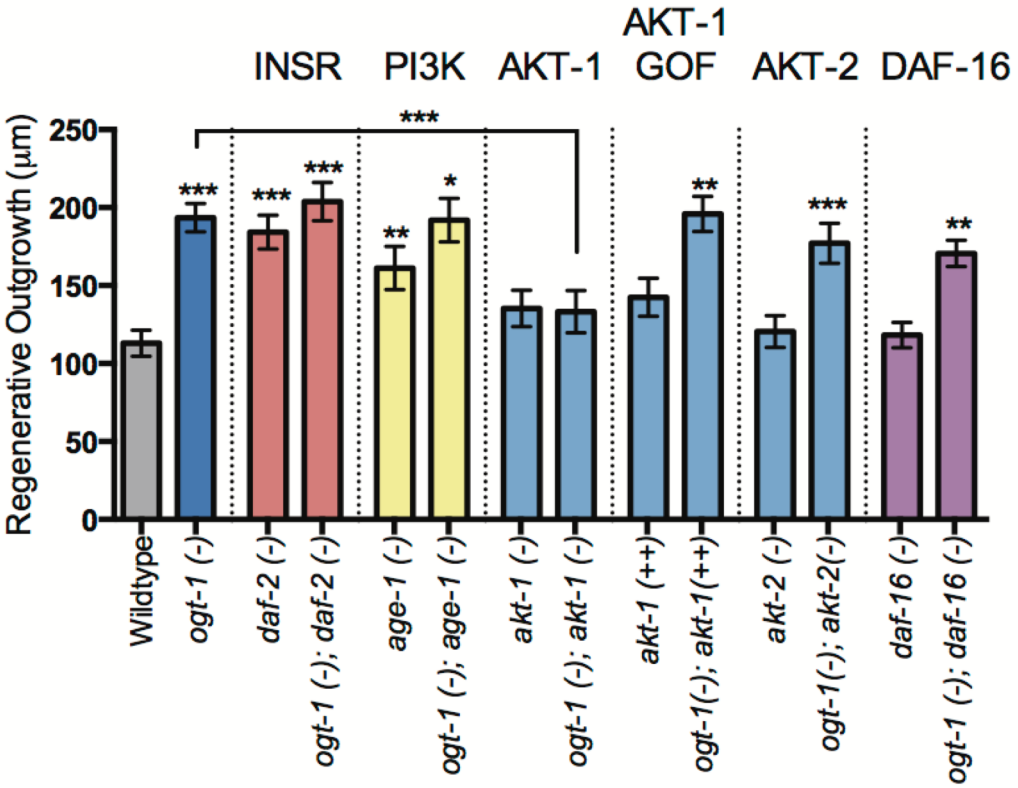

Figure 3.10 Insulin-Signaling Pathway Epistasis Analysis with *ogt-1* Mutants.

Loss-of-function mutants in *daf-2, age-1, akt-1, akt-2*, and *daf-16* in combination with the *ogt-1* mutant allele. (-) indicates loss-of-function allele and (++) indicates gain-of-function (gof) allele. Only loss-of-function in *akt-1* suppressed *ogt-1* mutant regeneration. Shown is mean ± s.e.m. One-way ANOVA ***$p<0.001$, **$p<0.01$, *$p<0.05$. Stars compare groups to wildtype control except for brackets that indicate specific comparisons.

Homology searches in *C. elegans* revealed that the ACK ortholog is *ark-1* with ~88% similarity. The mechanism of activation in mammalian systems occurs when ACK is activated through growth factor receptors or stress-induced signals and leads to the phosphorylation of tyrosine 186 of AKT. This then allows AKT to be recruited to the membrane for further activation. To examine if ACK/ARK-1 is involved in *ogt-1* mediated regeneration, we generated double mutants between *ogt-1;ark-1*. Interestingly, *ogt-1;ark-1* double mutants had significantly reduced outgrowth compared to ogt-1 mutants alone (Figure 3.11).

To determine whether ARK-1 lies upstream or downstream of AKT-1, we utilized an AKT-1 gain-of-function allele and restored AKT-1 activity in *ogt-1;ark-1* double mutants. The restoration of AKT-1 activity rescued the regeneration defect observed in *ogt-1;ark-1* mutants suggesting that AKT-1 is either downstream or acts in parallel to ARK-1 (Figure 3.11). To confirm that AKT-1 is downstream, we generated *ogt-1;ark-1;akt-1* loss-of-function mutants. Loss of both ARK-1 and AKT-1 did not further reduce the regeneration of *ogt-1;ark-1* mutants suggesting that ARK-1 and AKT-1 act within the same pathway and that ARK-1 is genetically upstream of AKT-1 (Figure 3.11).

3.9 Identification of Factors Downstream of AKT-1 that Mediate the Enhanced Regeneration of *ogt-1* mutants

Several signaling pathways have been identified that are downstream of AKT and act on axonal growth or regeneration. A prominent example is the mTOR signaling

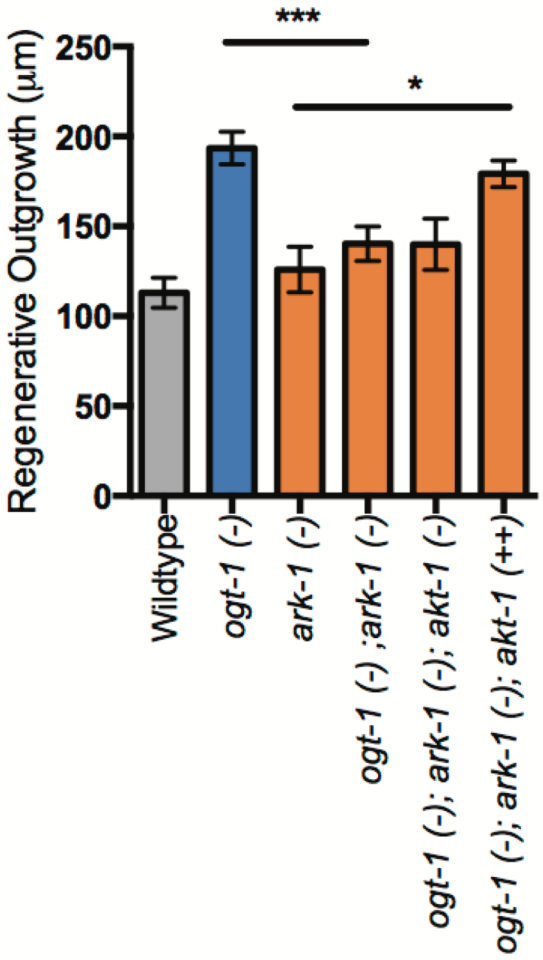

Figure 3.11 ARK-1 is Genetically Upstream of AKT-1 in *ogt-1* Mutant Regeneration

Genetic epistasis analysis between *ark-1, akt-1* and *ogt-1* mutants. (-) indicates loss-of-function allele and (++) indicates gain-of-function allele. Loss-of-function in *ark-1* suppressed *ogt-1* mutant regeneration. Gain-of-function in *akt-1* restored *ogt-1;akt-1* mutant regeneration. Shown is mean ± s.e.m. One-way ANOVA ***p<0.001, **p<0.01, *p<0.05. Stars compare groups to wildtype control except for brackets that indicate specific comparisons.

pathway, in which AKT can mediate mTOR activation resulting in enhanced regeneration through local protein translation and potentially metabolic means. To examine whether mTOR is important for *ogt-1* mutant regeneration, we treated animals with the mTOR inhibitor rapamycin. Treatment of wildtype animals with rapamycin had no effect on wildtype axon regeneration. As a positive control, treatment of PTEN/*daf-18* mutant animals, which display mTOR-dependent enhanced regeneration, was effectively eliminated with rapamycin treatment. However, we did not observe any decrease in *ogt-1* mutant regeneration upon rapamycin treatment (Figure 3.12). We further tested this by knocking down the regulatory associated protein of mTOR (RAPTOR/*daf-15*). Neuron-specific RNAi against *daf-15* had no effect on *ogt-1* mutant axon regeneration (data not shown). From this, we concluded that the enhanced regeneration of *ogt-1* mutants is independent of mTOR activity.

AKT is known to negatively regulate the glycogen synthase kinase 3 beta (GSK-3β) and many studies have linked GSK-3β to axonal growth and regeneration, although a consensus on whether it provides a positive or negative role remains controversial and may depend on neuronal type (Leibinger et al., 2017). Given that AKT is a negative downstream regulator of GSK-3β, we hypothesized that over-expression of GSK-3β may inhibit regeneration of *ogt-1* mutants. To test this, we utilized a heat-shock inducible *gsk-3* transgenic animal. Heat-shocking for two hours at 30°C after axonal injury was sufficient to significantly reduce 24-hour wildtype axonal regeneration. Performing the same

experiment in the *ogt-1* mutant background resulted in a slight but significant decrease in regeneration with an extent comparable to that seen in the wildtypes (Figure

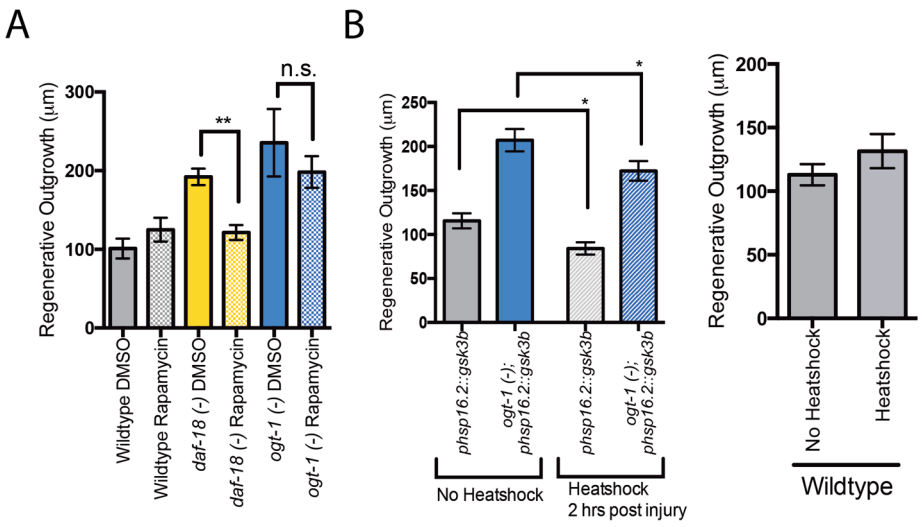

Figure 3.12 mTOR or GSK-3b Signaling is not Responsible for *ogt-1* Mutant Regeneration

A. mTOR inhibitor rapamycin is unable to suppress *ogt-1* mutant regeneration but able to suppress PTEN/*daf-18* regeneration.

B. (Left) Heat-shock inducible *gsk-3* expression mildly suppresses both wildtype and *ogt-1* mutant regeneration. The ratio of enhanced regeneration between wildtype and *ogt-1* remains conserved.

(Right) Heat-shocking has no effect on axon regeneration in wildtype controls without the heat-shock inducible *gsk-3* allele.

Shown is mean ± s.e.m. One-way ANOVA ***p<0.001, **p<0.01, *p<0.05. Stars compare groups to wildtype control except for brackets that indicate specific comparisons.

3.12). However, the regeneration observed in *ogt-1* mutants with *gsk-3* activation was still much higher than those of wildtypes. From this data, we concluded that while *gsk-3* has an effect on axon regeneration, it is independent from that of *ogt-1*.

Lastly, we examined the hypothesis that AKT may be regulating glycolysis. Notably, AKT has many roles in glucose homeostasis, including modulating cellular glucose uptake by acting on the GLUT4 transporter and affecting glycolysis. We examined both of these mechanisms. First, we knocked down every potential glucose transporter with neuron-specific RNAi to determine whether AKT was acting in a similar fashion to that in mammals. Knockdown of *aat-9, glt-1, fgt-1, swt-7, mct-2, mct-4, mct-5, mct-6*, and *ZK829.9* individually failed to inhibit axon regeneration in the *ogt-1* background (Figure 3.13). However, inhibition of all glucose transport pharmacologically with phorletin repressed regeneration suggesting multiple transporters may be acting in parallel.

To test whether glycolysis is involved, we again performed neuronal-specific RNAi against an enzyme important in glycolysis. *C. elegans* encodes multiple redundant genes for most of the glycolytic enzymes, preventing their analysis by RNAi. However, the phosphoglycerate kinase (*pgk-1*) is only encoded for by one gene and, therefore, we conducted a knockdown *of pgk-1* in *ogt-1* mutants. Interestingly, knockdown of *pgk-1* significantly reduced *ogt-1* mutant

regeneration (Figure 3.13). To confirm this, we used a loss-of-function mutant in the phosphofructokinase-1.1 (*pfk-1.1*) shown to be important in neuronal glycolysis in *C. elegans*. While *pfk-1.1* mutants failed to affect axon regeneration in a wildtype background, *pfk-1.1* loss-of-function significantly inhibited *ogt-1* enhanced regeneration (Figure 3.13). Taken together, these data strongly suggest that *ogt-1* mutants enhance regeneration through glycolysis. To further confirm this, we used a competitive inhibitor of glycolysis, 2-deoxy-D-glucose (DOG). Treatment of wildtype worms with either 5mM or 10mM DOG resulted in no effect on wildtype regeneration. However, treatment of *ogt-1* mutants resulted in a dose-dependent decrease in axon regeneration with 10mM being highly effective at inhibiting the enhanced regeneration (Figure 3.13E).

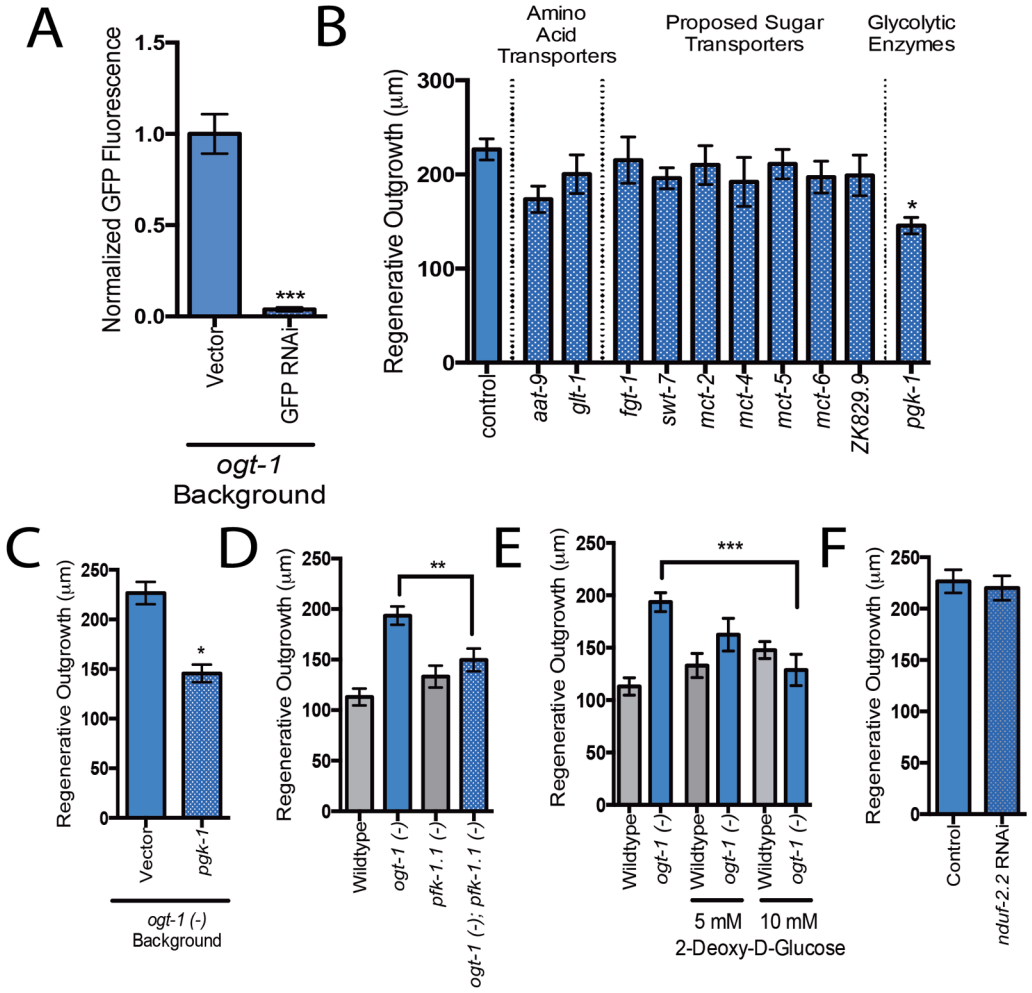

Figure 3.13 Glycolysis is Essential for *ogt-1* Mutant Regeneration

A. RNAi against GFP is able to inhibit GFP expression specifically in mechanosensory neurons.

B. Knockdown of glucose transporters did not affect *ogt-1* mutant regeneration.

C. Mechanosensory neuron-specific RNAi against the glycolytic enzyme phosphoglycerate kinase 1 (*pgk-1*) in the *ogt-1* background.

D. Mutation of phosphofructokinase-1.1 (*pfk-1.1*) in wildtype and *ogt-1* backgrounds.

E. Treatment of wildtype and *ogt-1* mutants with the non-hydrolyzable glucose analog 2-deoxy-D-glucose.

F. Mechanosensory neuron-specific RNAi against the NADH dehydrogenase iron-sulfur protein 2 (*nduf-2.2*) in the *ogt-1* background.

For all: Shown is mean ± s.e.m. One-way ANOVA ***p<0.001, **p<0.01,

To establish whether glycolysis is coupled to or independent of mitochondrial oxidative phosphorylation, we then knocked down an essential NADH dehydrogenase iron-sulfur protein 2 (*nduf-2.2*), a component of the electron-transport chain important for regeneration. Knocking down *nduf-2.2* had no effect on *ogt-1* mutant regeneration suggesting that the enhanced glycolysis is responsible for the regeneration independently of mitochondrial oxidative phosphorylation (Figure 3.13).

3.10 Abundance of O-GlcNAc Acts through the FOXO/DAF-16 transcription factor to enhance regeneration

As the *ogt-1* mutant regeneration was dependent on the insulin-signaling pathway, we wondered if the *oga-1* enhanced regeneration also relied on this pathway. We conducted a genetic epistasis analysis using loss-of-function mutants in the insulin-signaling pathway, as explained above. Unexpectedly, *oga-1;daf-2* mutants reduced *daf-2* regeneration to the extent of *oga-1* mutants (Figure 3.14). Examining the intermediate kinases AGE-1 and AKT-1 revealed no significant differences between double mutants and *oga-1* mutants. However, loss-of-function of the FOXO/DAF-16 transcription factor significantly reduced *oga-1*-dependent regeneration. This data suggested that *oga-1* acts downstream of *daf-2* but upstream of *daf-16* to enhance regeneration. We therefore examined another intermediate kinase, the Serum-Glucocorticoid Kinase 1 (SGK-1). Loss of

SGK-1 function significantly inhibited *oga-1* regeneration to wildtype levels. This suggests that *oga-1* acts at the level of SGK-1 to influence DAF-16 activity (Figure 3.14).

DAF-16 can be shuttled in and out of the nucleus upon deactivation or activation of insulin signaling, respectively. We examined whether O-GlcNAc status affected DAF-16 nuclear localization by examining a DAF-16::GFP-tagged strain in the O-GlcNAc mutant backgrounds. As a positive control, heat-shocking animals at 37°C resulted in the rapid nuclear localization of DAF-16. However, none of the O-GlcNAc mutants produced any difference in nuclear localization of DAF-16 (Figure 3.15). This suggests that *oga-1* mutants do not act on DAF-16 by altering its subcellular localization.

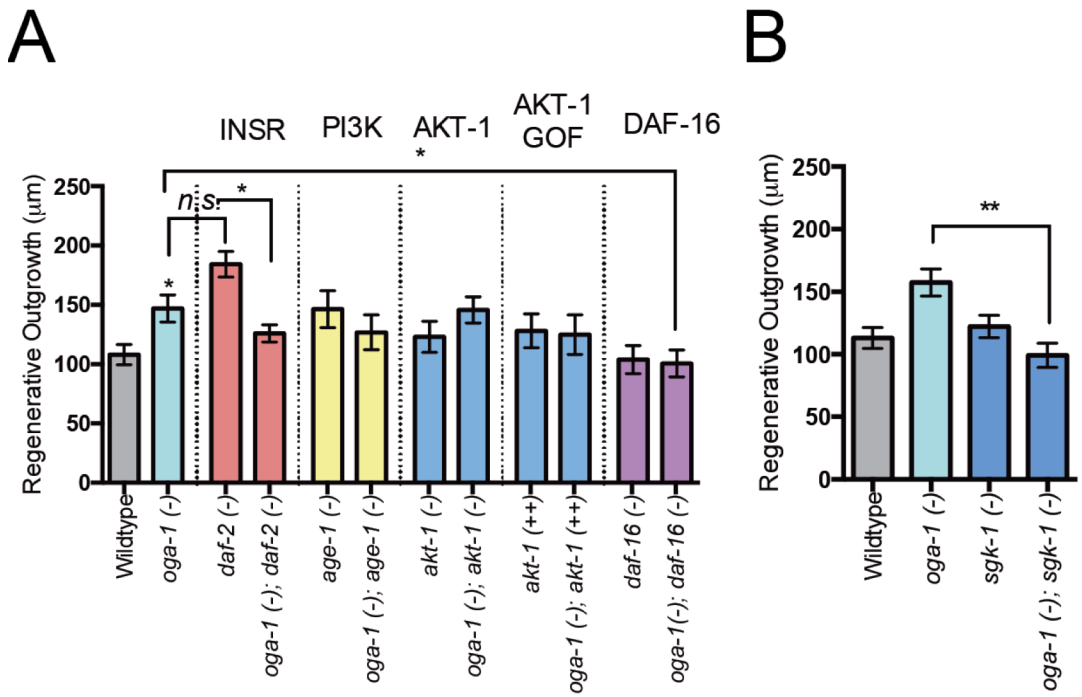

Figure 3.14 Insulin-Signaling Pathway Epistasis Analysis with *oga-1* Mutants.

(Left) Loss-of-function mutants in *daf-2, age-1, akt-1,* and *daf-16* in combination with the *oga-1* mutant allele. (-) indicates loss-of-function allele and (++) indicates gain-of-function allele. *oga-1* mutant allele was able to suppress *daf-2* regeneration whereas *oga-1* regeneration was dependent on *daf-16.*

(Right) Loss of *sgk-1* function suppresses *oga-1* mutant regeneration.
Shown is mean ± s.e.m. One-way ANOVA ***p<0.001, **p<0.01, *p<0.05. Stars compare groups to wildtype control except for brackets that indicate specific comparisons.

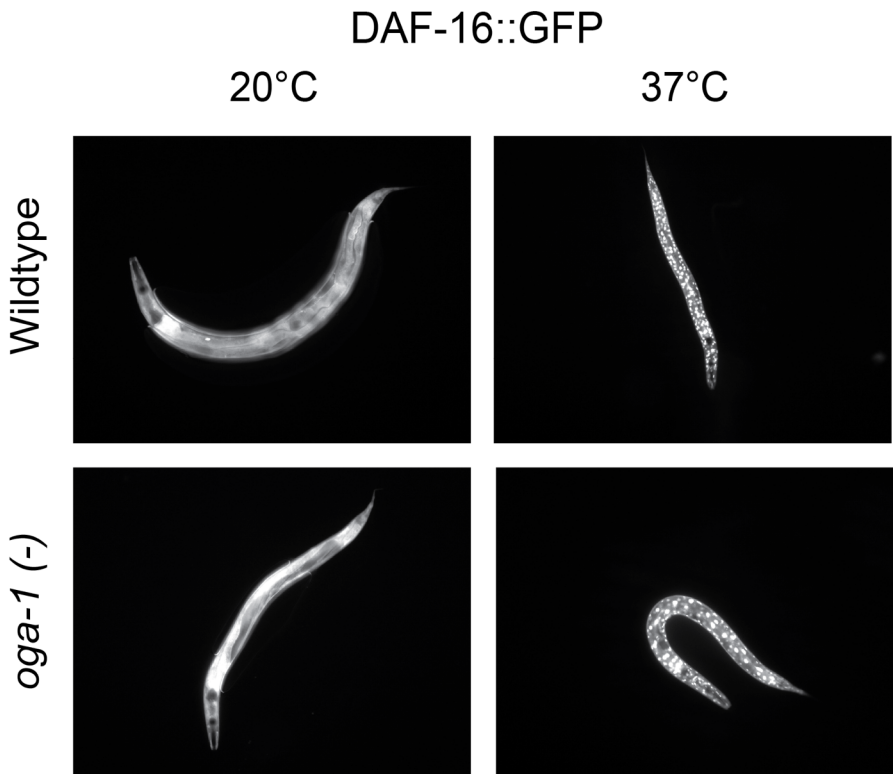

Figure 3.15 *oga-1* Mutants do not have Altered DAF-16 Localization

DAF-16::GFP is mostly cytosolic in *oga-1* mutants suggesting it does not act by altering DAF-16 localization. Heat shocking induces nuclear localization in both wildtypes and mutants as a positive control.

3.11 OGA-1 Mutants Have a Complex Mitochondrial Phenotype

Both O-GlcNAc and DAF-16 have been strongly linked to altering mitochondrial dynamics by invoking mitochondrial oxidative stress pathways and influencing mitochondrial transport. We examined whether *oga-1* mutants had enhanced mitochondrial oxidative stress resistance by using the mitoROGFP oxidative stress sensor. This sensor is a permutated GFP localized to the mitochondrial matrix that produces different ratios of emission depending on oxidative stress status. Before injury, oxidative environments were similar between wildtype and *oga-1* mutants. However, after injury, *oga-1* mutants were able to maintain a reduced environment compared to wildtypes 3 hours post axotomy (Figure 3.16).

Further, we examined mitochondrial locomotion dynamics by tagging mitochondria with RFP and generating five minute kymographs of their movements 24 hours after injury. O-GlcNAc addition has been previously shown to reduce mitochondrial motility by acting on the Milton protein complex. In accordance with this, we also observed that *oga-1* mutants exhibit significantly reduced motility, defined as the percentage of time in motion over a five-minute period (Figure 3.17). Differences in mitochondrial speed and total distance traveled were trending toward a reduced direction but did not reach significance.

Examining the *ogt-1* mutant revealed no differences between wildtype mitochondrial locomotion dynamics (Figure 3.17).

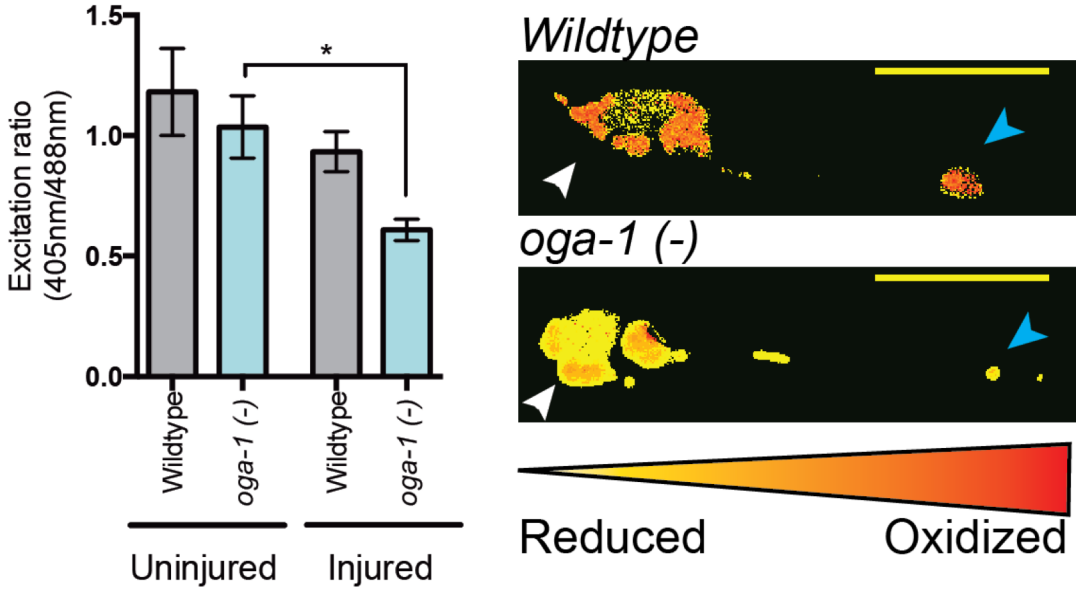

Figure 3.16 *oga-1* Mutants have Reduced Oxidative Stress upon Injury

(Left) mitoROGFP emission ratio changes in oxidative environments. Before injury, oxidative stress remains the same. After injury, *oga-1* mutants maintain a reduced environment.

(Right) Pseudocolored representative images of wildtypes and *oga-1* mutants post injury. Cell body is highlighted with a white arrow, axon cut site with a blue arrow.

Shown is mean ± s.e.m. One-way ANOVA *$p<0.05$. Stars compare groups to wildtype control except for brackets that indicate specific comparisons.

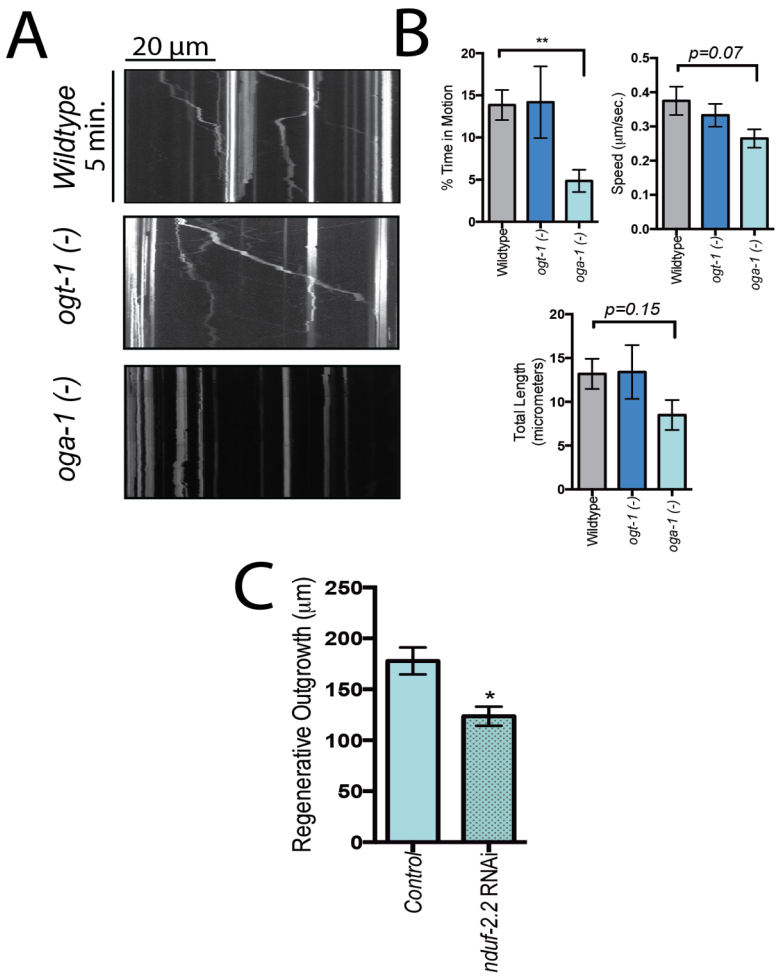

Figure 3.17 *oga-1* Mutants have Altered Mitochondrial Dynamics and Rely on Oxidative Phosphorylation for ATP Synthesis

A. Representative kymographs of mitochondrial movement in wildtype, *ogt-1*, and *oga-1* mutants 24 hours after injury.
B. Quantitative analysis of mitochondrial dynamics. Shown are the percent time in motion, the mean speed, and the total length traveled.
C. Mechanosensory neuron-specific RNAi against the NADH dehydrogenase iron-sulfur protein 2 (*nduf-2.2*) in the *oga-1* background compared to vector control.

Finally, we examined whether mitochondrial ATP synthesis was important in *oga-1* mutants. Interestingly, producing double mutants between *oga-1* and mutations of genes in the electron transport chain, such as *nuo-6* and *isp-1*, was not viable. To get around this, we knocked down with RNAi an essential NADH dehydrogenase iron-sulfur protein 2 (*nduf-2.2*), a component of the electron-transport chain important for regeneration. Knocking down *nduf-2.2* significantly reduced *oga-1* mutant regeneration suggesting that *oga-1* mutants rely on ATP generation from mitochondrial to fuel axon regeneration (Figure 3.17).

3.11 Canonical DAF-16 target genes are not responsible for *oga-1* mutant regeneration

A number of genes that are transcriptionally controlled by DAF-16 have been identified to play a role in the mitochondrial stress response and metabolism (Kaletsky et al., 2016). We conducted a targeted RNAi screen against these components using a list of recently identified mechanosensory neuron-specific DAF-16 target genes. We examined oxidative stress/stress response genes (*mtl-1, sip-1, sta-1*), fatty acid metabolism (*fat-3, T13C2.6*), mitochondrial genes (*nnt-1, hmgr-1*). However, knockdown of these genes produced no effect on *oga-1* mutant regeneration with the exception of *hmgr-1* (Figure 3.18). The *hmgr-1* gene is the homolog of the HMG CoA-reductase, the key rate-limiting enzyme of the mevalonate pathway. This pathway is responsible for the biosynthesis of

prenylation, Coenzyme Q, and dolichols. In contrast to mammals, *C. elegans* does not synthesize cholesterol via the mevalonate pathway and instead relies on dietary cholesterol for membranes. To confirm this hit, we knocked down enzymes downstream of the *hmgr-1* in the mevalonate pathway. However, knocking down the farnesyl diphosphate synthase (*R06C1.2*) produced no reduction in *oga-1* mutant regenerative outgrowth. Furthermore, inhibiting all downstream pathways including coenzyme Q synthesis (*coq-1*), protein prenylation (*R02D3.5, F23B12.6, M57.2,* and *Y48E1B.3*), or isopentyl tRNA synthesis (*gro-1*) also resulted in no effect in regenerative outgrowth (Figure 3.18). Taken together, we conclude that either *hmgr-1* could be a false positive in our screen or, excitingly, that a completely new branch of the mevalonate pathway exists.

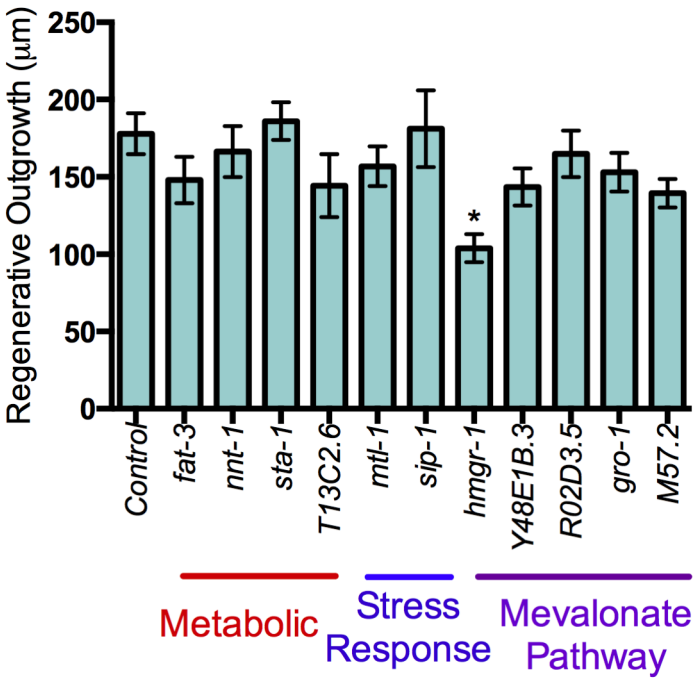

Figure 3.18 DAF-16 Target Gene Knockdown in the *oga-1* Mutant Background

RNAi knockdown of DAF-16 target genes involved in mitochondrial metabolism, the mitochondrial stress response, and the mevalonate pathway. One-way ANOVA. * p>0.01 compared to vector controls.

3.12 The effect of an OGT inhibitor on axon regeneration in mouse cortical neurons *in vitro*

We wondered whether acute inhibition of OGT could enhance axon regeneration in cultured mouse cortical neurons. We isolated day 18 embryonic cortical neurons and allowed them to grow for seven days in culture. We then treated the cultures with either 2 micromolar of ST045849, an OGT inhibitor, for 12 hours before inducing axonal injury with our laser ablation system. We confirmed that this dose of inhibitor successfully knocked down O-GlcNAc levels by Western blots (data not shown). We cut an axon approximately 60 micrometers from the cell body and observed its regenerative growth over six hours. Treatment with the OGT inhibitor ST045849 significantly increased the percentage of neurons displaying growth cones and trended toward an enhancement of axon regeneration, but did not reach significance, compared to vehicle treated controls (Figure 3.19). Further optimization of dose and treatment times need to be optimized before the results can be considered conclusive.

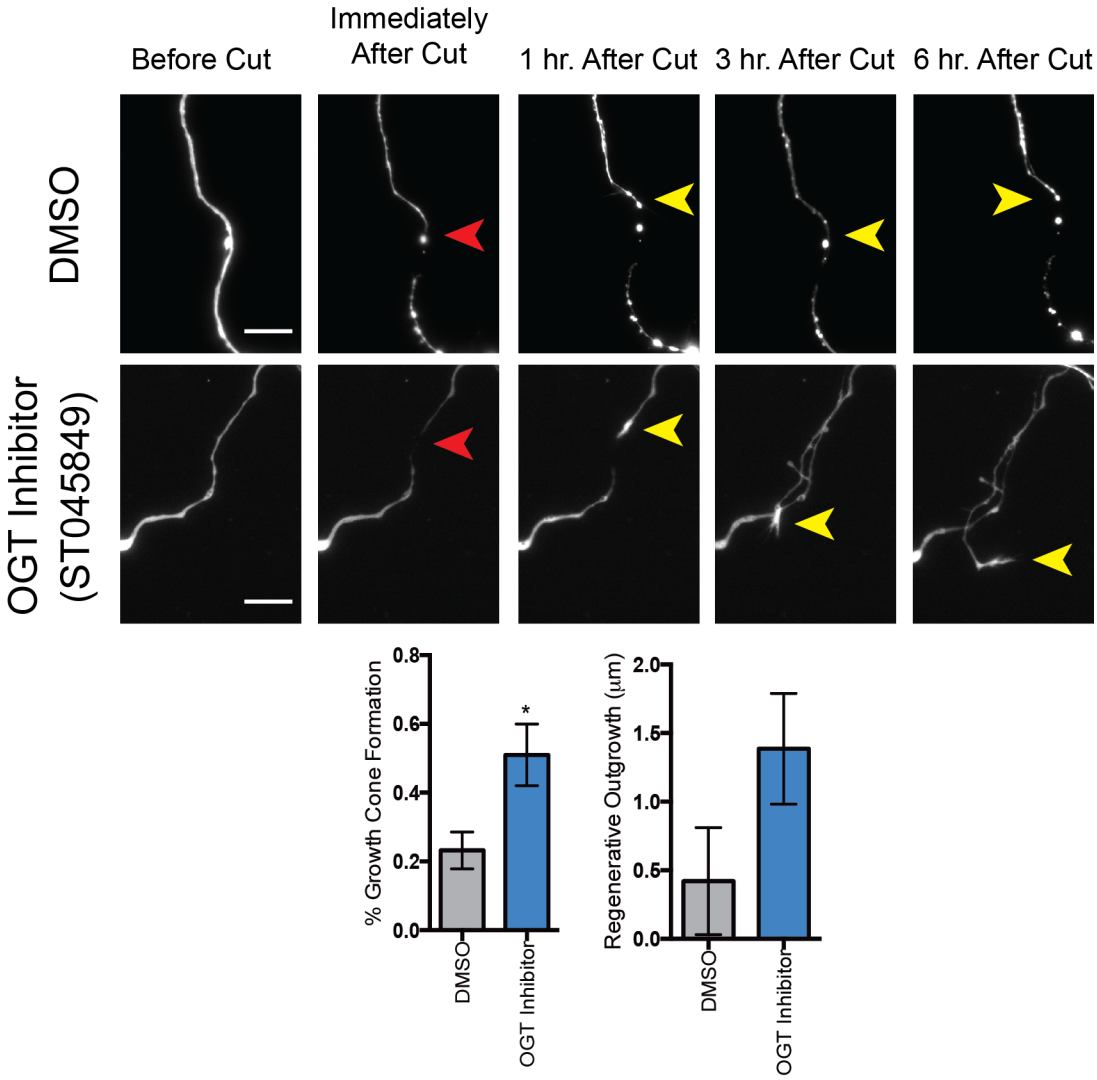

Figure 3.19 Inhibition of OGT in Regenerating Mouse Cortical Neurons

(Top) Timelapse analysis of axonal injury and regeneration over 6 hours. Red arrow shows injury site. Yellow arrow shows the growth cone.

(Bottom) Quantification of the percent of neurons displaying growth cones after damage and the amount of axonal regrowth.

3.12 The effect of OGT inhibition on axon regeneration in a mouse optic nerve crush injury model

We then assessed whether our findings in *C. elegans* and in cultured neurons could translate to an in vivo mouse model of axon regeneration. We utilized a mouse line with a floxed OGT allele, which upon Cre recombinase injection, would produce a functional null protein. This approach was essential due to the embryonic lethal nature of the constitutive OGT knockout. Therefore, we injected an adenoviral vector encoding Cre into the retina two weeks before optic nerve crush. We then crushed the optic nerve, waited two weeks, and then injected an axonal tracer, CTB-550, to assess the extent of regeneration of the retinal ganglion cells (RGCs). We also examined retinal ganglion cell death.

In stark contrast to our *C. elegans* model, inhibiting OGT produced no beneficial regenerative effect. The amount of regeneration was comparable to wildtype with potentially a slight increase at the first 200 micrometer point (Figure 3.20 A and B). We then examined cell death and cell morphology by staining whole-mount retinas for the RNA-binding protein with multiple splicing (RBPMS), a marker of all retinal ganglion cells, and osteopontin, a marker for the alpha-subtype retinal ganglion cells. Interestingly, we observe that total RGC number is significantly decreased in OGT knockouts and that the alpha-RGCs in particular are affected (Figure 3.20 C,D,E, and F). This suggests that any regeneration is likely originating from the other subtypes of RGCs, which under

normal conditions do not readily regenerate. The implications of this are detailed in the discussion.

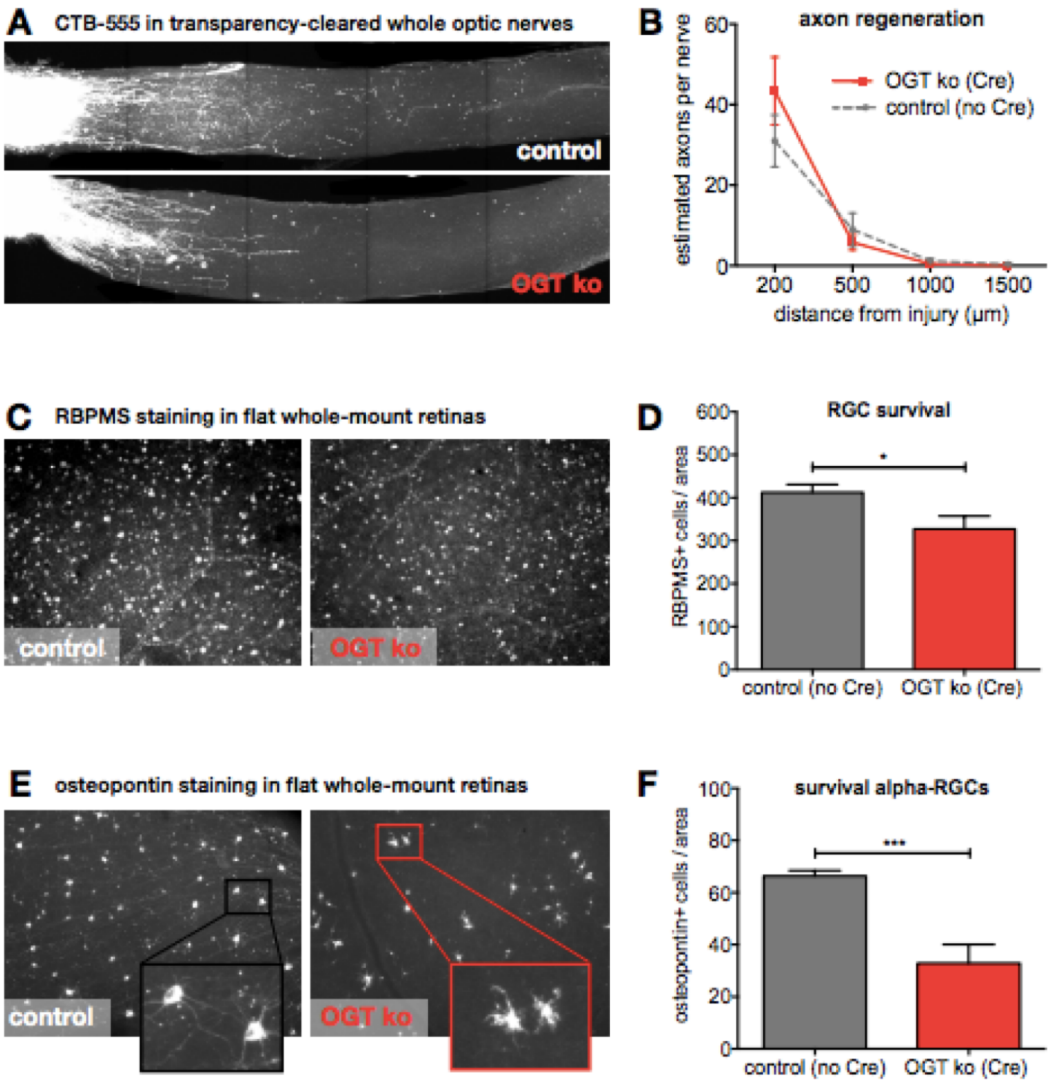

Figure 3.20 OGT Inhibition has no Effect on Regeneration but Induces Cell Death in Mouse Optic Nerve Injury Models

A. Whole-mount cleared optic nerves with axons stained with CTB-555 in control vs. OGT ko.
B. Quantification of regeneration.
C. RGC staining in flat mount retinas
D. Quantification of RGC survival
E. Alpha-RGC staining in whole mount retinas
F. Quantification of alpha-RGC survival

CHAPTER FOUR

Discussion

4.1 O-GlcNAc Manipulation Significantly Enhances Axon Regeneration through Novel Signaling Pathways

We have demonstrated for the first time that O-GlcNAc post-translational modifications have a dynamic and important role in axonal regeneration after injury. Interestingly, it appears that shifting the cellular O-GlcNAc state to one extreme or the other (i.e. complete lack of or an over-abundance of O-GlcNAc) can act as a switch to enhance regeneration through the insulin-signaling pathway (Figure 4.1). A loss of O-GlcNAc modifications enhances regeneration through non-canonical activation of AKT-1. Activation is mediated by the non-tyrosine receptor kinase ARK-1. Upon activation, our data suggests that AKT-1 mediates enhanced regeneration through glycolysis. In contrast, an abundance of O-GlcNAc modifications enhances regeneration through the SGK-1 kinase. This in turn acts on the transcription factor DAF-16/FOXO to up-regulate specific target genes. We further find that mitochondrial metabolism and function is affected suggesting that DAF-16 target genes play a role in regulating mitochondrial dynamics. This suggests a paradigm in which the perception of nutrients via O-GlcNAc levels can act as a metabolic switch in regenerating neurons. A lack of O-GlcNAc, conveying reduced nutrient availability, leads to the use of glycolysis for regeneration whereas an abundance of O-GlcNAc, conveying a nutrient abundance, leads to the use of mitochondrial metabolism for regeneration.

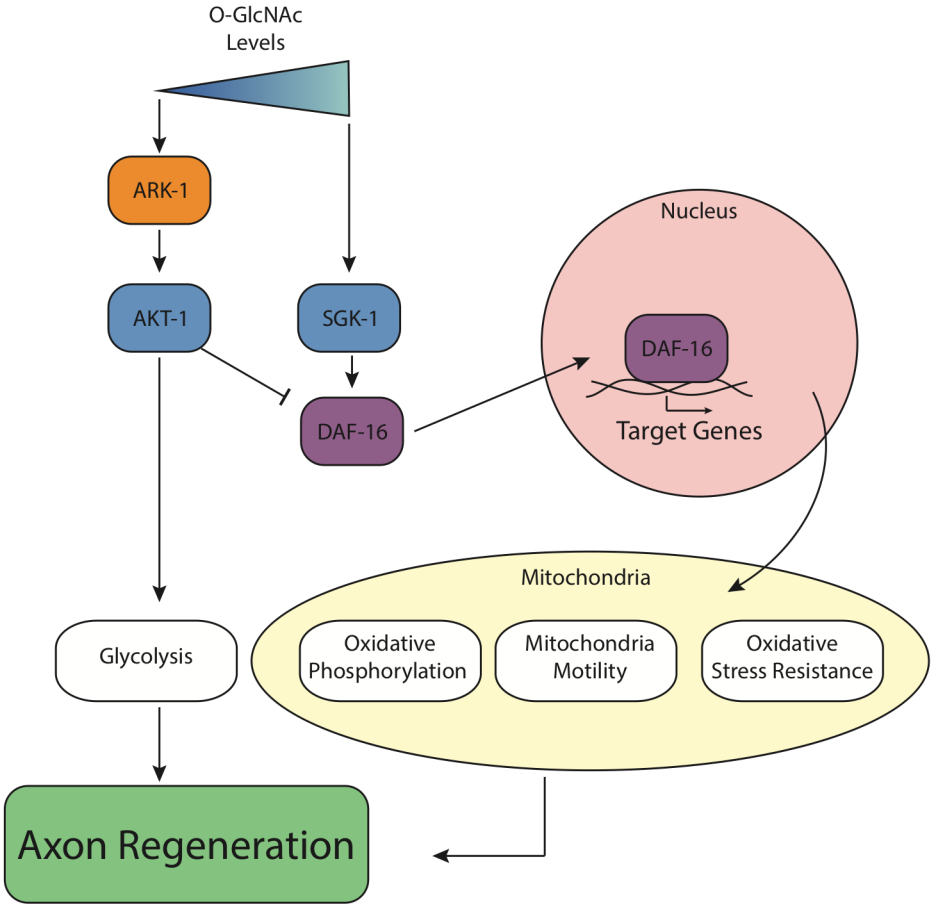

Figure 4.1 Proposed Model for How O-GlcNAc Enhances Axon Regeneration

Others have observed that manipulating O-GlcNAc levels in culture can alter axonal growth in a developmental paradigm. Culturing embryonic chicken neurons overexpressing the O-GlcNAcase revealed an enhancement of axonal growth and branching (Francisco et al., 2009). This effect was primarily due to an increased number of filopodia. In contrast, inhibiting the O-GlcNAcase with either PUGNAc or 9D did not produce any effects on axonal growth but significantly lowered the number of filopodia. The authors suggested that cAMP may be involved as O-GlcNAcase inhibition with 9D significantly inhibited the increased number of branches observed when culturing neurons with forskolin, a phosphodiesterase inhibitor (Francisco et al., 2009).

Another group also implicated O-GlcNAc in the cAMP pathway in axonal growth (Rexach et al., 2012). Cultured mouse cortical neurons depolarized with KCl exhibited an increase of CREB O-GlcNAcylation at Ser40, thereby repressing CREB activity. Interestingly, removing the O-GlcNAc Transferase resulted in increased axonal length whereas its overexpression significantly decreased length.

The role of cAMP and CREB in axonal regeneration is well-established in mammalian and *C. elegans* models. Elevations of cAMP lead to an enhancement of axon regeneration through distinct mechanisms in the two species. In mammals, CREB activation leads to the transcription of Arginase I and the production of polyamines (Cai et al., 2002). Through metabolism, polyamines are converted and lead to an unusual hypusination post-translational modification of the elongation initiation factor 5A

(eIF5A), which enhances its activity (He et al., 2016). This in turn is hypothesized to up-regulate p35 translation, leading to the activation of cyclin-dependent kinase 5 (Cdk5), and a reversal of the inhibition on axonal growth with myelin-based inhibitors (He et al., 2016). In contrast, *C. elegans* display CREB-independent enhancement of regeneration by cAMP. This is hypothesized to be through the activation of the CEBP-1/ETS-4 axis by Protein Kinase A to then activate MAPK-signaling (Li et al., 2015).

However, in our studies, the effect of O-GlcNAc on axon regeneration appears independent of cAMP/CREB (Figure 3.9). Loss-of-function mutation of the CREB transcription factor do not affect either *ogt-1* or *oga-1* mutants. In addition, loss-of-function of the phosphodiesterase, producing an enhancement of cellular cAMP levels, did not affect axon regeneration in O-GlcNAc mutants, although the double mutants were not additive suggesting either we have reached a ceiling for 24-hour regeneration or that the two pathways interact at an unknown level. Alternatively, as *C. elegans* does not have myelination, it could be that the effects of CREB activation and polyamine synthesis are not conserved or that the transcriptional targets of CREB in these two species may differ.

4.2 O-GlcNAc Enhances Axon Extension during a Later Stage of Regeneration

Axon regeneration follows distinct spatiotemporal steps: 1) membrane resealing 2) breakdown and cleanup of damaged cellular components 3) formation of a new growth

cone 4) axon extension 5) re-connecting with post-synaptic targets (Figure 1.3). Accordingly, the function of different pathways can begin to be assessed by analyzing when the regeneration phenotype is most prominent. Time-lapse analysis of regeneration determined that O-GlcNAc mutants likely act at a late stage of axon regeneration between 12 and 24 hours post injury with significant axon extension phenotypes observed at 24 hours (Figure 3.5). Interestingly, neuronal development in the *ogt-1* and *oga-1* mutants is not different from wildtypes, suggesting the impact of O-GlcNAc on axon extension is specific to injury and regeneration. Accordingly, early mediators of regeneration, such as calcium-signaling and *dlk-1* signaling, were determined to be independent of O-GlcNAc signaling in regeneration (Figure 3.6). Examination of early filopodial dynamics also revealed that O-GlcNAc mutants act in a similar manner to wildtypes between 1 and 3 hours post injury (Figure 3.5). Interestingly, *oga-1* mutants had reduced filopodial number at 5 hours post-injury compared to *ogt-1* and wildtypes. This could be due to a few factors. Often during regeneration, as in development, one major neurite is chosen to be the future presumptive axon and grows further than the rest of the other neurites. It could be that *oga-1* mutants select this presumptive axon sooner than wildtypes and repress filopodial dynamics earlier than wildtypes do. Alternatively, affinity purification coupled with mass spectrometry of heavily O-GlcNAcylated proteins in whole *C. elegans* and mammals have identified actin, certain actin binding proteins, and alpha-tubulin(Alfaro et al., 2012; Rahman et al., 2010). These are all important mediators of filopodial dynamics and O-GlcNAcylation may alter their properties.

Other aspects of the regeneration in O-GlcNAc mutants also appeared indistinguishable from wildtypes. Branching and anterior vs. posterior growth direction are not different from wildtype (Figure 3.5). This indicates that the numbers of branches/neurites are not different but that the growth of each neurite is longer in the *ogt-1* and *oga-1* mutants. As a whole, our data suggest that O-GlcNAc acts specifically during axon extension to enhance regeneration after injury.

4.3 O-GlcNAc Acts Cell Intrinsically to Enhance Axon Regeneration

As the effects of constitutive mutants are throughout the whole organism, we probed whether O-GlcNAc manipulation enhances regeneration in a cell-intrinsic or extrinsic manner. O-GlcNAc has been suggested previously to modify p27kip1, a cyclin-dependent kinase inhibitor, in astrocytes and lead to enhanced astrocyte migration and functional and histological improvement after a spinal cord contusion in rats (Mao et al., 2015). However, the majority of this study was conducted by mutating the serine that is O-GlcNAcylated to alanine resulting in a mutant than can neither be O-GlcNAcylated or phosphorylated. Whether the effects are due to phosphorylation, O-GlcNAcylation, or some complex interplay cannot be properly interpreted. In addition, no direct manipulation of O-GlcNAc *in vivo* was conducted. Regardless, the possibility that O-GlcNAc could act within neurons to improve functional recovery compelled us to examine where O-GlcNAc acts. To address this, we utilized a mechanosensory-neuron specific RNAi sensitive strain which exhibits RNAi sensitivity in the mechanosensory

neurons but RNAi resistance in all other tissues. When treated with *ogt-1* and *oga-1* mechanosensory-neuron specific RNAi, the axon regeneration was akin to that of the constitutive mutants (Figure 3.3). This strongly suggests the effect is cell-intrinsic. Future studies combining cell-specific rescues and mutagenesis could delineate the regions of the *ogt-1* and *oga-1* genes important for regeneration.

4.4 O-GlcNAc is a Nutrient-Responsive Post-Translational Modification in *C. elegans*

The O-GlcNAc modification is derived from glucose through the hexosamine biosynthetic pathway. It has been estimated that 2-5% of cellular glucose is directed into the hexosamine biosynthetic pathway and that the levels of cellular glucose can change the levels of protein O-GlcNAcylation. To assess whether O-GlcNAc is a nutrient-sensor in our system, we treated *C. elegans* with varying concentrations of glucose and measured the effect on O-GlcNAcylation. We found that treatment with 100mM glucose was sufficient to elevate levels of O-GlcNAc to the extent of the *oga-1* mutant (Figure 3.7). However, our analysis was conducted in whole *C. elegans* lysates in order to obtain enough protein for quantitative western blotting. The actual O-GlcNAc levels in a neuron in normal, injured, and regenerating settings could be different and dynamic. Future studies will address this by examining the levels of glucose and O-GlcNAc using FRET-sensors in a single ALM neurons during a regenerative response. A previous study found that the organismal glucose stress threshold, defined as the concentration of glucose that

affected fertility, was 250mM with a toxic threshold of 333mM (Mondoux et al., 2011). In addition, these concentrations facilitated an increase in O-GlcNAcylation. Our observations are conducted well below this toxic threshold and therefore, glucose toxicity is not a factor in our analysis.

To assess whether glucose levels affected regeneration, we treated wildtype, *ogt-1*, and *oga-1* mutants with either 100mM glucose or 1mM phloretin, a glucose transport inhibitor. Interestingly, we found that the treatment of wildtype *C. elegans* with glucose significantly enhanced regeneration to an extent comparable to *oga-1* mutants (Figure 3.2). Further, treatment of *oga-1* mutants with 100mM glucose did not have an additive effect on regeneration. Treatment of wildtypes with the glucose transporter inhibitor did not affect regeneration, as expected, but significantly decreased regeneration in *oga-1* mutants. This is expected as O-GlcNAc synthesis is dependent on glucose levels. We also found that treatment with the glucose transport inhibitor reduced *ogt-1* mutant regeneration (discussed further below). Taken together, this suggests that elevations of glucose produce elevations in O-GlcNAc levels leading to enhanced regeneration, akin to what is occurring in the *oga-1* mutant background.

Glucose was specifically advantageous for enhancing wildtype regeneration but does not appear essential, as wildtype regeneration remains unaffected by the glucose transport inhibitor. This is in accordance with a recent study (and this work) showing that inhibiting glycolysis does not affect wildtype axon regeneration in *C. elegans* (Han et al.,

2016) and suggests that while glucose utilization is not essential, it can be up-regulated to enhance the growth process. This will be elaborated on in a later section.

4.5 O-GlcNAc Acts through the Insulin-Signaling Pathway to Enhance Axon Regeneration

We screened many pathways important in axon regeneration to determine the genetic epistasis between these and the O-GlcNAc mutants to begin to determine the molecular underpinnings of the enhanced regeneration. Although O-GlcNAc has been implicated in calcium and cyclic AMP signaling in other settings, we did not find that the O-GlcNAc mutants depended on these pathways. Instead, we identified that the O-GlcNAc mutants depend on the insulin-signaling pathway to enhance regeneration. Genetic epistasis analysis between loss-of-function mutants in the insulin-signaling pathway revealed that the O-GlcNAc mutants differentially relied on specific kinases to mediate regenerative outgrowth. The *ogt-1* mutants specifically relied on *akt-1*, whereas the *oga-1* mutants relied on the parallel kinase, *sgk-1* (Figure 3.10 and 3.14).

The insulin-signaling pathway has previously been implicated in both axon regeneration and O-GlcNAc signaling in *C. elegans*. Insulin receptor/*daf-2* mutants were found to have enhanced regeneration in day 5 adults in the GABAergic motor neurons compared to wildtypes (Byrne et al., 2014). This effect was found to be dependent on the

FOXO transcription factor DAF-16, similar to DAF-2's effect on longevity. Examination of DAF-16 targets by ChIP-seq revealed DLK-1 in the MAPK-signaling pathway to be a target and important in age-related regeneration (Byrne et al., 2014).

In addition, O-GlcNAc mutants were previously found to have altered lifespans with *ogt-1* and *oga-1* mutants living modestly shorter and longer, respectively (Love et al., 2010; Rahman et al., 2010). As insulin-signaling is one of the major pathways controlling aging in *C. elegans*, its involvement was tested in O-GlcNAc mutants. Mutations in *daf-16* produced no effect on *ogt-1* mutant lifespan but did significantly decrease *oga-1* mutant longevity(Rahman et al., 2010). Epistasis analysis between other genes in the insulin-signaling pathway was inconclusive and many genes including *akt-1* and *akt-2* remained untested. Interestingly, they did find that *oga-1* mutations are able to suppress *daf-2* mediated lifespan suggesting that *oga-1* is acting downstream of *daf-2* but upstream of *daf-16* in longevity, similar to our observations in regeneration(Rahman et al., 2010). Another study examined O-GlcNAcylation with respect to the stress response and dauer. The authors found that O-GlcNAc can modify promoter regions of DNA that encode for stress-related genes including PIP3 interacting proteins and 14-3-3 proteins, both of which are known to intersect with the insulin-signaling pathway (Love et al., 2010). The authors also found that *daf-16* itself had promoter segments that were modified by O-GlcNAc. In addition to similar findings on aging, they found that *oga-1* mutants were better able to handle stress by modifying insulin signaling. Again, lack of more advanced epistasis analysis or mass spectrometry failed to identify whether O-

GlcNAc is acting at the transcriptional or protein level. Our findings shed light onto these studies. Our in-depth epistasis analysis of each gene in the insulin signaling pathway revealed the requirement of the intermediate kinases *akt-1* and *sgk-1*. This is likely to occur at the protein level as neither akt-1 or sgk-1 promoters are O-GlcNAcylated in *C. elegans*. Further, several studies have found that AKT1 is O-GlcNAcylated in mammals (Vosseller et al., 2002).

4.6 Activated CDC42 Non-Receptor Tyrosine Kinase/*ark-1* is a Novel Component of the Insulin-Signaling Pathway in *C. elegans*

While the phosphoinositide 3-kinase (PI3K), *age-1,* is the canonical upstream activator of *akt-1*, we interestingly found that this was not the case in *ogt-1* mutant regeneration. A similar phenomenon has also been observed in mammalian systems in which AKT is activated in a PI3K-independent manner (Mahajan et al., 2010). AKT activation follows discrete steps in which an inactive cytosolic protein is recruited to the plasma membrane upon increased PI3K activity. This is due to the action of PI3K to convert PIP2 to PIP3, which recruits AKT via its plextrin homology domain. Upon binding to PIP3, AKT becomes able to interact with other interacting factors, notably PDK and mTORC, and is phosphorylated at Thr308 and Ser473. Phospho-AKT is then active and can phosphorylate downstream targets. Activity can also be extinguished by certain phosphatases, notably PP2A. In contrast to this canonical mechanism of activation, others have found that mouse embryonic fibroblasts treated with EGF display

tyrosine phosphorylation of Akt1 at Tyr176 (Mahajan et al., 2010). This phosphorylation event alone was able to recruit AKT to the membrane for further activation. Treatment with a PI3K inhibitor did not abolish this effect and further studies identified that this phosphorylation is due to the action of the Activated CDC42 Non-Receptor Tyrosine Kinase (ACK). We conducted a homology search and found that the *C. elegans* gene ark-1 is roughly 88% similar at the amino acid level. In addition, a loss-of-function mutation in this gene significantly reduced *ogt-1* regeneration (Figure 3.11). Using a gain-of-function allele of *akt-1*, we further demonstrated that it can restore the *ogt-1;ark-1* double mutant regeneration to that of *ogt-1* levels. This demonstrates that in our system, *ark-1* is genetically upstream of *akt-1* and is necessary for *akt-1* activation.

This also demonstrates a new potential role for ACK/*ark-1* in the context of axonal injury. While loss of *ark-1* function alone does not affect regeneration, it is clear that its activation can have a beneficial role in mediating *akt-1* activity. ACK has been previously implicated in various cancers and in the dynamics of endocytosis (Wu et al., 2015; Wu et al., 2017; Yoo et al., 2004). In terms of cancer, ACK expression correlates with aggressive phenotypes in breast cancer and its knockdown significantly suppresses tumor growth in a rodent xenograft model (Wu et al., 2015). However, much is unknown about ACK signaling dynamics and targets. The ACK structure is divided into a N-terminal sterile-alpha motif and kinase domains, followed by an SH3 domain, a CRIB domain, a C-terminal proline-rich EGFR-binding domain and a ubiquitin associated domain. ACK can be activated by various growth factor receptors by associating with the

growth factor receptor-bound protein 2 (Grb2), an adapter protein. Activated growth factor receptor tyrosine kinases can bind Grb2 via its SH2 domain. ACK can then bind to Grb2's SH3 domain via its proline-rich C-terminal domain. Upon activation, ACK then proceeds to phosphorylate target tyrosines. A new study suggests that ACK can also have a role in the nucleus in governing histone dynamics (Mahajan et al., 2017). In a model of castration-resistant prostate cancer, the androgen receptor can recruit ACK to the androgen receptor promoter and phosphorylate Tyr88 of histone 4. This leads to the recruitment of the MLL2/WDR5 chromatin remodeling complex and a persistent activation of androgen receptor targets. Gene enrichment analysis found that these targets include cancer-related gene signatures involved in DNA-repair, proliferation, E2F, MYC, and estrogen-receptor targets. Therefore, whether ACK acts at the transcriptional level to regulate these pro-growth pathways in axon growth and regeneration is an interesting question. This could be examined by performing immunoprecipitation to see if ACK interacts with and phosphorylates histone 4 in mature neurons and during axon growth.

ACK is expressed in the developing mouse and rat brain although its function is unknown (La Torre et al., 2006; Urena et al., 2005). Northern blots revealed that ACK mRNA is upregulated throughout developmental time, peaking at the adult stage. *In situ* hybridization showed expression in the hippocampus, cortex, and cerebellum, although a moderate level of expression was detected throughout other brain regions (La Torre et al., 2006; Urena et al., 2005). Hippocampal neuronal cultures determined the localization of ACK throughout the soma, axon, and growth cone structures (Del Mar Masdeu et al.,

2017). However, genetic lesions of ACK in mice have not been performed. Given our results in *C. elegans*, whether or not a neurological phenotype exists in knockout/overexpression mouse models is an interesting area for future research. Likewise, whether the role of O-GlcNAc and ACK/*ark-1* in axon growth and regeneration is conserved is a key question for future studies. Mass spectrometry of mouse brains revealed that ACK is O-GlcNAcylated at T832 and T833, which lies in the proline-rich EGFR binding domain (Alfaro et al., 2012). O-GlcNAcylation of these residues may therefore inhibit the interaction of ACK with EGFR or result in an overall conformational change that impairs Grb2 interaction.

4.7 Glycolysis is Important for *ogt-1* Mutant Regeneration

Unexpectedly, we found that like the *oga-1* mutants, treatment of the *ogt-1* mutants with the glucose transport inhibitor phloretin significantly suppressed regeneration (Figure 3.2). This suggested that the regenerative response was dependent on glucose utilization. O-GlcNAc *C. elegans* mutants have been previously implicated in glucose metabolism and utilization. Whole animal lysates revealed that both *ogt-1* and *oga-1* mutants have increased levels of glycogen and trehalose and decreased levels of triacylglycerol (Forsythe et al., 2006). This is enigmatic in that if *ogt-1* mutants were utilizing glucose at higher rates, they might be expected to have lower glycogen stores. However, there may be differences between organismal and cellular metabolism. In addition, whether these neurons are in a permanent glycolytic state or react to damage by

enabling glycolysis remains a possibility. Evidence in mammalian hypoxic tumor cell line suggests that O-GlcNAc can act as a switch between glycolysis and the pentose phosphate pathway with a lack of O-GlcNAcylation supporting glycolysis (Yi et al., 2012). The glycolytic enzyme phosphofructokinase-1 is modified by O-GlcNAc at Ser529. Over-expression of OGT, and therefore enhancing O-GlcNAc levels, results in a decrease in the glycolytic rate. This effect is abolished when Ser529 is mutated suggesting that O-GlcNAcylation at this residue is important for controlling glycolytic flux. This residue is conserved in *C. elegans* and whether or not this is important in *ogt-1/oga-1* mutant regeneration is unknown. However, given that the regeneration is dependent on insulin-signaling, it is unlikely that the modification of a glycolytic enzyme alone that enhances regeneration. Given that the regeneration of *ogt-1* mutants is dependent on *akt-1*, a kinase known to be involved in a number of metabolic pathways, we screened a number of pathways downstream of AKT to begin to establish how regeneration is enhanced mechanistically in *ogt-1* mutants. While FOXO/*daf-16*, mTOR, and GSK-3 were negative, we found an important role for glycolysis, agreeing with our findings above. Inhibition of glycolysis, but not oxidative phosphorylation, produced a specific decrease in *ogt-1* mutant regeneration. AKT is a well-known mediator of metabolic flux and is a key player in cancer cells using glycolysis even in oxygen permissive conditions, known as the Warburg effect (Ward and Thompson, 2012). AKT can enable this by acting directly and indirectly (Robey and Hay, 2009). Direct phosphorylation of glycolytic enzymes, hexokinase and phosphofructokinase, by AKT can enhance their activity (Robey and Hay, 2009). Indirectly, AKT can activate other

protein effectors of metabolism such as mTOR (Memmott and Dennis, 2009). Further, AKT could have indirect effects on transcription of metabolic genes. For example, AKT is a negative regulator of p53 and MDM2, which are known tumor-suppressors (Gottlieb et al., 2002). AKT activation therefore inhibits p53's regulation of glycolysis by releasing the transcriptional block in glycolytic genes like hexokinase, phosphoglycerate mutase, and glucose transporters. As *C. elegans* lacks homologs of p53 and MDM2 and we have ruled out mTOR and GSK-3, we favor a model in which AKT directly influences glycolytic enzymes. Further, we have shown inhibiting glycolytic enzymes represses *ogt-1* mutant regeneration. Examining whether this occurs in *C. elegans* and mammalian neurons after damage will be important to address. Future work utilizing glucose FRET sensors in *C. elegans* may demonstrate increased glucose utilization upon injury. However, a detailed analysis requires examining glycolysis in mouse neuronal cultures before and after injury and examining the involvement of AKT. Mass spectrometry could identify residues of specific glycolytic enzymes that are phosphorylated by AKT and these residues can then be mutated and examined functionally.

4.8 OGT Inhibition Enhances the Regenerative Response in Injured Mammalian Cortical Neurons *in vitro* but not *in vivo*

To examine if our findings in *C. elegans* translated into a mammalian system, we first determined whether inhibition of OGT using the pharmacological inhibitor ST045849 could enhance regeneration after laser-induced injury of cultured mouse

cortical neurons. We found that by 6 hours after injury the number of axons with growth cones, structures indicating new axonal growth, was significantly elevated in OGT inhibitor treated neurons while axon growth trended upward but did not reach significance. Other studies have examined axon regeneration in cultured neurons over a 24-hour period with growth cone structures appearing 1 to 6 hours after injury and axonal extension occurring later. We hypothesize that looking at later time-points in regeneration, optimizing dose and timing of treatment may be beneficial in enhancing this regenerative response.

Given these encouraging initial results, we examined the effect of OGT inhibition in an in vivo mouse model of axon regeneration. Surprisingly, we found that genetic ablation of OGT had no or a mild effect on regeneration. Further, retinal ganglion cell (RGC) cell death was significantly elevated in OGT ablated mice. While this is in stark contrast to what we observe in our *C. elegans* and cell culture model, others have observed cell death in OGT ablated sensory neurons in mice (Su and Schwarz, 2017). Why does OGT ablation cause cell death in this model? Previous work has suggested that many types of neurons are developmentally glycolytic but then rely on mitochondrial oxidative phosphorylation for energy generation once mature (Zheng et al., 2016). Whether this is the case for retinal ganglion cells is unknown but many forms of inherited disease of RGCs stem from mutations in mitochondrial metabolism, highlighting its importance (Ito and Di Polo, 2017). If our model is correct, then ablating OGT and favoring glycolysis over mitochondrial metabolism, at a time when none of the glycolytic

machinery is present, may induce an energy crisis and cell death. In contrast, in our cell culture model, the neurons are still developmentally primed (isolated at E18.5) and have access to excess glucose in the culture media. Alternatively, the role of O-GlcNAc may not be evolutionarily conserved. However, our preliminary results in culture suggest that under the right conditions, enhancement of regeneration by knocking down OGT may be beneficial.

4.9 Serum Glucocorticoid Kinase (*sgk-1*) is Important for *oga-1* Mutant Regeneration

The regeneration of *oga-1* mutants did not rely on *age-1, akt-1*, or *akt-2*. Through epistasis experiments, we interestingly found that *oga-1* acted downstream of *daf-2* and upstream of *daf-16* (Figure 3.13). A lesser known kinase in the insulin-signaling pathway that fit these criteria is the serum glucocorticoid kinase, *sgk-1*. Loss-of-function of this kinase specifically inhibited *oga-1* regeneration while leaving wildtypes unaffected. The role of *sgk-1* in the insulin-signaling pathway is less defined than the other components. In terms of lifespan, the predominant phenotype of insulin-signaling mutants, *sgk-1* mutants have been contradictorily reported to have lowered or enhanced lifespan. In an assessment of the genetic components underlying the enhanced lifespan of O-GlcNAc mutants, the authors observed a moderate enhancement of lifespan in *sgk-1* mutants similar to the lifespan extension of *daf-2*/INSR mutants. However, the addition of *oga-1*

mutations in an *sgk-1* mutant background had no effect on lifespan, suggesting the two are potentially acting in a similar pathway in lifespan (Rahman et al., 2010).

Previous studies have demonstrated that *sgk-1* can act on the DAF-16 transcription factor to upregulate specific DAF-16 target genes. SGK-1 can directly phosphorylate DAF-16 *in vitro* but the consequences of this phosphorylation remain unclear (Hertweck et al., 2004). Others have suggested that this interaction either alone or in combination with other factors allows the regulation of a subset of DAF-16 target genes (Chen et al., 2013). Analysis of DAF-16 target genes regulated by AKT-1 and SGK-1 revealed an important disparity, suggesting that SGK-1 acts on DAF-16 in a more complex way than previously recognized (Chen et al., 2013). We favor a model in which the activation of *sgk-1* can result in the regulation of a subset of DAF-16 genes that are important for the regenerative response seen in *oga-1* mutants. While our genetic epistasis data supports this, a more detailed biochemical evaluation is required. Further, examining expression levels of subsets of DAF-16 target genes and subsequently knocking down genes which are regulated by SGK-1 may be fruitful in understanding the interaction between SGK-1, DAF-16, and regeneration.

Further, whether SGK-1 itself is O-GlcNAcylated or there remains a missing interacting protein is unclear. Previous mass spectrometry studies have not identified SGK1 as an O-GlcNAcylated protein (Alfaro et al., 2012). However, these studies have identified the PDK-class protein kinase (PDK-1) protein as being O-GlcNAcylated and

this may play a functional role in insulin-signaling (Whelan et al., 2010). Upon insulin stimulation of 3T3-L1 adipocytes, PDK1 and OGT interact and PDK1 O-GlcNAcylation occurs. This is proposed to inhibit insulin-signaling, potentially at the level of AKT. Activation of SGK can occur through PDK1. Therefore, O-GlcNAc modification of PDK-1 may lead to SGK-1 activation (Whelan et al., 2010). Alternatively, it has been proposed in *C. elegans* that AKT-1, AKT-2, and SGK-1 form a complex (Hertweck et al., 2004).O-GlcNAcylation of one or more of these components leading to alterations in complex constituents or activity could be a potential mechanism of balancing AKT vs. SGK activation.

4.10 O-GlcNAcase (*oga-1*) Mutants have a Global Effect on Mitochondrial Function

Both DAF-16 and O-GlcNAc have been heavily implicated in altering mitochondrial function. As a transcription factor, DAF-16 regulates a number of mitochondrial genes. For example, upon oxidative stress, DAF-16 up-regulation of the superoxide dismutase 3 (SOD-3) to mitigate oxidative damage is a well-known example (Chavez et al., 2007). However, a statistical analysis of DAF-16 targets shows no over-representation of mitochondrial genes. Further, mechanosensory neuron-specific targets of DAF-16 reveal a completely different set of genes compared with whole *C. elegans* lysates (Kaletsky et al., 2016). In this case, the number of genes with mitochondrial annotation is much fewer and DAF-16 appears to regulate genes with neuronal specific

functions such as synaptic transmission. Whether the effect of DAF-16 on mitochondria is therefore direct or indirect remains to be seen.

Regardless, DAF-16 has several effects on mitochondria. First, DAF-16 over-expression or DAF-2 mutation resulting in DAF-16 activation results in enhanced oxidative stress resistance (Tullet et al., 2017). DAF-16 has been proposed to accomplish this by the regulation of SOD-3 and metallothionein-1 (MTL-1), a key metal-binding protein involved in the stress response. However, transcriptomes of the mechanosensory neurons show that *sod-3* is not expressed (Kaletsky et al., 2016). Further, we have shown that RNAi against *mtl-1* has no effect on *oga-1* regeneration suggesting it is also not involved. Exactly how DAF-16 is able to achieve a reduced oxidative environment in neurons is unknown. Second, DAF-16 is implicated in mitochondrial motility, although the exact role is unknown. Mitochondrial motility declines with age in ALM neurons and this can be prevented by *daf-2* loss-of-function or dietary restriction via *eat-2* mutation (Morsci et al., 2016). Our study is another example, and excellent model, to assess the effect of DAF-16 on mitochondrial function given that we can monitor multiple aspects of mitochondrial function at a single cell level. We plan to interrogate this further with the help of neuron specific RNAi.

Akin to DAF-2/DAF-16 genetic lesions, O-GlcNAc modifications have also been shown to impact mitochondrial function. At the organelle level, O-GlcNAc overexpression alters mitochondrial morphology making longer mitochondria with less

organized cristae (Tan et al., 2017). The consequences of these morphological alterations are not understood but several mitochondrial phenotypes have been observed. O-GlcNAc overexpression is protective against oxidative stress and heat-shock and this is dependent on GSK-3beta, HIF1, and heatshock proteins (Zachara et al., 2004). Further, respiration in these mitochondria is blunted (Tan et al., 2017). Finally, mitochondrial motility is affected by O-GlcNAc level through post-translational modification of mitochondrial motor adapter proteins. High O-GlcNAc levels, and therefore high O-GlcNAc modification of the mitochondrial motor adapter protein Milton, results in less motile mitochondria (Pekkurnaz et al., 2014).

We also observed effects of high O-GlcNAc levels on mitochondrial function (Figure 3.17). Oxidative stress resistance, mitochondrial respiration, and mitochondrial motility were all affected in *oga-1* mutant regeneration. The mitochondrial motility phenotype is particularly interesting. Motility has been previously linked to regenerative potential. Armcx1 is a mitochondria-localized protein which plays a key role in governing motility. Overexpression of Armcx1 results in enhanced motility and enhanced regenerative outgrowth (Cartoni et al., 2017). Further, increased mitochondrial motility correlates well with regenerative capacity of axons after injury (Cartoni et al., 2017; Han et al., 2016). This also appears to be conserved in *C. elegans* models. Knocking down the key mitochondrial motor adaptor complex protein *miro-1*, decreased mitochondrial abundance in the regenerating axon and regenerative outgrowth whereas overexpression of *miro-1* resulted in increased mitochondrial abundance and regenerative outgrowth

(Han et al., 2016). However, in our *oga-1* mutants that have increased regenerative outgrowth, mitochondrial motility is substantially reduced (Figure 3.17). This suggests that while motility is helpful for enhanced regeneration, it may not be necessary and other mitochondrial phenotypes, such as oxidative stress resistance, may be more important.

The role of oxidative stress in axon growth is still underexplored. While excess levels of reactive oxygen species (H_2O_2, O_2^-, and HO+) are clearly detrimental through irreversible damage of proteins and lipids, some optimal level may be important. In particular, the cytoskeleton is sensitive to the oxidative environment. Actin polymerization is inhibited by oxidative environments and some studies have suggested that a redox balance is necessary for proper growth cone formation and axon outgrowth (Wilson and Gonzalez-Billault, 2015). Our study suggests that the ability to maintain a reduced environment is key for regeneration (Figure 3.16). If regenerating axons of *oga-1* mutants are predominantly utilizing mitochondrial metabolism, then keeping a reductive environment may be beneficial.

From the list of genes regulated by DAF-16 in mechanosensory neurons, we identified a subset of metabolic and/or mitochondrial genes. However, RNAi against these genes did not impact *oga-1* regeneration (Figure 3.18). Exactly how OGA-1 and DAF-16 act to alter global mitochondrial dynamics remains unclear. Given that OGA-1 mutants appear to alter mitochondrial dynamics as a whole, as opposed to one aspect of mitochondrial biology, it is reasonable to propose that O-GlcNAc and/or DAF-16 are

acting on a global regulator of mitochondrial function such as a transcription factor. Examination of DAF-16 target genes that have mitochondrial functional annotation and are transcription factors identify only one, MEX-6, the *C. elegans* homolog of tristetraprolin. This is particularly interesting because tristetraprolin has been implicated in mitochondrial function. Overexpression of tristetraprolin results in elongated mitochondria, reduced mitochondrial membrane potential, decreased ATP production, and increased reactive oxygen species production (Vo et al., 2017). While some of these phenotypes match the *oga-1* mutants, others are opposites. This could be due to the experimental system used or the distant homology (~17% conservation). If MEX-6 is involved, then knocking down *mex-6* should suppress the regeneration observed in *oga-1* mutants and be redundant with *daf-16*.

Alternatively, DAF-16 could be regulating numerous mitochondrial genes in parallel. DAF-16 regulates 12 genes, which we have identified, that have annotated mitochondrial function with functions that range from maintaining the mitochondrial membrane potential to oxidative stress resistance. Additive mutants/RNAi should be able to distinguish whether this is a possibility in the future.

4.11 Metabolism of Injured and Regenerating Neurons

Ultimately, our results suggest that certain metabolic pathways are more advantageous for a regenerative response. Recent research in axon regeneration has

focused on the important role of mitochondria, as discussed above. Experiments in *C. elegans* have begun to delineate a role for not only mitochondrial motility and density, but also components of the electron transport chain as having roles in regeneration. Interestingly, components of complex I (*gas-1, nduf-2.2, nduf-7)* and complex II/III (*rad-8* and *isp-1*) were identified as important for regeneration while components of complex II, III, Ubiquinone, and the ATP Synthase were found to be non-essential. Oddly, only certain components in each complex were important (Knowlton et al., 2017). For example, in complex I, *nduf-2.2* mutants displayed reduced regeneration whereas *nuo-6* mutants did not even though they both have deficits in ATP synthesis. This discrepancy may be due to the severity of each loss-of-function mutation (as complete loss-of-function of these components are lethal) or the neuronal subtypes analyzed. Interestingly, overexpression of only *nduf-2.2* and *isp-1*, is able to enhance regeneration whereas the others are unable (Knowlton et al., 2017). This suggests a dose-dependent effect for some of these components as well. The above results were obtained in the Posterior Lateral Microtubule (PLM) neuron or the motor neurons. My results in the Anterior Lateral Microtubule (ALM) neuron suggest that *nduf-2.2* knockdown via RNAi or *nuo-6* genetic loss-of-function have no impact on wildtype regeneration suggesting neuronal subtype is indeed important.

Our results also reveal the previously underappreciated role of glycolytic metabolism in axon growth. Whether neurons utilize glycolysis, mitochondrial oxidative phosphorylation, the pentose phosphate pathway, or some combination of the above is

highly debated and may be neuronal subtype or species dependent. However, recent advances made in metabolic imaging using FRET-based biosensors have revealed an important role for neuronal glycolytic metabolism during neuronal stimulation or periods of energy stress. In *C. elegans*, neuronal stimulation leads to the formation of clusters of glycolytic enzymes at synapses and this is essential to power the synaptic cycle (Jang et al., 2016). Further, glycolytic enzymes, but not mitochondrial oxidative phosphorylation, were essential to sustain synaptic activity under high neuronal stimulus regimes. In mouse models, a similar picture is emerging. Previous models have suggested that upon neuronal stimulation, glutamate is released and triggers glucose metabolism in astrocytes. The lactate produced by the astrocytes could then be shuttled to neurons for ATP production through mitochondrial oxidative phosphorylation (Pellerin et al., 2007). This data was supported by the relatively high levels of expression of glycolytic enzymes in astrocytes and low levels in neurons coupled with metabolic measurements made in cell culture models (Pellerin and Magistretti, 1994; Zhang et al., 2014). However, FRET-based biosensors *in vivo* and in cultured hippocampal slices have suggested that under stimulation, neurons are largely glycolytic whereas basal metabolism is mitochondrial (Diaz-Garcia et al., 2017). Future efforts to examine these discrepancies should provide fruitful information into the metabolic allotment of neurons.

Our data in *ogt-1* mutants is in line with neurons utilizing glycolysis under conditions of energy stress (i.e. neuronal injury and regeneration). Why is this source of energy generation more advantageous? Although the amount of ATP produced by

glycolysis is lower than oxidative phosphorylation, it can occur at much faster rates (Pfeiffer et al., 2001). This may be advantageous during an injury as energy is needed rapidly to mitigate damage and enable regrowth. Our work demonstrates that glycolysis, as well as finding other mutants that enhance glycolysis, may be key to optimizing regrowth. As many of the glycolytic enzymes are controlled allosterically by metabolic products, finding therapeutics that lock glycolytic enzymes into an active conformation may also be an interesting avenue.

4.12 Concluding Remarks

The regeneration of damaged axons remains a key goal in regenerative medicine. Our results demonstrate a unique mechanism by which O-GlcNAc post-translational modifications can orchestrate the metabolic response after injury to improve regeneration. We hypothesize that O-GlcNAc levels may interpret cellular nutrient status and act as a switch governing either glycolytic or mitochondrial metabolism. In the case of *ogt-1* mutants, a perceived absence of nutrients (i.e. low glucose) may trigger glucose metabolism to create more of the O-GlcNAc moiety. In contrast, in the *oga-1* mutants, a perceived abundance of nutrients (i.e. high glucose) triggers mitochondrial oxidative phosphorylation. This is accomplished by a dueling-kinases scenario where low O-GlcNAc activates AKT, whereas high O-GlcNAc activates SGK. Whether this model is conserved across neuronal injury models and whether this can be therapeutically targeted remains a critical question.

APPENDIX

Appendix 1: Strains Used and Sample Sizes

Gene Name	Allele(s) Used	Strain Name	N
WT (zdis5 pmec-4::GFP)		SK4005	40
ogt-1	ok1474	RB1342	40
oga-1	ok1207	RB1169	40
daf-2	e1370	CB1370	17
ogt-1;daf-2		CG121	22
oga-1;daf-2		CG122	20
age-1	hx546	TJ1052	18
ogt-1;age-1		CG123	21
oga-1;age-1		CG124	11
akt-1	ok525, mg144	RB759, GR1310	20, 18
akt-1(ok525)			18
ogt-1;akt-1(ok525)		CG125	17
oga-1;akt-1(ok525)		CG126	20
akt-1(mg144)			16
ogt-1;akt-1(mg144)		CG127	18
oga-1;akt-1(mg144)		CG128	10
sgk-1	ok538	VC345	13
oga-1;sgk-1		CG129	15
ark-1	sy247	PS1461	15
ogt-1;ark-1		CG130	29
ogt-1;ark-1;akt-1(mg144)		CG131	21
ogt-1;ark-1;akt-1(ok525)		CG132	17
daf-16	mu86	CF1038	14
ogt-1;daf-16		CG133	19
oga-1;daf-16		CG134	17
akt-2	ok393	VC204	23
ogt-1;akt-2		CG135	25
pfk-1.1	ola72	DCR3791	20
ogt-1;pfk-1.1		CG136	18
nuo-6	qm200	MQ1333	14

ogt-1;nuo-6		CG137	16
ogt-1;itr-1	sa73	N/A	13
pde-4	ce268	KG744	20
ogt-1;pde-4		N/A	20
oga-1;pde-4		N/A	20
crh-1	tz2	YT17	20
ogt-1;crh-1		N/A	19
oga-1;crh-1		N/A	20
PLM Neuron			
WT (zdis5 pmec-4::GFP)			19
ogt-1			30
oga-1			10
MitoROGFP Oxidative Stress			
Uncut			
pha-1(e2123); him-5(e1490); zhsEx17[Pmec-4mitoLS::ROGFP]		PTN73	15
oga-1; pha-1(e2123); him-5(e1490); zhsEx17[Pmec-4mitoLS::ROGFP]		CG138	15
Cut			
pha-1(e2123); him-5(e1490); zhsEx17[Pmec-4mitoLS::ROGFP]		PTN73	15
oga-1; pha-1(e2123); him-5(e1490); zhsEx17[Pmec-4mitoLS::ROGFP]		CG138	15
DAF-16::GFP Localization			
Non-heatshocked			
muIs61 [(pKL78) daf-16::GFP + rol-6(su1006)]; daf-16 (mu86)		CF1139	20
oga-1; muIs61 [(pKL78) daf-16::GFP + rol-6(su1006)]; daf-16 (mu86)		CG139	24
Heatshocked			
muIs61 [(pKL78) daf-16::GFP + rol-6(su1006)]; daf-16 (mu86)		CF1139	14
oga-1; muIs61 [(pKL78) daf-16::GFP + rol-6(su1006)]; daf-16 (mu86)		CG139	11

GSK-3b Overexpression			
Non-heatshocked			
(phsp16.2::gsk-3b;pmec-7::GFP)		KN131	20
ogt-1; (phsp16.2::gsk-3b;pmec-7::GFP)		CG140	18
Heatshocked			
(phsp16.2::gsk-3b;pmec-7::GFP)		KN131	22
ogt-1; (phsp16.2::gsk-3b;pmec-7::GFP)		CG140	20
WT zdis5		SK4005	15
Drug Treatments			
WT zdis5 (DMSO)		SK4005	7
WT zdis5 (Rapamycin)			10
daf-18 (DMSO)	ok480	RB712	10
daf-18 (Rapamycin)			16
ogt-1 (DMSO)	ok1474	RB1342	6
ogt-1 (Rapamycin)			11
WT zdis5 (100mM D-mannitol)			19
WT zdis5 (100mM glucose)			27
WT zdis5 (1mM phloretin)			18
WT zdis5 (5mM 2-deoxy-D-glucose)			20
WT zdis5 (10mM 2-deoxy-D-glucose)			20
ogt-1 (100mM glucose)			19
ogt-1 (1mM phloretin)			14
ogt-1 (5mM 2-deoxy-D-glucose)			21
ogt-1(10mM 2-deoxy-D-glucose)			15
oga-1 (100mM glucose)			12
oga-1(1mM phloretin)			17
WT zdis5 (EtOH controls for Thiamet G)			19
WT zdis5 (2uM Thiamet G)			20
oga-1 (2uM Thiamet G)			19
WT zdis5 (DMSO controls for ST045849)			19
WT zdis5 (50uM ST045849)			22

ogt-1 (50uM ST045849)			18
WT (7.5mM EGTA)			11
ogt-1 (7.5mM EGTA)			15
RNAi			
GFP Vector Control			10
GFP RNAi			9
Vector Control WT TU3568			21
ogt-1 RNAi			13
oga-1 RNAi			15
nduf-2.2 RNAi			14
OGT-1 RNAi Targets			
ogt-1;TU3568 Vector			9
glt-1 RNAi			10
fgt-1 RNAi			14
swt-7 RNAi			13
mct-2 RNAi			8
mct-4 RNAi			9
mct-5 RNAi			9
mct-6 RNAi			23
aat-9 RNAi			21
ZK829.9 RNAi			12
pgk-1 RNAi			23
nduf-2.2 RNAi			18
OGA-1 RNAi Targets			
oga-1; TU3568 Vector			19
nduf-2.2 RNAi			22
Timelapse Dynamics			
WT zdis5			
1 hr			17
3 hr			17
5 hr			17
12 hr			16
24 hr			40
ogt-1			
1 hr			21
3 hr			21

5 hr			21
12 hr			22
24 hr			40
oga-1			
1 hr			20
3 hr			20
5 hr			20
12 hr			19
24 hr			40
Mitochondrial Dynamics			
Wildtype zdis5 (C. elegans N)			18
ogt-1 (C. elegans N)			8
oga-1 (C. elegans N)			12
Wildtype zdis5 (mitochondria N)			259
ogt-1 (mitochondria N)			159
oga-1 (mitochondria N)			140

BIBLIOGRAPHY

Alfaro, J.F., Gong, C.X., Monroe, M.E., Aldrich, J.T., Clauss, T.R., Purvine, S.O., Wang, Z., Camp, D.G., 2nd, Shabanowitz, J., Stanley, P.*, et al.* (2012). Tandem mass spectrometry identifies many mouse brain O-GlcNAcylated proteins including EGF domain-specific O-GlcNAc transferase targets. Proceedings of the National Academy of Sciences U S A *109*, 7280-7285.

Beifuss, K.K., and Gumienny, T.L. (2012). RNAi screening to identify postembryonic phenotypes in C. elegans. Journal of Visualized Experiments, e3442.

Bianchi, L., Gerstbrein, B., Frokjaer-Jensen, C., Royal, D.C., Mukherjee, G., Royal, M.A., Xue, J., Schafer, W.R., and Driscoll, M. (2004). The neurotoxic MEC-4(d) DEG/ENaC sodium channel conducts calcium: implications for necrosis initiation. Nature Neuroscience *7*, 1337-1344.

Brenner, S. (1974). The genetics of Caenorhabditis elegans. Genetics *77*, 71-94.

Byrne, A.B., Walradt, T., Gardner, K.E., Hubbert, A., Reinke, V., and Hammarlund, M. (2014). Insulin/IGF1 signaling inhibits age-dependent axon regeneration. Neuron *81*, 561-573.

Cai, D., Deng, K., Mellado, W., Lee, J., Ratan, R.R., and Filbin, M.T. (2002). Arginase I and polyamines act downstream from cyclic AMP in overcoming inhibition of axonal growth MAG and myelin in vitro. Neuron *35*, 711-719.

Cai, D., Shen, Y., De Bellard, M., Tang, S., and Filbin, M.T. (1999). Prior exposure to neurotrophins blocks inhibition of axonal regeneration by MAG and myelin via a cAMP-dependent mechanism. Neuron *22*, 89-101.

Calixto, A., Chelur, D., Topalidou, I., Chen, X., and Chalfie, M. (2010). Enhanced neuronal RNAi in C. elegans using SID-1. Nature Methods *7*, 554-559.

Cartoni, R., Norsworthy, M.W., Bei, F., Wang, C., Li, S., Zhang, Y., Gabel, C.V., Schwarz, T.L., and He, Z. (2017). The Mammalian-Specific Protein Armcx1 Regulates Mitochondrial Transport during Axon Regeneration. Neuron *94*, 689.

Chalfie, M., and Sulston, J. (1981). Developmental genetics of the mechanosensory neurons of Caenorhabditis elegans. Developmental Biology *82*, 358-370.

Chavez, V., Mohri-Shiomi, A., Maadani, A., Vega, L.A., and Garsin, D.A. (2007). Oxidative stress enzymes are required for DAF-16-mediated immunity due to generation of reactive oxygen species by Caenorhabditis elegans. Genetics *176*, 1567-1577.

Chen, A.T., Guo, C., Dumas, K.J., Ashrafi, K., and Hu, P.J. (2013). Effects of Caenorhabditis elegans sgk-1 mutations on lifespan, stress resistance, and DAF-16/FoxO regulation. Aging Cell *12*, 932-940.

Cho, Y., Sloutsky, R., Naegle, K.M., and Cavalli, V. (2015). Injury-Induced HDAC5 Nuclear Export Is Essential for Axon Regeneration. Cell *161*, 691.

Chung, S.H., Awal, M.R., Shay, J., McLoed, M.M., Mazur, E., and Gabel, C.V. (2016). Novel DLK-independent neuronal regeneration in Caenorhabditis elegans shares links with activity-dependent ectopic outgrowth. Proceedings of the National Academy of Sciences U S A *113*, E2852-2860.

Consortium, C.e.D.M. (2012). large-scale screening for targeted knockouts in the Caenorhabditis elegans genome. G3 (Bethesda) *2*, 1415-1425.

Consortium, C.e.S. (1998). Genome sequence of the nematode C. elegans: a platform for investigating biology. Science *282*, 2012-2018.

Corsi, A.K., Wightman, B., and Chalfie, M. (2015). A Transparent Window into Biology: A Primer on Caenorhabditis elegans. Genetics *200*, 387-407.

Del Mar Masdeu, M., Armendariz, B.G., Torre, A., Soriano, E., Burgaya, F., and Urena, J.M. (2017). Identification of novel Ack1-interacting proteins and Ack1 phosphorylated sites in mouse brain by mass spectrometry. Oncotarget *8*, 101146-101157.

Diaz-Garcia, C.M., Mongeon, R., Lahmann, C., Koveal, D., Zucker, H., and Yellen, G. (2017). Neuronal Stimulation Triggers Neuronal Glycolysis and Not Lactate Uptake. Cell Metabolism *26*, 361-374 e364.

Dickinson, D.J., and Goldstein, B. (2016). CRISPR-Based Methods for Caenorhabditis elegans Genome Engineering. Genetics *202*, 885-901.

Dickson, B.J., and Gilestro, G.F. (2006). Regulation of commissural axon pathfinding by slit and its Robo receptors. Annual Reviews in Cell and Developmental Biology *22*, 651-675.

Dorman, J.B., Albinder, B., Shroyer, T., and Kenyon, C. (1995). The age-1 and daf-2 genes function in a common pathway to control the lifespan of Caenorhabditis elegans. Genetics *141*, 1399-1406.

Erickson, J.R., Pereira, L., Wang, L., Han, G., Ferguson, A., Dao, K., Copeland, R.J., Despa, F., Hart, G.W., Ripplinger, C.M.*, et al.* (2013). Diabetic hyperglycaemia activates CaMKII and arrhythmias by O-linked glycosylation. Nature *502*, 372-376.

Forsythe, M.E., Love, D.C., Lazarus, B.D., Kim, E.J., Prinz, W.A., Ashwell, G., Krause, M.W., and Hanover, J.A. (2006). Caenorhabditis elegans ortholog of a diabetes susceptibility locus: oga-1 (O-GlcNAcase) knockout impacts O-GlcNAc cycling, metabolism, and dauer. Proceedings of the National Academy of Sciences U S A *103*, 11952-11957.

Francisco, H., Kollins, K., Varghis, N., Vocadlo, D., Vosseller, K., and Gallo, G. (2009). O-GLcNAc post-translational modifications regulate the entry of neurons into an axon branching program. Developmental Neurobiology *69*, 162-173.

Furuyama, T., Nakazawa, T., Nakano, I., and Mori, N. (2000). Identification of the differential distribution patterns of mRNAs and consensus binding sequences for mouse DAF-16 homologues. Biochemical Journal *349*, 629-634.

Gabel, C.V. (2008). Femtosecond lasers in biology: nanoscale surgery with ultrafast optics. Contemporary Physics *49*, 391-411.

Gabel, C.V., Antoine, F., Chuang, C.F., Samuel, A.D., and Chang, C. (2008). Distinct cellular and molecular mechanisms mediate initial axon development and adult-stage axon regeneration in C. elegans. Development *135*, 1129-1136.

Ghosh-Roy, A., Wu, Z., Goncharov, A., Jin, Y., and Chisholm, A.D. (2010). Calcium and cyclic AMP promote axonal regeneration in Caenorhabditis elegans and require DLK-1 kinase. Journal of Neuroscience *30*, 3175-3183.

Gottlieb, T.M., Leal, J.F., Seger, R., Taya, Y., and Oren, M. (2002). Cross-talk between Akt, p53 and Mdm2: possible implications for the regulation of apoptosis. Oncogene *21*, 1299-1303.

Hammarlund, M., Nix, P., Hauth, L., Jorgensen, E.M., and Bastiani, M. (2009). Axon regeneration requires a conserved MAP kinase pathway. Science *323*, 802-806.

Han, S.M., Baig, H.S., and Hammarlund, M. (2016). Mitochondria Localize to Injured Axons to Support Regeneration. Neuron *92*, 1308-1323.

Hanover, J.A., Forsythe, M.E., Hennessey, P.T., Brodigan, T.M., Love, D.C., Ashwell, G., and Krause, M. (2005). A Caenorhabditis elegans model of insulin resistance: altered macronutrient storage and dauer formation in an OGT-1 knockout. Proceedings of the National Academy of Sciences U S A *102*, 11266-11271.

Hart, G.W., Housley, M.P., and Slawson, C. (2007). Cycling of O-linked beta-N-acetylglucosamine on nucleocytoplasmic proteins. Nature *446*, 1017-1022.

He, H., Deng, K., Siddiq, M.M., Pyie, A., Mellado, W., Hannila, S.S., and Filbin, M.T. (2016). Cyclic AMP and Polyamines Overcome Inhibition by Myelin-Associated Glycoprotein through eIF5A-Mediated Increases in p35 Expression and Activation of Cdk5. Journal of Neuroscience *36*, 3079-3091.

He, Z., and Jin, Y. (2016). Intrinsic Control of Axon Regeneration. Neuron *90*, 437-451.

Hertweck, M., Gobel, C., and Baumeister, R. (2004). C. elegans SGK-1 is the critical component in the Akt/PKB kinase complex to control stress response and life span. Developmental Cell *6*, 577-588.

Ito, Y.A., and Di Polo, A. (2017). Mitochondrial dynamics, transport, and quality control: A bottleneck for retinal ganglion cell viability in optic neuropathies. Mitochondrion *36*, 186-192.

Jang, S., Nelson, J.C., Bend, E.G., Rodriguez-Laureano, L., Tueros, F.G., Cartagenova, L., Underwood, K., Jorgensen, E.M., and Colon-Ramos, D.A. (2016). Glycolytic Enzymes Localize to Synapses under Energy Stress to Support Synaptic Function. Neuron *90*, 278-291.

Kaletsky, R., Lakhina, V., Arey, R., Williams, A., Landis, J., Ashraf, J., and Murphy, C.T. (2016). The C. elegans adult neuronal IIS/FOXO transcriptome reveals adult phenotype regulators. Nature *529*, 92-96.

Kamath, R.S., and Ahringer, J. (2003). Genome-wide RNAi screening in Caenorhabditis elegans. Methods *30*, 313-321.

Keembiyehetty, C., Love, D.C., Harwood, K.R., Gavrilova, O., Comly, M.E., and Hanover, J.A. (2015). Conditional knock-out reveals a requirement for O-linked N-Acetylglucosaminase (O-GlcNAcase) in metabolic homeostasis. Journal of Biological Chemistry *290*, 7097-7113.

Kim, E., Sun, L., Gabel, C.V., and Fang-Yen, C. (2013). Long-term imaging of Caenorhabditis elegans using nanoparticle-mediated immobilization. PLoS One *8*, e53419.

Kimura, K.D., Tissenbaum, H.A., Liu, Y., and Ruvkun, G. (1997). daf-2, an insulin receptor-like gene that regulates longevity and diapause in Caenorhabditis elegans. Science *277*, 942-946.

Knowlton, W.M., Hubert, T., Wu, Z., Chisholm, A.D., and Jin, Y. (2017). A Select Subset of Electron Transport Chain Genes Associated with Optic Atrophy Link Mitochondria to Axon Regeneration in Caenorhabditis elegans. Frontiers in Neuroscience *11*, 263.

Korswagen, H.C., Coudreuse, D.Y., Betist, M.C., van de Water, S., Zivkovic, D., and Clevers, H.C. (2002). The Axin-like protein PRY-1 is a negative regulator of a canonical Wnt pathway in C. elegans. Genes and Development *16*, 1291-1302.

Kumar, J., Choudhary, B.C., Metpally, R., Zheng, Q., Nonet, M.L., Ramanathan, S., Klopfenstein, D.R., and Koushika, S.P. (2010). The Caenorhabditis elegans Kinesin-3 motor UNC-104/KIF1A is degraded upon loss of specific binding to cargo. PLoS Genetics *6*, e1001200.

Kwon, E.S., Narasimhan, S.D., Yen, K., and Tissenbaum, H.A. (2010). A new DAF-16 isoform regulates longevity. Nature *466*, 498-502.

La Torre, A., del Rio, J.A., Soriano, E., and Urena, J.M. (2006). Expression pattern of ACK1 tyrosine kinase during brain development in the mouse. Gene Expression Patterns *6*, 886-892.

Lagerlof, O., Slocomb, J.E., Hong, I., Aponte, Y., Blackshaw, S., Hart, G.W., and Huganir, R.L. (2016). The nutrient sensor OGT in PVN neurons regulates feeding. Science *351*, 1293-1296.

Lehman, D.M., Fu, D.J., Freeman, A.B., Hunt, K.J., Leach, R.J., Johnson-Pais, T., Hamlington, J., Dyer, T.D., Arya, R., Abboud, H.*, et al.* (2005). A single nucleotide polymorphism in MGEA5 encoding O-GlcNAc-selective N-acetyl-beta-D glucosaminidase is associated with type 2 diabetes in Mexican Americans. Diabetes *54*, 1214-1221.

Leibinger, M., Andreadaki, A., Golla, R., Levin, E., Hilla, A.M., Diekmann, H., and Fischer, D. (2017). Boosting CNS axon regeneration by harnessing antagonistic effects of GSK3 activity. Proceedings of the National Academy of Sciences U S A *114*, E5454-E5463.

Li, C., Hisamoto, N., and Matsumoto, K. (2015). Axon Regeneration Is Regulated by Ets-C/EBP Transcription Complexes Generated by Activation of the cAMP/Ca2+ Signaling Pathways. PLoS Genetics *11*, e1005603.

Lin, K., Hsin, H., Libina, N., and Kenyon, C. (2001). Regulation of the Caenorhabditis elegans longevity protein DAF-16 by insulin/IGF-1 and germline signaling. Nature Genetics *28*, 139-145.

Liu, Q., Hollopeter, G., and Jorgensen, E.M. (2009). Graded synaptic transmission at the Caenorhabditis elegans neuromuscular junction. Proceedings of the National Academy of Sciences U S A *106*, 10823-10828.

Love, D.C., Ghosh, S., Mondoux, M.A., Fukushige, T., Wang, P., Wilson, M.A., Iser, W.B., Wolkow, C.A., Krause, M.W., and Hanover, J.A. (2010). Dynamic O-GlcNAc cycling at promoters of Caenorhabditis elegans genes regulating longevity, stress, and immunity. Proceedings of the National Academy of Sciences U S A *107*, 7413-7418.

Mahajan, K., Coppola, D., Challa, S., Fang, B., Chen, Y.A., Zhu, W., Lopez, A.S., Koomen, J., Engelman, R.W., Rivera, C.*, et al.* (2010). Ack1 mediated AKT/PKB tyrosine 176 phosphorylation regulates its activation. PLoS One *5*, e9646.

Mahajan, K., Malla, P., Lawrence, H.R., Chen, Z., Kumar-Sinha, C., Malik, R., Shukla, S., Kim, J., Coppola, D., Lawrence, N.J.*, et al.* (2017). ACK1/TNK2 Regulates Histone H4 Tyr88-phosphorylation and AR Gene Expression in Castration-Resistant Prostate Cancer. Cancer Cell *31*, 790-803 e798.

Mao, X., Zhang, D., Tao, T., Liu, X., Sun, X., Wang, Y., and Shen, A. (2015). O-GlcNAc glycosylation of p27(kip1) promotes astrocyte migration and functional recovery after spinal cord contusion. Experimental Cell Research *339*, 197-205.

Marshall, S., Bacote, V., and Traxinger, R.R. (1991). Discovery of a metabolic pathway mediating glucose-induced desensitization of the glucose transport system. Role of hexosamine biosynthesis in the induction of insulin resistance. Journal of Biological Chemistry *266*, 4706-4712.

McClain, D.A., and Crook, E.D. (1996). Hexosamines and insulin resistance. Diabetes *45*, 1003-1009.

Melentijevic, I., Toth, M.L., Arnold, M.L., Guasp, R.J., Harinath, G., Nguyen, K.C., Taub, D., Parker, J.A., Neri, C., Gabel, C.V.*, et al.* (2017). C. elegans neurons jettison protein aggregates and mitochondria under neurotoxic stress. Nature *542*, 367-371.

Memmott, R.M., and Dennis, P.A. (2009). Akt-dependent and -independent mechanisms of mTOR regulation in cancer. Cell Signal *21*, 656-664.

Mondoux, M.A., Love, D.C., Ghosh, S.K., Fukushige, T., Bond, M., Weerasinghe, G.R., Hanover, J.A., and Krause, M.W. (2011). O-linked-N-acetylglucosamine cycling and insulin signaling are required for the glucose stress response in Caenorhabditis elegans. Genetics *188*, 369-382.

Morsci, N.S., Hall, D.H., Driscoll, M., and Sheng, Z.H. (2016). Age-Related Phasic Patterns of Mitochondrial Maintenance in Adult Caenorhabditis elegans Neurons. Journal of Neuroscience *36*, 1373-1385.

Murphy, C.T., and Hu, P.J. (2013). Insulin/insulin-like growth factor signaling in C. elegans. WormBook, 1-43.

Ngoh, G.A., Watson, L.J., Facundo, H.T., and Jones, S.P. (2011). Augmented O-GlcNAc signaling attenuates oxidative stress and calcium overload in cardiomyocytes. Amino Acids *40*, 895-911.

Nix, P., Hammarlund, M., Hauth, L., Lachnit, M., Jorgensen, E.M., and Bastiani, M. (2014). Axon regeneration genes identified by RNAi screening in C. elegans. Journal of Neuroscience *34*, 629-645.

Nix, P., Hisamoto, N., Matsumoto, K., and Bastiani, M. (2011). Axon regeneration requires coordinate activation of p38 and JNK MAPK pathways. Proceedings of the National Academy of Sciences U S A *108*, 10738-10743.

O'Donnell, N., Zachara, N.E., Hart, G.W., and Marth, J.D. (2004). Ogt-dependent X-chromosome-linked protein glycosylation is a requisite modification in somatic cell function and embryo viability. Molecular and Cellular Biology *24*, 1680-1690.

O'Hagan, R., Chalfie, M., and Goodman, M.B. (2005). The MEC-4 DEG/ENaC channel of Caenorhabditis elegans touch receptor neurons transduces mechanical signals. Nature Neuroscience *8*, 43-50.

Olivier-Van Stichelen, S., Wang, P., Comly, M., Love, D.C., and Hanover, J.A. (2017). Nutrient-driven O-linked N-acetylglucosamine (O-GlcNAc) cycling impacts neurodevelopmental timing and metabolism. Journal of Biological Chemistry *292*, 6076-6085.

Park, K.K., Liu, K., Hu, Y., Smith, P.D., Wang, C., Cai, B., Xu, B., Connolly, L., Kramvis, I., Sahin, M.*, et al.* (2008). Promoting axon regeneration in the adult CNS by modulation of the PTEN/mTOR pathway. Science *322*, 963-966.

Pekkurnaz, G., Trinidad, J.C., Wang, X., Kong, D., and Schwarz, T.L. (2014). Glucose regulates mitochondrial motility via Milton modification by O-GlcNAc transferase. Cell *158*, 54-68.

Pellerin, L., Bouzier-Sore, A.K., Aubert, A., Serres, S., Merle, M., Costalat, R., and Magistretti, P.J. (2007). Activity-dependent regulation of energy metabolism by astrocytes: an update. Glia *55*, 1251-1262.

Pellerin, L., and Magistretti, P.J. (1994). Glutamate uptake into astrocytes stimulates aerobic glycolysis: a mechanism coupling neuronal activity to glucose utilization. Proceedings of the National Academy of Sciences U S A *91*, 10625-10629.

Pfeiffer, T., Schuster, S., and Bonhoeffer, S. (2001). Cooperation and competition in the evolution of ATP-producing pathways. Science *292*, 504-507.

Pinan-Lucarre, B., Gabel, C.V., Reina, C.P., Hulme, S.E., Shevkoplyas, S.S., Slone, R.D., Xue, J., Qiao, Y., Weisberg, S., Roodhouse, K.*, et al.* (2012). The core apoptotic executioner proteins CED-3 and CED-4 promote initiation of neuronal regeneration in Caenorhabditis elegans. PLoS Biology *10*, e1001331.

Rahman, M.M., Stuchlick, O., El-Karim, E.G., Stuart, R., Kipreos, E.T., and Wells, L. (2010). Intracellular protein glycosylation modulates insulin mediated lifespan in C.elegans. Aging (Albany NY) *2*, 678-690.

Rengifo, J., Gibson, C.J., Winkler, E., Collin, T., and Ehrlich, B.E. (2007). Regulation of the inositol 1,4,5-trisphosphate receptor type I by O-GlcNAc glycosylation. Journal of Neuroscience *27*, 13813-13821.

Rexach, J.E., Clark, P.M., Mason, D.E., Neve, R.L., Peters, E.C., and Hsieh-Wilson, L.C. (2012). Dynamic O-GlcNAc modification regulates CREB-mediated gene expression and memory formation. Nature Chemical Biology *8*, 253-261.

Robey, R.B., and Hay, N. (2009). Is Akt the "Warburg kinase"?-Akt-energy metabolism interactions and oncogenesis. Seminars in Cancer Biology *19*, 25-31.

Shafi, R., Iyer, S.P., Ellies, L.G., O'Donnell, N., Marek, K.W., Chui, D., Hart, G.W., and Marth, J.D. (2000). The O-GlcNAc transferase gene resides on the X chromosome and is essential for embryonic stem cell viability and mouse ontogeny. Proceedings of the National Academy of Sciences U S A *97*, 5735-5739.

Song, H.J., and Poo, M.M. (1999). Signal transduction underlying growth cone guidance by diffusible factors. Currrent Opinions in Neurobiology *9*, 355-363.

Stiess, M., and Bradke, F. (2011). Neuronal polarization: the cytoskeleton leads the way. Developmental Neurobiology *71*, 430-444.

Su, C., and Schwarz, T.L. (2017). O-GlcNAc Transferase Is Essential for Sensory Neuron Survival and Maintenance. Journal of Neuroscience *37*, 2125-2136.

Sun, L., Shay, J., McLoed, M., Roodhouse, K., Chung, S.H., Clark, C.M., Pirri, J.K., Alkema, M.J., and Gabel, C.V. (2014). Neuronal regeneration in C. elegans requires subcellular calcium release by ryanodine receptor channels and can be enhanced by optogenetic stimulation. Journal of Neuroscience *34*, 15947-15956.

Tan, E.P., McGreal, S.R., Graw, S., Tessman, R., Koppel, S.J., Dhakal, P., Zhang, Z., Machacek, M., Zachara, N.E., Koestler, D.C.*, et al.* (2017). Sustained O-GlcNAcylation reprograms mitochondrial function to regulate energy metabolism. Journal of Biological Chemistry *292*, 14940-14962.

Tullet, J.M.A., Green, J.W., Au, C., Benedetto, A., Thompson, M.A., Clark, E., Gilliat, A.F., Young, A., Schmeisser, K., and Gems, D. (2017). The SKN-1/Nrf2 transcription factor can protect against oxidative stress and increase lifespan in C. elegans by distinct mechanisms. Aging Cell *16*, 1191-1194.

Urena, J.M., La Torre, A., Martinez, A., Lowenstein, E., Franco, N., Winsky-Sommerer, R., Fontana, X., Casaroli-Marano, R., Ibanez-Sabio, M.A., Pascual, M.*, et al.* (2005). Expression, synaptic localization, and developmental regulation of Ack1/Pyk1, a cytoplasmic tyrosine kinase highly expressed in the developing and adult brain. Journal of Comparative Neurology *490*, 119-132.

Vaidyanathan, K., Niranjan, T., Selvan, N., Teo, C.F., May, M., Patel, S., Weatherly, B., Skinner, C., Opitz, J., Carey, J.*, et al.* (2017). Identification and characterization of a missense mutation in the O-linked beta-N-acetylglucosamine (O-GlcNAc) transferase gene that segregates with X-linked intellectual disability. Journal of Biological Chemistry *292*, 8948-8963.

Vo, M.T., Choi, S.H., Lee, J.H., Hong, C.H., Kim, J.S., Lee, U.H., Chung, H.M., Lee, B.J., Park, J.W., and Cho, W.J. (2017). Tristetraprolin inhibits mitochondrial function through suppression of alpha-Synuclein expression in cancer cells. Oncotarget *8*, 41903-41920.

Vosseller, K., Wells, L., Lane, M.D., and Hart, G.W. (2002). Elevated nucleocytoplasmic glycosylation by O-GlcNAc results in insulin resistance associated with defects in Akt activation in 3T3-L1 adipocytes. Proceedings of the National Academy of Sciences U S A *99*, 5313-5318.

Wang, P., Lazarus, B.D., Forsythe, M.E., Love, D.C., Krause, M.W., and Hanover, J.A. (2012). O-GlcNAc cycling mutants modulate proteotoxicity in Caenorhabditis elegans models of human neurodegenerative diseases. Proceedings of the National Academy of Sciences U S A *109*, 17669-17674.

Ward, P.S., and Thompson, C.B. (2012). Signaling in control of cell growth and metabolism. Cold Spring Harbor Perspectives in Biology *4*, a006783.

Whelan, S.A., Dias, W.B., Thiruneelakantapillai, L., Lane, M.D., and Hart, G.W. (2010). Regulation of insulin receptor substrate 1 (IRS-1)/AKT kinase-mediated insulin signaling by O-Linked beta-N-acetylglucosamine in 3T3-L1 adipocytes. Journal of Biological Chemistry *285*, 5204-5211.

White, J.G., Southgate, E., Thomson, J.N., and Brenner, S. (1986). The structure of the nervous system of the nematode Caenorhabditis elegans. Philosophical Transactions of the Royal Society of London B Biological Sciences *314*, 1-340.

Willems, A.P., Gundogdu, M., Kempers, M.J.E., Giltay, J.C., Pfundt, R., Elferink, M., Loza, B.F., Fuijkschot, J., Ferenbach, A.T., van Gassen, K.L.I.*, et al.* (2017). Mutations in N-acetylglucosamine (O-GlcNAc) transferase in patients with X-linked intellectual disability. Journal of Biological Chemistry *292*, 12621-12631.

Wilson, C., and Gonzalez-Billault, C. (2015). Regulation of cytoskeletal dynamics by redox signaling and oxidative stress: implications for neuronal development and trafficking. Frontiers in Cellular Neuroscience *9*, 381.

Wu, X., Zahari, M.S., Ma, B., Liu, R., Renuse, S., Sahasrabuddhe, N.A., Chen, L., Chaerkady, R., Kim, M.S., Zhong, J.*, et al.* (2015). Global phosphotyrosine survey in triple-negative breast cancer reveals activation of multiple tyrosine kinase signaling pathways. Oncotarget *6*, 29143-29160.

Wu, X., Zahari, M.S., Renuse, S., Kelkar, D.S., Barbhuiya, M.A., Rojas, P.L., Stearns, V., Gabrielson, E., Malla, P., Sukumar, S.*, et al.* (2017). The non-receptor tyrosine kinase TNK2/ACK1 is a novel therapeutic target in triple negative breast cancer. Oncotarget *8*, 2971-2983.

Xiao, R., Zhang, B., Dong, Y., Gong, J., Xu, T., Liu, J., and Xu, X.Z. (2013). A genetic program promotes C. elegans longevity at cold temperatures via a thermosensitive TRP channel. Cell *152*, 806-817.

Yan, D., and Jin, Y. (2012). Regulation of DLK-1 kinase activity by calcium-mediated dissociation from an inhibitory isoform. Neuron *76*, 534-548.

Yi, W., Clark, P.M., Mason, D.E., Keenan, M.C., Hill, C., Goddard, W.A., 3rd, Peters, E.C., Driggers, E.M., and Hsieh-Wilson, L.C. (2012). Phosphofructokinase 1 glycosylation regulates cell growth and metabolism. Science *337*, 975-980.

Yoo, A.S., Bais, C., and Greenwald, I. (2004). Crosstalk between the EGFR and LIN-12/Notch pathways in C. elegans vulval development. Science *303*, 663-666.

Zachara, N.E., O'Donnell, N., Cheung, W.D., Mercer, J.J., Marth, J.D., and Hart, G.W. (2004). Dynamic O-GlcNAc modification of nucleocytoplasmic proteins in response to stress. A survival response of mammalian cells. Journal of Biological Chemistry *279*, 30133-30142.

Zhang, Y., Chen, K., Sloan, S.A., Bennett, M.L., Scholze, A.R., O'Keeffe, S., Phatnani, H.P., Guarnieri, P., Caneda, C., Ruderisch, N.*, et al.* (2014). An RNA-sequencing transcriptome and splicing database of glia, neurons, and vascular cells of the cerebral cortex. Journal of Neuroscience *34*, 11929-11947.

Zheng, X., Boyer, L., Jin, M., Mertens, J., Kim, Y., Ma, L., Ma, L., Hamm, M., Gage, F.H., and Hunter, T. (2016). Metabolic reprogramming during neuronal differentiation from aerobic glycolysis to neuronal oxidative phosphorylation. Elife *5*.

CURRICULUM VITAE